UCRL-18369

cy.2

University of California

Ernest O. Lawrence Radiation Laboratory

RECEIVED
LAWRENCE
RADIATION LABORATORY

DEC 19 1968

LIBRARY AND
DOCUMENTS SECTION

COMPARISON OF π^+ AND π^- LIFETIMES AS A TEST OF CPT INVARIANCE

David S. Ayres

(Ph. D. Thesis)

October 1, 1968

TWO-WEEK LOAN COPY

This is a Library Circulating Copy which may be borrowed for two weeks. For a personal retention copy, call Tech. Info. Division, Ext. 5545

UCRL-18369 cy.2

DISCLAIMER

This document was prepared as an account of work sponsored by the United States Government. While this document is believed to contain correct information, neither the United States Government nor any agency thereof, nor the Regents of the University of California, nor any of their employees, makes any warranty, express or implied, or assumes any legal responsibility for the accuracy, completeness, or usefulness of any information, apparatus, product, or process disclosed, or represents that its use would not infringe privately owned rights. Reference herein to any specific commercial product, process, or service by its trade name, trademark, manufacturer, or otherwise, does not necessarily constitute or imply its endorsement, recommendation, or favoring by the United States Government or any agency thereof, or the Regents of the University of California. The views and opinions of authors expressed herein do not necessarily state or reflect those of the United States Government or any agency thereof or the Regents of the University of California.

UCRL-18369

UNIVERSITY OF CALIFORNIA

Lawrence Radiation Laboratory
Berkeley California

AEC Contract No. W-7405-eng-48

COMPARISON OF π^+ AND π^- LIFETIMES AS A TEST OF CPT INVARIANCE

David S. Ayres

(Ph.D. Thesis)

October 1, 1968

COMPARISON OF π^+ AND π^- LIFETIMES AS A TEST OF CPT INVARIANCE

Contents

Abstract. v

I. Introduction. 1

II. Theory

A. The Reflection Symmetries 8

B. The CPT Theorem 13

C. Consequences of the CPT Theorem 16

D. Experimental Checks on CPT Invariance 20

E. The Pion Decay Interaction. 23

III. Experimental Method

A. The Beam. 26

B. The Liquid-Deuterium Cerenkov Counters, CM and CP

1. Choice of the Cerenkov Medium 38

2. The Optical System. 39

3. Cryogenic Problems. 49

4. Performance Tests 57

C. Electronics 74

D. Data-Taking Procedure 82

IV. Systematic Errors

A. Equality of Momenta of the Positive and Negative Beams. 85

B. Beam Containment Along the Decay Path 99

C. CP Performance. 106

D. Biases Related to the Use of Liquid Hydrogen. 111

E. Changes in the Experimental Method. 115

V. Data Analysis

A. Derivation of Formulae Used. 123

B. Data Analysis for a Particular Run 131

C. Data Selection and Final Compilation 137

VI. Conclusions. 142

Acknowledgements 145

References 147

COMPARISON OF π^+ AND π^- LIFETIMES AS A TEST OF CPT INVARIANCE

Lawrence Radiation Laboratory
University of California
Berkeley, California

ABSTRACT

One of the consequences of the CPT theorem is the prediction that a particle and its antiparticle will have equal lifetimes. The experiment described here tests that prediction by comparing the mean lifetimes of π^+ and its antiparticle π^-. The result of the measurement was $\tau_{\pi^+}/\tau_{\pi^-} = 1.00055 \pm 0.00071$, which is consistent with the prediction of the CPT theorem.

The experimental method was to measure the fraction of surviving pions at several positions along a 35-ft (one-half lifetime) decay path. The beam polarity was alternated frequently between positive and negative particles, and many precautions were taken to insure that the π^+ and π^- beams were identical in their spatial and momentum distributions. Most of the running time was spent investigating possible sources of systematic bias which might make the lifetimes appear to be different, and a number of these systematic errors were found and eliminated. This experiment represents a considerable improvement over an earlier one at the 184-in. cyclotron, in which the author also participated. The most significant changes were a 100-fold increase in the pion beam intensity, and the use of charge-symmetric liquid deuterium in the focusing Cerenkov counter which detected pions along the decay path.

I. INTRODUCTION

The CPT theorem states that all interaction Hamiltonians are invariant under the combined operations of C, P, and T, applied in any order. One consequence of this invariance which is fairly simple to test experimentally is the prediction that the total lifetimes of particle and antiparticle must be equal. The experiment described here is a comparison of the mean lifetimes of π^+ and its antiparticle π^-, performed at the Lawrence Radiation Laboratory's 184-in. cyclotron. The result of the measurement was $\tau_{\pi^+}/\tau_{\pi^-} = 1.00055 \pm 0.00071$, which is consistent with the invariance under CPT of the Hamiltonian responsible for the decay, and thus with the prediction of the CPT theorem. Since CPT invariance is a sufficient, but not a necessary condition for the equality of lifetimes of particle and antiparticle, it is still possible that CPT is not conserved in the charged pion decay and that the observed equality of lifetimes results from some other symmetry, for instance CP invariance.

The most accurate recent determinations of $\tau_{\pi^+}/\tau_{\pi^-}$ are listed below:

Columbia (1966)[1]	1.004 ± 0.007
Rochester-Brookhaven (1966)[2]	1.0023 ± 0.0040
Berkeley-Santa Barbara (1967)[3]	1.0056 ± 0.0028
Dubna (1968)[4]	0.9986 ± 0.0029
This experiment (1968)[5]	1.00055 ± 0.00071

This tabulation indicates one of the reasons for our interest in measuring the lifetime ratio: while each of the first three results is consistent with equality of lifetimes, when taken together they suggest that π^+ might be longer lived than π^-. The third measurement was the result of an earlier experiment in which the author participated, and used many of the same techniques as the experiment reported here.

The mean lifetime of the positive pion is usually measured by bringing pions to rest in a block of material (scintillator, for instance), and then observing the distribution of the decay muons as a function of time after the pion has entered the block.[6] Unfortunately, the lifetime of the negative pion cannot be measured in this way, since when it is brought to rest in matter, it is immediately captured by the Coulomb field of a nucleus, cascades to an orbit which overlaps the nucleus, and undergoes a strong interaction with that nucleus before it has an appreciable chance to decay. For the small fraction of negative pions which do decay before they are captured, the decay products will be hopelessly confused with reaction products from the great majority of pions which are captured. For this reason, the π^- lifetime must be measured in flight, and in an experiment to compare the π^+ and π^- lifetimes, it is important that both lifetimes be measured in the same way. Thus we have chosen to measure both lifetimes by an in-flight method.

A nearly parallel beam of pions, kept smaller than 5.5 in. in diameter over its entire 35-ft length, was produced at the Lawrence Radiation Laboratory's 184-in. cyclotron. The pion intensity was monitored by a system of counters upstream of this 35-ft decay path, and the fraction of pions which had not decayed was measured by a movable detector at different distances along the decay path. Because of pion decay in flight, the fraction of surviving pions fell off with increasing distance, and it was possible to measure the pions' lifetime in the laboratory reference frame by determining this fraction as a function of distance. In our beam, $\beta = 0.92$, so the lifetime was nearly three times as long in the laboratory as in the pion rest frame, and the decay

path was equivalent to about one-half of a pion mean lifetime in the laboratory. The pion beam could be easily alternated between π^+ and π^- by changing the polarities of the secondary-beam magnets. If the velocities of the positive and negative beams were equal, a measurement of the lifetime ratio in the laboratory system could be transformed to the rest system without knowing the beam velocity very accurately. On the other hand, a precise measurement of the absolute pion lifetime (in the rest frame) required a precise determination of the pion velocity. For this reason, it was possible for us to measure the ratio of the pion lifetimes to considerably higher precision than either of the absolute lifetimes.

At the heart of the experiment were two focusing Cerenkov counters which responded only to the pions in the beam, and did not count the other beam particles. One of these was placed upstream of the decay path, and was part of the pion intensity monitor, while the other was the movable detector used to measure the fraction of surviving pions along the decay path. The detectors used either liquid hydrogen or liquid deuterium as the radiating medium. While these liquids were difficult to handle and maintain in a stable condition, the relatively low multiple scattering and nuclear interaction cross sections made them far superior to other radiating media. Because our 285-MeV/c pion momentum was nearly at the peak of the first $J = 3/2$, $I = 3/2$ pion-nucleon resonance, nuclear interaction cross sections would have been large for any radiating medium, but were lowest for liquid hydrogen. Liquid deuterium was actually used for the data running, however, because of the very different cross sections of π^+ and π^- on hydrogen (200 mb for π^+p and 80 mb for π^-p). The π^+d and π^-d cross sections were equal due

charge independence, although larger than that for π^+p.

This experiment grew out of an earlier one at the 184-in. cyclotron, in which the author also participated, and which used the same basic approach to measure the π^+-π^- lifetime ratio.[3] While the earlier experiment provided invaluable experience in the construction and operation of liquid-hydrogen Cerenkov counters, and in many other aspects of the running, it was plagued by serious difficulties which limited the accuracy attainable. The results obtained from this first experiment were $\tau_{\pi^+}/\tau_{\pi^-} = 1.0056 \pm 0.0028$, and $\tau_{\pi^+} = 26.6 \pm 0.2$ nsec. The lifetime ratio differs from unity by two standard deviations, while the absolute lifetime is three standard deviations higher than the currently accepted world average. Both of these effects are now believed to be due to systematic biases which were uncovered and eliminated during the second experiment reported here.

The beam layout for the first experiment is shown in Fig. 1. Since this beam contains no focusing elements except for bending-magnet fringe-field focusing, the pion flux was very low: 35 π^+/sec and 7 π^-/sec. The low pion intensity not only limited the ultimate accuracy to 0.3%, but also made it impossible to investigate systematic errors to even that precision without spending prohibitively long periods of time. By way of contrast, the π^+ flux in the second experiment was 5000/sec, and it was possible to investigate many systematic effects to high precision in a short time.

The movable liquid-hydrogen Cerenkov counter used in the first experiment[7] is shown in Fig. 2. This counter always used liquid hydrogen as the radiating medium, and we now believe that if liquid deuterium had

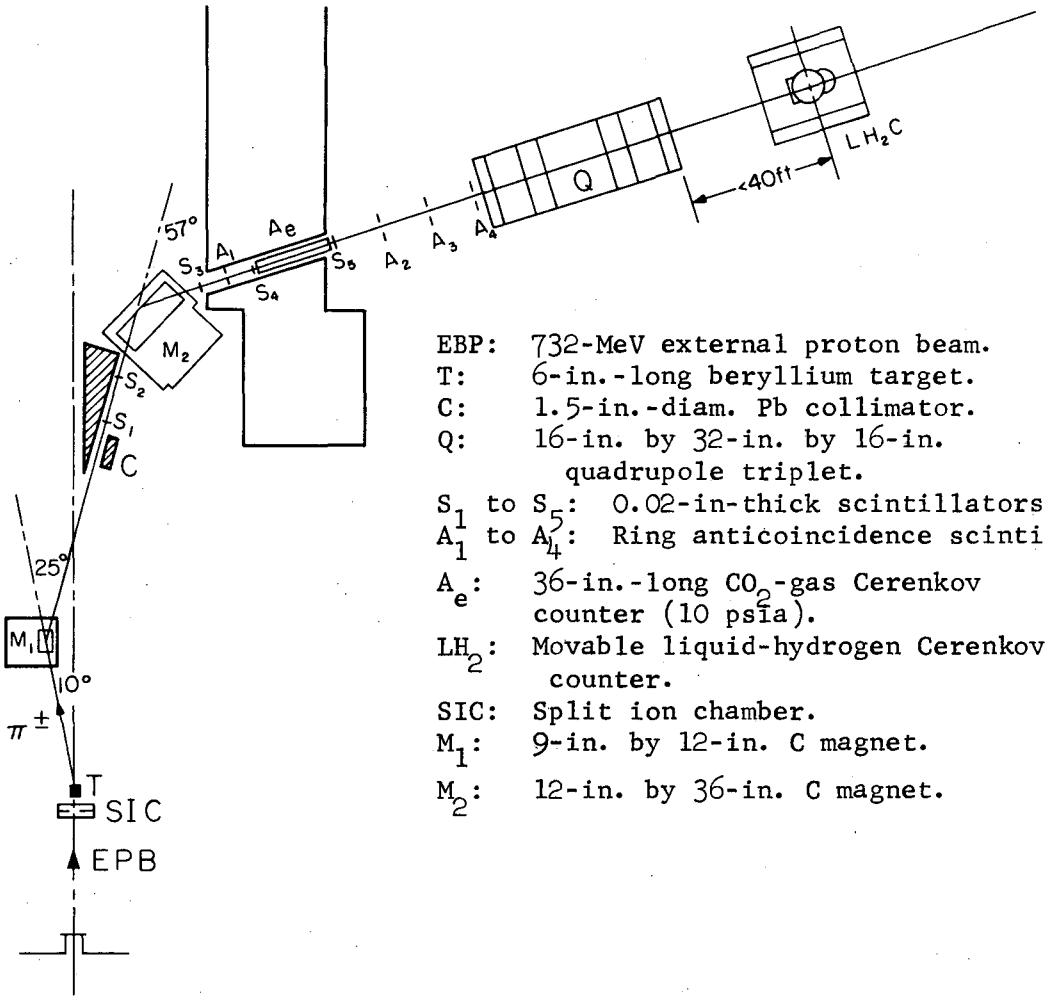

Fig. 1. Experimental arrangement of the first experiment.

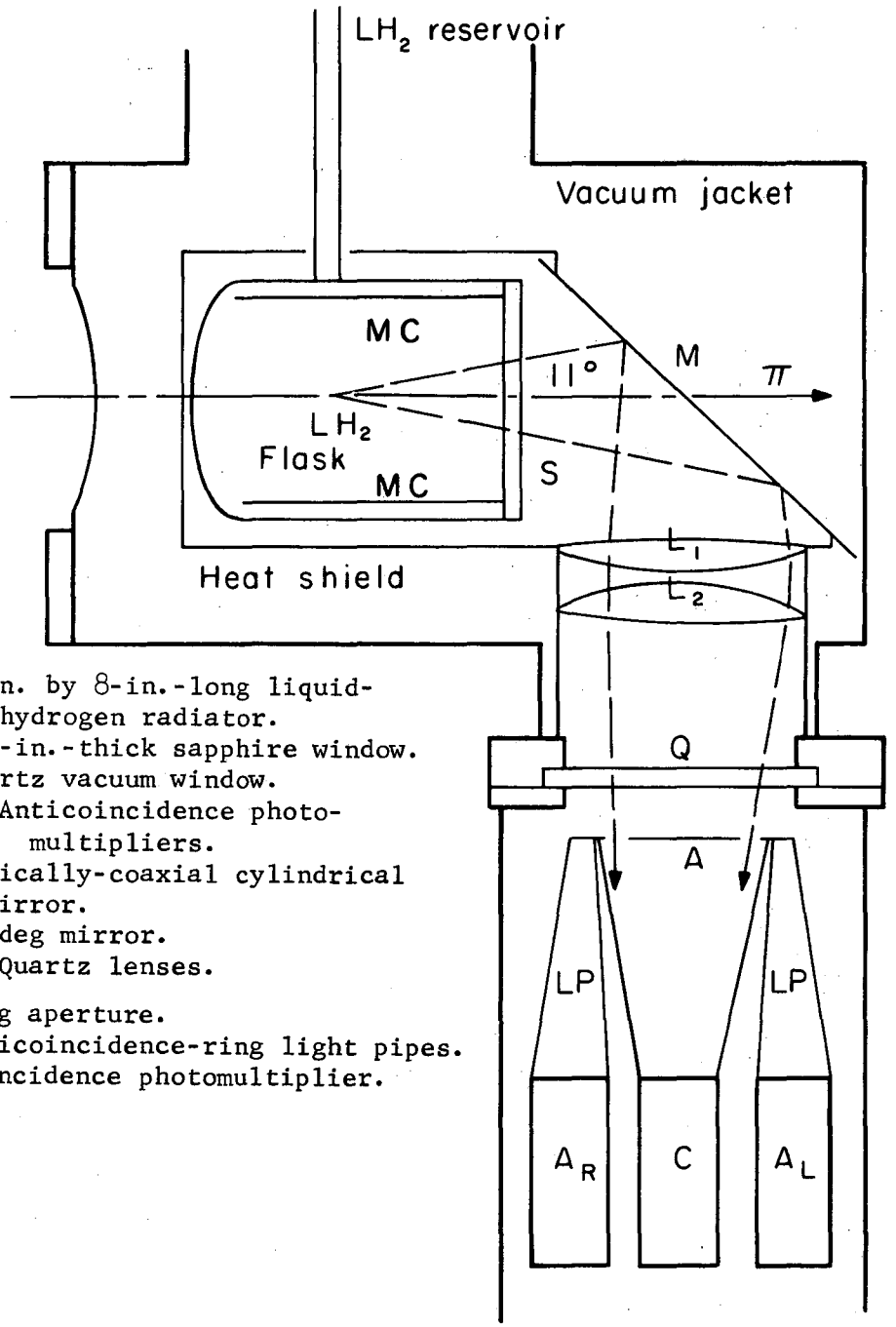

LH_2: 4-in. by 8-in.-long liquid-hydrogen radiator.
S: 1/4-in.-thick sapphire window.
Q: Quartz vacuum window.
A_R, A_L: Anticoincidence photomultipliers.
MC: Optically-coaxial cylindrical mirror.
M: 45-deg mirror.
L_1, L_2: Quartz lenses.
A: Ring aperture.
LP: Anticoincidence-ring light pipes.
C: Coincidence photomultiplier.

MUB-13668-A

Fig. 2. Movable liquid-hydrogen Cerenkov counter used in the first experiment (side view).

been used, the lifetime ratio would have been considerably closer to unity than the number quoted above. Note also that the pion intensity monitor contained no positive identification of pions, while in the second experiment an additional Cerenkov counter was used to identify pions in the monitor.

Notice in Fig. 2 that the flask window S, through which the Cerenkov light left the liquid hydrogen, was actually in the particle beam. The window was originally made of quartz, but Cerenkov light from particles in the window was counted with high efficiency by the central phototube, so this window was replaced by a sapphire one. Becuase of the high index of refraction of the sapphire, the Cerenkov light produced in the window was trapped by total internal reflection, and could not escape into the optical system. Due to flaws in the sapphire, however, some light actually did escape, and the Cerenkov counter detected beam particles with 0.6% efficiency without liquid hydrogen. Both counters used in the second experiment had their optical windows located out of the particle beam, and had counter-empty counting efficiencies of less than 0.01% of their counter-full efficiencies.

In addition to the improvements noted above, the experiment reported here involved completely new counters and electronics. Several of the experimenters who worked on the second experiment had not been involved in the first, and their new points of view contributed significantly to our success. Thus, although the second experiment grew out of the first one, had the benefit of the earlier experience, and was partially motivated by the results of the first experiment, its validity is in no way tied to the first experiment, and it stands as a self-contained, independent investigation.

II. THEORY

A. The Reflection Symmetries

Symmetry laws occupy a central place in high-energy physics today. Ironically their importance has grown in the last 12 years since the discovery that nature was not symmetric under the parity operation, so that today it is of more interest to study the ways in which certain symmetry laws are violated than it is to consider other laws still believed to be exact. This is particularly true of the three reflection symmetries: parity (P), charge conjugation (C), and time reversal (T). Nature was once believed to be symmetric under each of these individually, but there is now conclusive evidence that this is not the case. All that remains is the hope that symmetry under the operation CPT, or under T, will remain exact, while it has already been demonstrated that invariance under P, C, and the product operation CP is only approximate.[8-10]

What is meant by the statement that nature is symmetric under a particular operation? In particle physics the physical meaning is simple: for every reaction observed to occur in nature, the transformed reaction must also be a possible reaction, and must occur with the same probability. The transformed reaction is the result of applying the symmetry operation in question to the observed reaction. For example, the decay of the positive pion, $\pi^+ \rightarrow \mu^+\nu$, is observed to occur with the muon and neutrino both having negative helicity (spin opposite to the direction of motion). Under the charge conjugation operation C, all particles are replaced by their antiparticles, and if nature is symmetric under C we expect the resultant decay $\pi^- \rightarrow \mu^-\bar{\nu}$ to occur in the same way as the π^+ decay. In particular, the muon and anti-neutrino helicities

are still expected to be negative. But in fact the observed decay of the π^- produces both muon and anti-neutrino with positive helicity, so the reaction is not symmetric under C.[9] Speaking loosely, it is often said that C is not conserved in the decay interaction.

In a similar fashion, we can see that this decay also violates parity, for when P operates on the π^+ decay all the helicities are reversed. But the decay is never observed to occur unless the muon and neutrino come out with negative helicities, so the parity-inverted decay is not equally probable, and parity is not conserved. It seems likely, and in fact it is believed to be the case, that pion decay is symmetric under the operation CP (also PC), for CP changes particles into anti-particles and reverses spin directions.

There are other ways of applying symmetry laws. If an isolated system is in an eigenstate of the operation in question (i.e., the operation changes the system into itself, multiplied by a numerical eigenvalue), then it must always remain in an eigenstate with the same eigenvalue regardless of how complicated its internal interactions may be. An example of this sort of application is the decay of the long-lived neutral kaon: $K_L^0 \rightarrow \pi^+\pi^-$. The decay is forbidden by CP invariance if K_L^0 is in an eigenstate of CP which is odd (eigenvalue = -1), while the two pions are always in an even CP state (eigenvalue = +1). This is easily seen since P interchanges the two pions, and C interchanges them again. This CP-violating decay was first seen in 1964.[10] The smallness of the violation is shown by the fact that K_L^0 has a branching ratio of 35% for decay into three pions (CP = -1), but only of 0.5% for the two-pion modes (CP = +1).

Finally, we can view the symmetry laws from a more quantitative point of view: the Hamiltonian describing the interactions of a system

of particles must be literally invariant under the symmetry operation, i.e., it must be transformed into itself by the operation in question. For example, if pion decay is to be invariant under P, then the Hamiltonian describing the interaction cannot contain terms like $\vec{\sigma}_\mu \cdot \vec{p}_\mu$ which are odd (see Table I) under the parity transformation $\left[P(\vec{\sigma}_\mu \cdot \vec{p}_\mu) = (+\vec{\sigma}_\mu) \cdot (-\vec{p}_\mu) = -\vec{\sigma}_\mu \cdot \vec{p}_\mu\right]$. We have already seen that this condition is violated since the decay probability is strongly dependent on the muon helicity.

Until 1957, when it was discovered that the Hamiltonian for the weak interaction was not invariant under P and C, symmetry under these operations had been assumed without solid experimental evidence in all types of interactions.[11] It seemed extremely reasonable that nature should not distinguish between right and left and that particles and antiparticles should enter into reactions in symmetric ways. There was strong experimental evidence for symmetry under parity in the electromagnetic interactions, where transitions forbidden by parity considerations were never observed to occur. It seemed only logical that the strong and the weak interactions should observe the same rules. The fact that particles and antiparticles had equal masses, lifetimes, and magnetic moments was regarded as good evidence of invariance under C, although this requirement is now seen to follow from CPT symmetry. Theoretically however, it was easy to construct Hamiltonians[12] which violated C, P and even T, so it was not difficult to come up with a number of possible mechanisms when C and P violations were actually observed in nature. On the other hand, it had already been noted that it was very difficult to construct Hamiltonians which violated CPT symmetry and at the same time respected more conventional laws like

Table I. Effect of Reflection Operators on Physical Quantities.

	Physical Properties								
Operators	Q	B	S	I_z	$\vec{x}$	$\vec{p}$	$\vec{J}$	$\vec{E}$	$\vec{B}$
C	R	R	R	R	I	I	I	R	R
P	I	I	I	I	R	R	I	R	I
T	I	I	I	I	I	R	R	I	R
CP	R	R	R	R	R	R	I	I	R
CPT	R	R	R	R	R	I	R	I	I

Key

I = property unchanged by operation

R = property undergoes sign change under the operation

Q = electric charge

B = baryon number

S = strangeness

I_z = third component of isotopic spin

$\vec{x}$ = position

$\vec{p}$ = momentum

$\vec{J}$ = angular momentum

$\vec{E}$ = electric field

$\vec{B}$ = magnetic field

like Lorentz invariance and the usual spin-statistics relation.[12-14] These considerations had been made explicit in 1957 by Lüders, who proved the CPT theorem. This theorem proved the invariance of any reasonable field theory under CPT, providing the theory was invariant also under proper Lorentz transformations.

The CPT theorem immediately puts CPT symmetry on a very different foundation from its component operations C, P, T, and CP. It is tied intimately to the ideas of field theory, although not to any one form of field theory, and if CPT is found to be violated anywhere, a complete reworking of the basis of field theory will be required. The observed CP violation in the decay of the neutral kaon implies that either T or CPT is violated in that decay also. CPT is regarded as the more fundamental symmetry, and it is generally assumed that T is violated in such a way as to preserve CPT symmetry in the decay, although no <u>direct</u> evidence of T noninvariance has been found in the neutral kaon system or in any other interaction. Evidence of T violation has been sought in the strong, electromagnetic, and weak interactions by many investigators.[15] The fact that no violation has been seen may only be a consequence of the smallness of the effect (the branching ratio of $K_L^0 \rightarrow \pi^+\pi^-$ is only 0.2%), but it is becoming increasingly relevant to look for possible noninvariance under CPT as well. One of the many consequences of CPT symmetry is the equality of total lifetimes of particle and antiparticle, which provides the motivation for this experiment.

B. The CPT Theorem

There are many ways of "proving" the CPT theorem, depending on the assumptions made about the type of field theory to be shown invariant under CPT. In this section I shall indicate briefly the lines of reasoning used to prove the theorem for the Hamiltonian version of field theory, and list the assumptions involved. Without actually going through the details, I shall outline a proof set forth in Sakurai,[16] which was first given by Lüders in 1957.[17]

The proof consists of two parts: (a) demonstration that a wide class of field theories is invariant under "strong reflection" (defined below), and (b) proof that CPT is equivalent to strong reflection followed by Hermitian conjugation. From this, any reasonable Hamiltonian is seen to be invariant under CPT. The first part of the proof is due to Pauli,[14] and the second to Lüders;[13,17] hence the theorem is often called the Pauli-Lüders theorem.

Strong reflection is defined in the following table, in terms of its effect on the quantities which can be used to construct Hamiltonians: four-vectors, x; scalar fields, $\phi(x)$; vector fields, $A_\mu(x)$; and Dirac fields, $\psi(x)$.

Strong Reflection

(a) $x \to -x$

(b) $\phi(x) \to \phi(-x)$, $\phi^+(x) \to \phi^+(-x)$

(c) $A_\mu(x) \to -A_\mu(-x)$

(d) $\psi(x) \to \gamma_5\, \psi(-x)$; $\bar{\psi}(x) \to -\bar{\psi}(x)\gamma_5$

(e) Reverse the order of factors in operator algebra

It is easily seen that the various commutation relations, which form the basis of field theory, are invariant under strong reflection.

Furthermore it can be shown that Lagrangian and Hamiltonian densities, made up of boson and fermion fields, are invariant under strong reflection providing they are also invariant under proper Lorentz transformations, are properly symmetrized (or antisymmetrized), and are consistent with the normal spin-statistics relation.

Finally, if we examine the properties of $\phi(x)$, $A_\mu(x)$, $\psi(x)$, ∂_μ, and c-numbers under the operation of strong reflection followed by Hermitian conjugation, we get the same result for each of these quantities as we get by applying sequentially C, P, and T in any order. The last result holds providing we choose the arbitrary difference between phases for the eigenvalues of C, P, and T in the proper way. Thus the CPT theorem is proved for all reasonable field theories using the Hamiltonian formalism. The assumptions made are:

(a) Invariance of the Hamiltonian under proper orthochronous Lorentz transformations (i.e., <u>not</u> involving space or time inversions).

(b) Local interaction densities, constructed only of field operators and their derivatives (of finite order).

(c) The usual spin-statistics relation.

(d) Interaction densities properly symmetrized or antisymmetrized.

(e) Hermitian interaction densities.

Outside the frame work of Hamiltonian field theory, it is possible to prove that the CPT theorem is equivalent to the assumption of <u>weak local commutativity</u>, often called microcausality, for any Lorentz-invariant theory.[18] Simply stated, the assumption means that two events are not allowed to influence each other if they are separated by space-like distances, i.e., if they cannot be connected by a light signal.

In fact, if CPT invariance should break down in nature, it seems most likely that the root of the trouble would have to be in either the assumption of microcausality (i.e., causality might break down at very small distances) or the assumption of locality (that the interaction of the two fields can be represented by an integration over all possible point interactions). The physical mechanism by which such a breakdown of quantum mechanics at small distances might occur is not at all clear, however, and so far has not suggested any logical places to look for CPT violations.

C. Consequences of the CPT Theorem

If the CPT operation is applied to an isolated system of particles, the following changes are induced:

(a) particles are changed to antiparticles,

(b) momenta are unchanged,

(c) all spins are reversed,

(d) all matrix elements are replaced by their complex conjugates.

This can be verified by referring to Table I, where the effect of the reflection operators is shown for various physical quantities. The complex conjugation of matrix elements comes from the T operation which involves complex conjugation (and is thus neither linear or unitary).

If CPT is applied to an isolated particle, its only effect is to replace the particle by its antiparticle with reversed spin (the latter change has no consequence in the rest system of the particle). For this reason, it is possible to define the particle-antiparticle relationship using the CPT operator rather than C alone: $CPT|\text{particle}> = |\text{antiparticle}>$. From this it follows directly that particle and antiparticle have equal masses, equal and opposite charges and magnetic moments, and equal total lifetimes. It is of course this last consequence which is of most concern to us here. Although the equality of lifetimes can be proved without recourse to a perturbation expansion in the interaction Hamiltonian,[19] it is more instructive to consider the proof to first order in the weak Hamiltonian H_w.[20] We assume that the decay interaction is weak and that H_w commutes with CPT by the CPT theorem.

Consider the decay of particle A into decay products B, $A \rightarrow B$, and the corresponding decay $\bar{A} \rightarrow \bar{B}$, where $|\bar{A}> \equiv C|A>$ and $|\bar{B}> \equiv C|B>$. Since the decay is to be represented by the matrix element $<B|H_w|A>$,

the state of B must be understood to represent an <u>entire set</u> (or several sets) of decay channels which communicate with each other via possible final-state interactions. This is because H_w contains no information about the final-state interactions, and thus the matrix element above cannot possibly describe transitions into only one channel of a number of channels communicating via strong final-state interactions.

The operator T represents Wigner time reversal and can be written $T = UK$, where U is a unitary operator and K is complex conjugation.[16] Since T also reverses spins, $T|A(m)> = |A(-m)>^*$ where m denotes the spin of A. The decay rate of $A \to B$ can be written

$$1/\tau \propto \sum_m |< B(m)|H_w|A(m)>|^2 .$$

Hence, to prove that the rate of $A \to B$ is the same as the rate $\bar{A} \to \bar{B}$ we need to show that:

$$\sum_m |< B(m)|H_w|A|(m)>|^2 = \sum_m |< \bar{B}(m)|H_w|\bar{A}(m)>|^2 .$$

Now, let $H_w = H_+ + H_-$ where $PH_\pm P^{-1} = \pm H_\pm$. Then we can write:

$$< B(m)|H_\pm|A(m)>^* = < B(m)|T^{-1}TH_\pm T^{-1}T|A(m)>^*$$

$$= < B(-m)|UH_\pm U^{-1}|A(-m)>,$$

where we have used

$$T = UK \text{ and } H_\pm^* = H_\pm .$$

But, by the CPT theorem,

$$PCT\, H_\pm T^{-1}C^{-1}P^{-1} = H_\pm$$

so

$$T\, H_\pm T^{-1} = C^{-1}P^{-1}H_\pm PC = U\, H_\pm\, U^{-1} .$$

Thus,

$$< B(m)|H_{\pm}|A(m) >^{*} = < B(-m)|C^{-1}P^{-1}H_{\pm}PC|A(-m) >$$

$$= \pm < \bar{B}(-m)|H_{\pm}|\bar{A}(-m) > .$$

Hence,

$$| < B(m)|H_{\pm}|A(m) >|^2 = | < \bar{B}(-m)|H_{\pm}|\bar{A}(-m) >|^2.$$

But

$$1/\tau \propto \sum_m | < B(m)|H_+ + H_-|A(m) >|^2$$

$$= \sum_m \left[|< B(m)|H_+|A(m) >|^2 + |< B(m)|H_-|A(m) >|^2 \right]$$

$$= \sum_m \left[| < \bar{B}(-m)|H_+|\bar{A}(-m) >|^2 + | < \bar{B}(-m)|H_-|\bar{A}(-m) >|^2 \right] ,$$

where the cross terms in H_+H_- must be zero, since they are pseudoscalar and τ must be scalar. Thus we have shown

$$\sum_m | < B(m)|H_w|A(m) >|^2 = \sum_m | < \bar{B}(-m)|H_w|\bar{A}(-m) >|^2,$$

and since the sum over spins includes both +m and -m, $\bar{\tau} = \tau$.

The state B may include any or all of the possible final states available to the decay, with the condition that it must not include only part of a set of states connected by final-state interactions. If one such state is included, all other communicating states must also be included. Thus, if there are no final-state interactions, the CPT theorem guarantees equality of the <u>partial</u> lifetimes, into each individual channel. However, if there are final-state interactions then the CPT theorem requires only that the total decay rates into whole sets of channels, connected by final-state interactions, are equal for particle and antiparticle. Of course it always guarantees that the <u>total</u> decay rates into all channels are equal.

As an example, consider the decays of the charged kaons, K^+ and K^-, which are particle and antiparticle. The CPT theorem requires:

(a) the total decay rates of K^+ into all modes = total decay rate for K^-.

(b) $K^+ \to \mu^+\nu$ and $K^- \to \mu^-\nu$ occur at the same rate (no final-state interactions).

(c) Rate $(K^+ \to \pi^+\pi^-\pi^+)$ + Rate $(K^+ \to \pi^+\pi^0\pi^0)$ = Rate $(K^- \to \pi^-\pi^-\pi^+)$ + Rate $(K^- \to \pi^-\pi^0\pi^0)$,

since these two final states are connected by strong interactions.

D. Experimental Checks on CPT Invariance

In recent years a number of experiments have been performed to check the predictions of the CPT theorem, usually by measuring corresponding properties for particle and antiparticle. Some of these are listed below for reference.

$m(\pi^+)/m(\pi^-) = 1.00014 \pm 0.00036$	Barkas (1965)[21]
$m(\bar{p})/m(p) = 1.008 \pm 0.005$	Cocconi et al. (1960)[22]
$m(e^-)/m(e^+) = 1.000101 \pm 0.000185$	Muller et al. (1952)[23]
$m(K^o) - m(\bar{K}^o) \leq 2 \times 10^{-16}\, m(K^o)$	from $K_L^0 - K_S^0$ mass difference[24]

The first two mass equalities check invariance of the strong interaction Hamiltonian, which is responsible for masses to first order. The equality of electron masses is consistent with invariance of the electromagnetic interaction under CPT, and the comparison of neutral kaon masses is approaching the level of checking invariance of the weak interaction Hamiltonian, and is certainly consistent with invariance of the strong interaction Hamiltonian under CPT to a very high accuracy.

There are also several comparisons of particle-antiparticle lifetimes which check the invariance of the weak interaction Hamiltonian under CPT:

$\tau(\mu^+)/\tau(\mu^-) = 1.000 \pm 0.001$	Meyer et al. (1963)[25]
$\tau(K^+)/\tau(K^-) = 0.99910 \pm 0.00078$	Lobkowicz et al. (1966)[2]
$\tau(\pi^+)/\tau(\pi^-) = 1.00055 \pm 0.00071$	This experiment (1968)[5]

The predicted equality of the gyromagnetic ratios of electrons and positrons and of positive and negative muons has been checked with the results:

$1/2(g_{e^+} - g_{e^-}) = (1.5 \pm 2)\alpha^2/\pi^2$	Rich and Crane (1966)[26]

$1/2(g_{\mu^+} - g_{\mu^-}) = (-0.09 \pm 0.19)\alpha^2/\pi^2$ Williams et al. (1968)[27]

This list of experimental results is not intended to be exhaustive, but only to give an idea of the most accurate tests of CPT invariance available at this time.

It should be noted that all checks of equality of total lifetimes have a common fault: they do not check the full content of CPT invariance,[28] but rather involve averages over various spins and final states. As stated at the outset, the CPT operation involves changing particle to antiparticle, reversing spins, and complex conjugating matrix elements. Each of these operations could, in principle at least, be checked against the detailed kinematics of various decays via H_{weak}, as part of a complete program to look for CPT violations. Unfortunately, one of the most important aspects of such a program would be a study of the polarization of decay products, which in most cases would be nearly impossible to do with any precision. There are several notable exceptions however.

As an example of a more detailed use of CPT invariance, consider the $K_{\mu 3}$ decays:

$$K^+ \rightarrow \pi^o \mu^+ \nu$$

$$K^- \rightarrow \pi^o \mu^- \bar{\nu}.$$

Since there are no strong final state interactions, CPT invariance requires these partial decay rates to be equal. But it also places a more stringent condition on the muon spin directions which can be checked experimentally, using the electron angular distribution asymmetry in muon decay as a convenient indicator of the muon polarization. The CPT operation transforms the $K^+_{\mu 3}$ decay into the $K^-_{\mu 3}$ decay and at the same time reverses the muon spin direction. Thus, if the muon were to be

polarized in the $K^+_{\mu 3}$ decay, an equal and opposite polarization must exist in the $K^-_{\mu 3}$ decay. Such a polarization could be detected by observing the angular distribution of the electrons from the subsequent $\mu^{\pm}$ decays. (e^+ tend to be emitted with positive helicity, and hence preferentially in the direction of the μ^+ spin, while e^- tend to come off opposite the direction of the μ^- spin.)

This example is unfortunately complicated by time-reversal invariance, which controls the muon polarization perpendicular to the $\pi^o\mu$ plane. Such polarization would be present only if a term proportional to $\vec{\sigma}_\mu \cdot (\vec{p}_\mu \times \vec{p}_{\pi^o})$ were present in the decay Hamiltonian. But such a term is odd under time-reversal, since $\vec{\sigma}_\mu$, $\vec{p}_\mu$, and $\vec{p}_{\pi^o}$ all change sign under T. Thus, if the Hamiltonian is invariant under T, there can be no muon polarization perpendicular to the $\pi^o\mu$ plane, eliminating the sort of CPT-violating asymmetry which would be easiest to detect experimentally. It has already been observed that such polarization in K^+ decay is $\leq 10\%$, as a check on time-reversal invariance.[29]

E. The Pion Decay Interaction

This experiment has shown that any difference in the π^+ and π^- lifetimes is less than 0.07%, and it is important to make explicit the implications of this result for CPT invariance. In particular, it should be pointed out that CPT is a sufficient, but not necessary condition for the equality of lifetimes of particle and antiparticle. That is, our null result does not "prove" that the pion decay Hamiltonian is invariant under CPT, since there are other ways that the lifetimes could be equal even if CPT were violated in the decay. For instance, CP invariance also requires equal lifetimes (as does C invariance, but we already know that C is not conserved in the decay[9]). Of course, if a lifetime difference had been observed, it would have been direct evidence for the violation of both CPT and CP.

It is interesting to speculate what such a violation might mean in physical terms. An absolute distinction between π^+ and π^-, in terms of one being long-lived and the other short-lived, allows us to define positive charge and negative charge in absolute terms (e.g., positive electrical charge is associated with the long lived pion). This in turn allows us to define matter and antimatter in absolute terms (e.g. protons have the same charge as the long-lived pion; antiprotons have the opposite charge), and also to define right and left in an absolute sense (e.g., through helicity of the polarized muons from pion decay). The ability to make such distinctions in absolute terms would destroy the fundamental symmetry between matter and antimatter which is now believed to prevail in the universe.

Even if we do take the equality of lifetimes of the charged pions as an indication of the smallness of a possible CPT violation, it should

be kept in mind that this limit applies only to the part of the weak interaction Hamiltonian describing pion decay. In particular, the result says nothing at all about the strangeness-changing part of the weak interaction Hamiltonian, which operates for instance in kaon decay. Because the interaction responsible for pion decay is quite well understood, it is possible to be even more explicit about the nature of the interaction involved.

Pion decay can be described to lowest order by the diagrams:

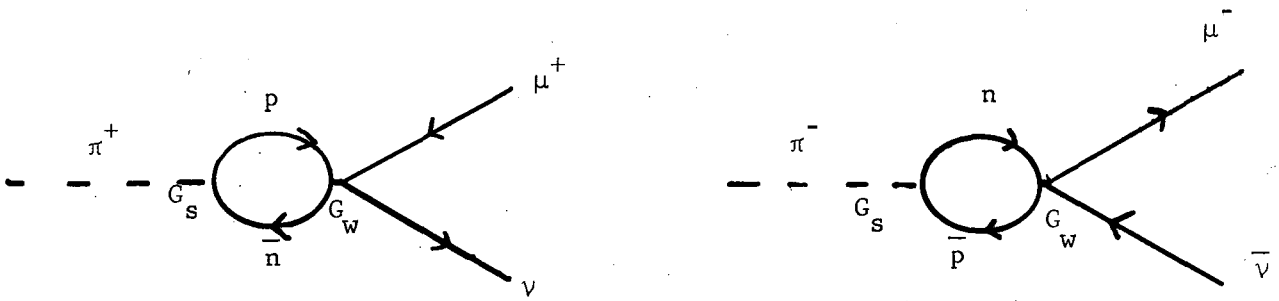

Thus, the pion can dissociate into a virtual nucleon-antinucleon pair, via its strong interactions, at the vertex labelled G_s. According to the diagrams, decay can only take place when the nucleon-antinucleon annihilate at a four-fermion vertex, labelled G_w. This vertex is described accurately by the standard V-A theory of weak interactions, and is exactly the same as the interaction responsible for μ capture: $\mu^- p \rightarrow n\nu$.

Evidence for the correctness of this picture comes from several sources:

(a) The observed polarization of the muon agrees with that predicted by V-A theory and the two-component theory of the neutrino.[30]

(b) The branching ratio $\frac{\pi \rightarrow e\nu}{\pi \rightarrow \mu\nu} = 1.2 \times 10^{-4}$ experimentally.[31] The G_s vertex is the same in both decays, and the four-fermion vertex as described by V-A theory gives the observed branching ratio. (On the

basis of phase space alone, the branching ratio should be about 3.3!)

(c) The fact that the diagram drawn is dominant in the decay is strikingly confirmed by the dispersion-relation calculation of Goldberger and Treiman,[32] who used the axial-vector coupling constant from beta decay, the pion-nucleon coupling constant from scattering experiments, and only the intermediate nucleon-antinucleon state shown in the diagram, to calculate correctly the absolute value of the pion lifetime to within a few percent.

III. EXPERIMENTAL METHOD

A. The Beam

The beam layout is shown in Fig. 3, and a photograph of the decay path in Fig. 4. Beryllium was used for the pion-production target to maximize the π^- flux. Because the target was 73 ft from the cyclotron itself, the proton beam was kept under vacuum and was refocused on the beryllium target by two quadrupole doublets (not shown on the drawing). The proton beam cross section was roughly 2.5-in. wide by 1-in. high at the target. The entire secondary beam system was set up as far downstream in the external proton beam as feasible, in order that the cyclotron fringe field be as small as possible along the beam line. This nearly-vertical field was thus kept to less than 3 gauss along the pion beam line, and was further reduced to less than 0.2 gauss by wrapping the beam vacuum pipe with six layers of thin transformer steel.[33] The entire beam path was magnetically shielded in this way, from the production target to the movable liquid-deuterium Cerenkov counter, CP.

The proton-beam position at the target tended to wander horizontally, and this in turn changed the electron contamination of the pion beam (by varying the amount of material available for pair production from π^0-produced gamma rays). In order to keep the electron fraction constant, the proton-beam position at the beryllium target was monitored by a split ion chamber (not shown in Fig. 3) which allowed the proton-beam position to be held constant within 1 mm during the running. The proton-beam intensity was measured by a secondary-emission monitor (not shown in Fig. 3) which was placed in the proton beam about 3-ft downstream of the beryllium target. Both the beam position and intensity were read out on strip-chart recorders in the counting house and monitored visually during

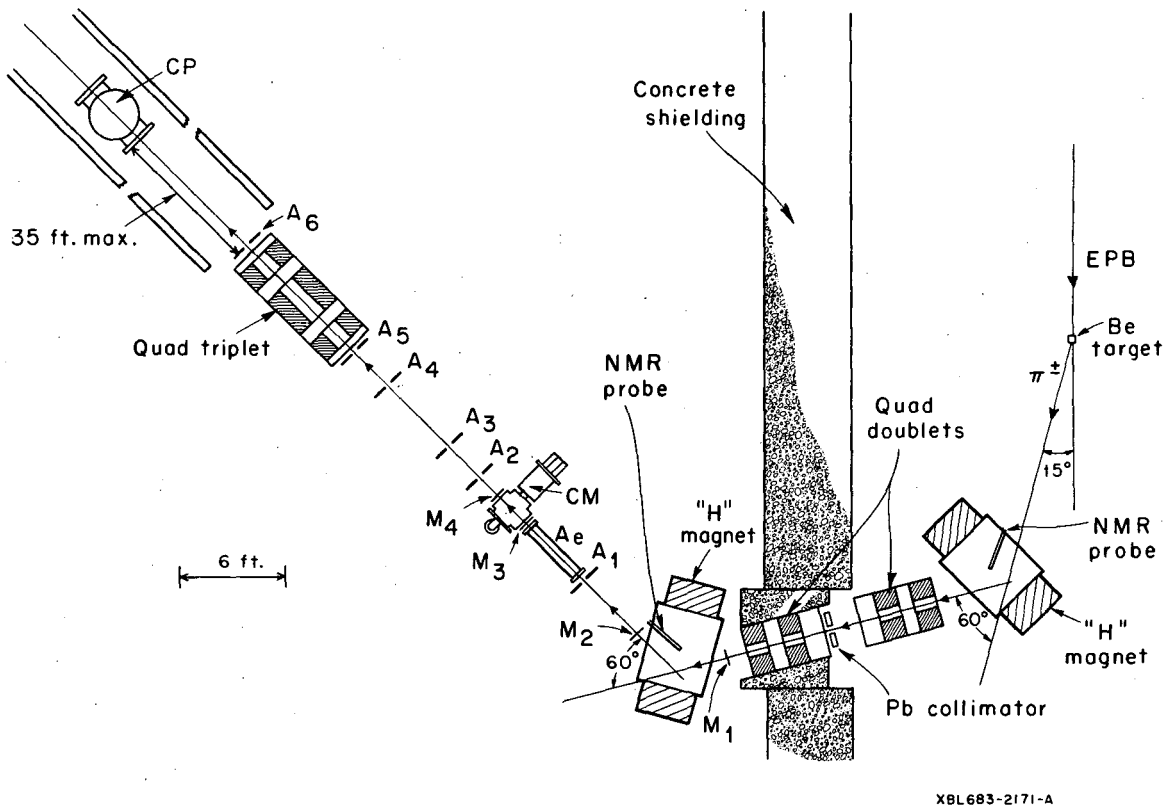

Fig. 3. Beam layout for this experiment.

EPB: 732-MeV external proton beam of the 184-in. cyclotron.
Be target: beryllium target, 2-in. wide by 1.75-in. high as viewed from the pion beam.
NMR probes: nuclear magnetic resonance probes.
In order of occurrence, the quadrupole-doublet sections have the following focusing properties in the horizontal plane: diverging, converging, converging, diverging.
M_1 to M_4: Thin scintillation counters.
A_1 to A_6: Scintillation anticoincidence counters.
A_e: Electron veto counter.
CM and CP: Focusing liquid-deuterium Cerenkov counters.

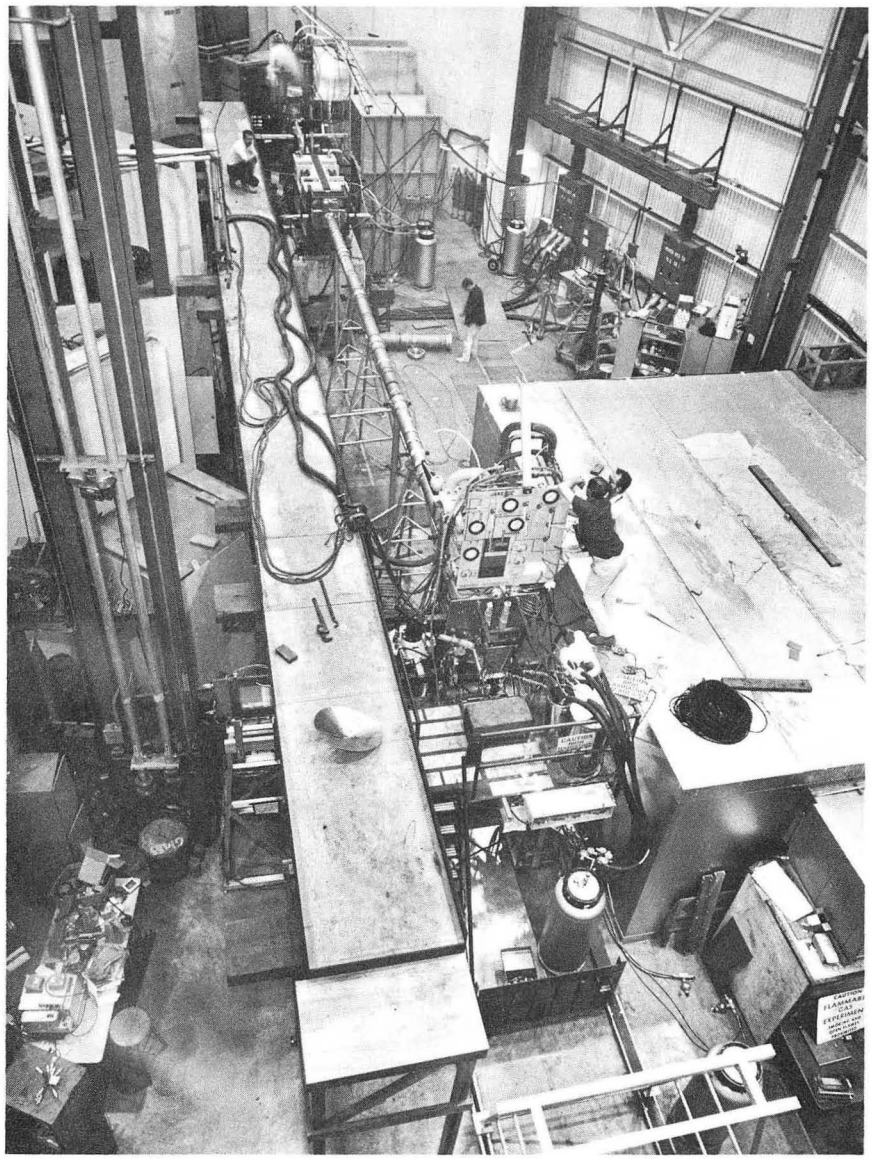

CBB 679-5660

Fig. 4. Photograph of the experimental set-up. The second H magnet is at the very top of the picture, followed by CM (under the white liquid-nitrogen exhaust), and the quadrupole triplet. In the center of the picture is the vacuum pipe leading to the movable counter CP. The two technicians working on CP are standing on top of the counting house. The long elevated ramp to the left of the beam path carries the vent lines from CP.

the running, corrections being made as necessary.

Pions produced at 15 deg were momentum analyzed and brought to an image at the 2-in.-thick lead collimator, which defined the beam momentum acceptance. Horizontal and vertical magnifications were each 0.40 at the collimator, and the dispersion was $\Delta p/p = 1.1\%$/inch. These were the design values predicted by the beam analysis program OPTIK,[34] and were verified experimentally by "wire orbiting"[35] before the start of the running. The pion beam was symmetric about the collimator, and so a second, dispersionless image of the production target was formed at counter M_4. The horizontal and vertical magnifications at this point were unity, and the lead collimator aperture was chosen to give $\Delta p/p = \pm 0.5\%$ (half-width-half-maximum). Finally, the 12-in.-diameter quadrupole triplet brought the particles diverging from M_4 to a focus 35-ft downstream from the quadrupole exit, with horizontal and vertical magnifications of about three.

Before the actual running began, wire-orbit[35] measurements were made on the magnet system in three sections: beryllium target to collimator, collimator to M_4, and M_4 to the end of the decay path. For the first two sections these measurements were made at six different momenta between 240 and 550 MeV/c, while the final triplet (which was run very weakly, far from saturation) was done only at 320 and 360 MeV/c (the momentum used during the running was about 300 MeV/c). The results verified that the beam was magnetically symmetric about the collimator and gave us experimental values of the magnet currents needed to produce images at the desired positions. The magnet settings found from the wire orbit work were different from the values predicted by OPTIK by as much as 15%, due to the fringe-field focusing of the bending magnets, which was not

properly estimated by the program for the large bending angles used. The wire orbiting also showed that the magnet currents could be scaled linearly with momentum up to about 450 MeV/c (where saturation effects started to set in), a fact which was used frequently during later beam tuning.

The wire-orbit measurements provided only a starting point for the beam tuning, which was completed after the magnets and vacuum system were fully assembled from the beryllium target to A_6. Final optimization was done using the coincidences $M_1M_2M_3M_4\bar{A}_1\bar{A}_e\ CM\overline{CMA}\ \bar{A}_2\bar{A}_3\bar{A}_4\bar{A}_5\bar{A}_6$ as a monitor of pion flux and the integrated secondary emission monitor current as a measure of the number of incident protons. Each magnet current was changed through a range of currents about the wire-orbit value, while the other magnet currents were held fixed. The current was finally set at the value which gave the maximum number of pions per incident proton, and the next magnet in the system varied in a similar fashion. The first bending magnet was not varied, but was set at its wire-orbit current which served to define the momentum for the rest of the beam. The current in the second bending magnet was optimized first in order to steer the beam properly through the counter telescope. Then the current in each of the four quadrupole-doublet sections was optimized proceeding downstream in order. Since the current in a particular quadrupole section which produced maximum pion flux depended on the currents in the other three quadrupoles, this process of successive optimization was repeated cyclically until it converged on a set of self-consistent currents for maximum pion flux. About six cycles were required before the final solution was reached, with a net increase in flux of about 30%.

The final magnet currents were considerably different from the wire-

orbit values: the first two quadrupole sections had to be lowered by 15% and 30% respectively, but the doublet after the collimator remained within 1% of the wire-orbit settings. The large changes in the first doublet were of some concern at first, until it was realized that the position along the beam line of the image at the collimator was quite insensitive to the quadrupole currents, and the new values corresponded to moving the image position less than 3 in. Furthermore, the focusing studies done during wire-orbiting did not take into account the finite size of the collimator. Later studies of the spatial properties and the momentum distribution of the pion beam revealed that the end result of the beam tuning was indistinguishable from the beam predicted by OPTIK.

The pion beam travelled in vacuum where possible, although M_1, M_2, M_3 and M_4 could not be included in the vacuum system for reasons of safety: in the event of an accidentally broken vacuum window, tests showed that these thin counters would have shattered and become sharp projectiles capable of breaking many other windows in the system. For this reason, all four counters were in air, separated from the vacuum by a 0.005-in. Mylar window on either side. The anticoincidence counters, A_1 to A_6, were designed to veto particles which had scattered upstream, and consisted of a thick sheet of scintillator, 8-in. square, with the beam passing through a central hole (see Table II). These counters were mounted inside the vacuum system, and had no wrappings around the hole edges, so that any particle which scattered in them also produced enough light to veto itself. The counters A_2 to A_6 were particularly important in eliminating particles which scattered in M_4, and they also served to define the unscattered beam going into the quadrupole triplet, insuring

Table II. Dimensions of counters.

M_1:	1/16-in. thick by 3.5-in. wide by 5.75-in. high (rectangular).
M_2:	3/32-in. thick by 4.0-in. wide by 5.75-in. high (rectangular).
M_3:	1/16-in. thick, 3.0-in. diameter (circular).
M_4:	1/16-in. thick, 4.0-in. diameter (circular).
A_1:	4.75-in.-diam. circular hole in 1/2-in.-thick, 8-in.-square. scintillator.
A_2:	2.36-in-diam. circular hole in 1/2-in.-thick, 8-in. square. scintillator.
A_3:	2-in.-diam. circular hole in 1/4-in.-thick, 8-in.-square. scintillator.*
A_4:	5-in.-diam. circular hole in 1/2-in.-thick, 8-in.-square. scintillator.
A_5:	4.5-in.-diam. circular hole in 1/4-in.-thick, 8-in.-square. scintillator.*
A_6:	4.5-in.-diam. circular hole in 1/4-in.-thick, 8-in.-square. scintillator.*
A_e:	5-in.-diam. circular aperture (inner diameter of cylindrical. mirror).
CM:	4-in.-diam, circular aperture (inner diameter of cylindrical mirror).
CP:	7-in.-diam. circular aperture (inner diameter of cylindrical mirror).

*A_3, A_5, and A_6 were each viewed from opposite sides by two 56-AVP photomultipliers. Other counters were viewed by a single photomultiplier each.

that the beam was contained within a 5.5-in.-diameter envelope along the decay path. Thus, there was continuous vacuum from M_4 to CP, and it was impossible for particles to scatter without producing light in one of the anticoincidence counters. The final veto counter, A_6, also served to veto the very small number of large-angle decay muons which were focused by the quadrupole triplet and emerged roughly parallel to the axis but more than 2.25-in. from the axis. The most important veto counters were A_3, A_5, and A_6, since they were responsible for vetoing 75% of the unscattered pion beam. These were made of thinner scintillator (to present less edge surface area to the beam) and were each viewed by two photomultiplier tubes, one on either side of the hole. The dimensions of all counters are tabulated in Table II.

M_1, M_2, M_3, and M_4 were the principle elements of the counter telescope, and were kept as thin as possible to minimize absorption and scattering. The effects of absorption were of particular concern because of the very different cross sections for nuclear scattering of π^+ and π^- at the 3-3 resonance. The dimensions of the M counters are given in Table II. Their shapes were chosen from the beam envelope predicted by OPTIK, and particles which did not pass through one of the M counters had presumably been scattered somewhere upstream. A "good" beam particle was one which counted in all four M counters, and not in any of the veto counters, A_1 to A_6.

The counter telescope described above defines the particle beam, but does not distinguish between the different types of particles in the beam. Because these particles have the same momentum, but different masses, they will have different velocities, and we used this fact to distinguish the pions from the other beam components. A_e was a 36-in.-

long, 45-psia threshold Cerenkov counter, which responded only to electrons in the beam, all other particles having velocities well below threshold. We were particularly concerned about the electrons for several reasons: typically, they accounted for 35% of the negative beam, but only 7% of the positive beam, and they produced so much light in the movable Cerenkov counter that they counted with up to 7% efficiency. For these reasons they were the potential source of a large, systematic bias, and it was important that they be identified and vetoed with high efficiency in the monitor counters. A_e was shown to have an efficiency of 99.3% $\pm$ 0.1% by identifying electrons independently by their time-of-flight to the end of the decay path, where they arrived 8 nsec sooner than pions. Since the monitor Cerenkov counter detected electrons with only 1% efficiency (when filled with deuterium), the overall efficiency of the pion monitor for counting electrons was 0.007%. The construction of A_e is shown in Fig. 5. The only material in the beam were the 0.007-in. vacuum windows, the 0.001-in. aluminized Mylar plane mirror, and the CO_2 gas itself. The cylindrical mirror and the conical mirror were lacquer-dipped and vacuum plated with aluminum, and had excellent reflectivity in the visible and ultraviolet regions. The quartz optical window and the quartz-faced photomultiplier both improved the performance of the counter by transmitting the strong ultraviolet components of the Cerenkov light. This light was nearly parallel to the axis, and so was collected with high efficiency by the conical mirror. The cylindrical mirror was needed only for those particles travelling far from the axis.

The most effective particle selection was done by the monitor Cerenkov counter CM. Like CP, this counter was designed to respond only to particles (in this case pions) with velocity $\beta = 0.920 \pm 0.005$,

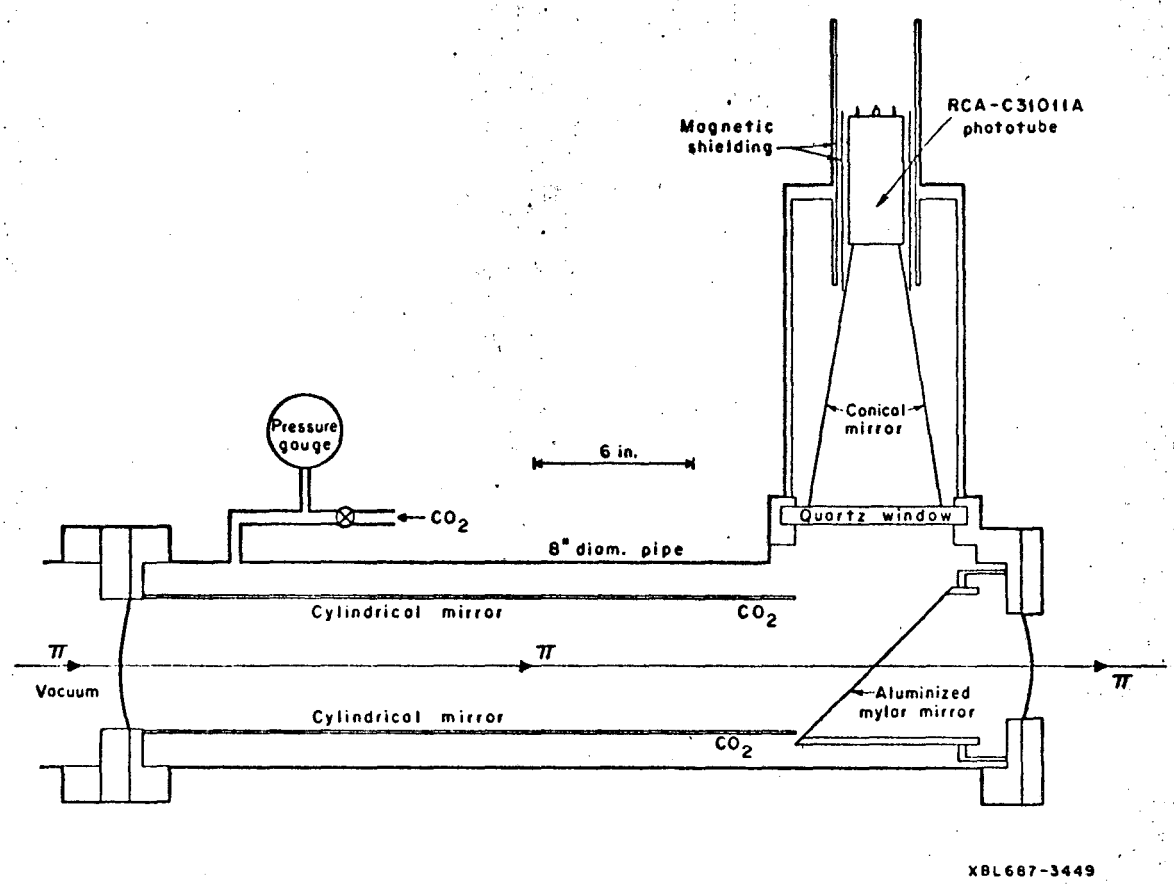

Fig. 5. Electron veto counter A_e (side view). All dimensions are roughly to scale except for the 36-in. length of cylindrical mirror, which has been shortened for compactness of the drawing.

travelling parallel to the axis. The operation of this counter will be described in more detail in the next section. For the moment, it is sufficient to note that CM had an efficiency of greater than 99% for pions, and less than 1% for electrons (as determined from A_e-CM coincidences). Thus it improved the rejection of electrons by two orders of magnitude. It did not respond to momentum-analyzed "beam" muons ($\beta = 0.95$) produced by pion decays upstream of the first bending magnet (as distinct from "decay" muons from pion decay after the second bending magnet). The beam muons constituted 10% of the positive and 8% of the negative beam, after the electrons were vetoed. Beam muons counted in CM with less than 0.1% efficiency. The net efficiencies of the system of monitor counters for pions, muons, and electrons is discussed in detail in the section on electronics.

Protons constituted a potentially dangerous component of the positive beam, which had no counterpart in the negative beam. The apparatus discriminated against these particles in many ways, however. Although the absolute proton flux was comparable to the positive pion flux, the protons lost a much larger fraction of their energy in M_1 due to their lower velocity ($\beta = 0.32$), and so were bent more strongly by the second bending magnet, reducing their flux to about 10% of the pion flux at M_3. The time-of-flight difference between pions and protons from M_1 to M_4 was 36 nsec, so the protons were eliminated by the coincidence requirement on the pions. Finally, all of the protons were physically stopped in the first inch of liquid deuterium in CM, and produced no counts in CM. The only real effect of the protons was to make the singles rates in counters M_1 and M_2 twice as high on positives as on negatives (for the same pion rates) and this was not a serious problem with many

other counters in the coincidence.

One final important asymmetry between the π^+ and π^- beams remains, and this is the fact that the production cross section of π^+ is five times that of π^- for 732-MeV protons on beryllium (which was chosen for maximum π^- production). For this reason, the proton beam level was reduced to 20% of full intensity during data taking on positive particles, while negative-particle data was taken with full beam intensity. A number of systematic effects were nevertheless investigated using the full positive beam, for instance measurement of the lateral and vertical uniformity of response of the movable Cerenkov counter. All important checks had to be done eventually on both polarities, but much preliminary study was done using only the high-intensity positive beam. This procedure was particularly useful since the positive beam was more likely to be affected by nuclear interactions than the negative, and was therefore the logical place to look first for certain systematic effects.

B. The Liquid-Deuterium Cerenkov Counters, CM and CP

1. Choice of the Cerenkov Medium

One of the first questions which is often raised about this experiment concerns our use of liquid hydrogen and deuterium as the radiating media in the Cerenkov counters. These substances are difficult to handle under the best of conditions, and our requirements of internal reflective optics and large optical windows only adds to the problems. Although the counters we utilized are certainly not a unique solution to the problems faced in the design of the experiment, it is instructive to retrace the lines of reasoning that led to the decision to use them.

In a highly precise experiment of this type, it is necessary to understand completely the nature of the beam, the operation of the counters, and to track down and eliminate the many possible sources of systematic bias which are bound to appear in any experiment at the 0.1% level. For this reason the decision was made to perform the experiment at the 184-in. cyclotron. At the Bevatron, the pressures to do a fast experiment were much greater. The decision to use focusing liquid-hydrogen Cerenkov counters of the type finally employed was based on the experience of Dr. David O. Caldwell, one of the initial proponents of the first experiment and an active participant in both experiments. Dr. Caldwell had been impressed with the performance of a Cerenkov counter which he helped develop at M. I. T. using the same optical system as our counters, but with a high pressure gas as the radiating medium.[36] The excellent velocity resolution of this type of counter made it ideal for the lifetime-comparison experiment.

The most stringent requirement on our counter was that it be able to distinguish clearly between pions and their decay products (muons).

The Cerenkov light emitted by a particle moving with velocity β in a material medium of index of refraction n is produced at an angle θ to the direction of motion, and these quantities are related by

$$\cos\theta = 1/n\beta.$$

In order to find the velocity resolution, we differentiate this expression and find

$$d\beta/\beta = \tan\theta\, d\theta.$$

Thus, for the fixed velocity difference $d\beta$ between pions and decay muons, we desire the largest possible $d\theta$, and therefore small values of θ. These considerations must be balanced against the fact that the intensity of the Cerenkov light is proportional to $\sin^2\theta$, and hence goes to zero at small angles.[37] The desire to operate at a momentum near the maximum for pion production at the cyclotron, and the requirement of small Cerenkov angle leads to a pion velocity $\beta = 0.92$, and an index of refraction $n = 1.1$, corresponding to a Cerenkov angle of 11 deg. Such an index is obtainable from a high pressure gas maintained near its critical point,[36] or from a substance like liquid hydrogen. The latter substance minimizes multiple Coulomb scattering and energy loss, therefore tending to increase the resolution of the counter. Furthermore, it became clear during this experiment that the nuclear interaction of pions with the radiating medium of the movable counter was a fundamental limitation on the accuracy attainable, and this again makes the use of liquid hydrogen or deuterium very desirable.

2. <u>The Optical System</u>

The monitor Cerenkov counter CM is shown in Fig. 6 and a photograph of the CM flask in Fig. 7. The movable counter CP is similarly depicted

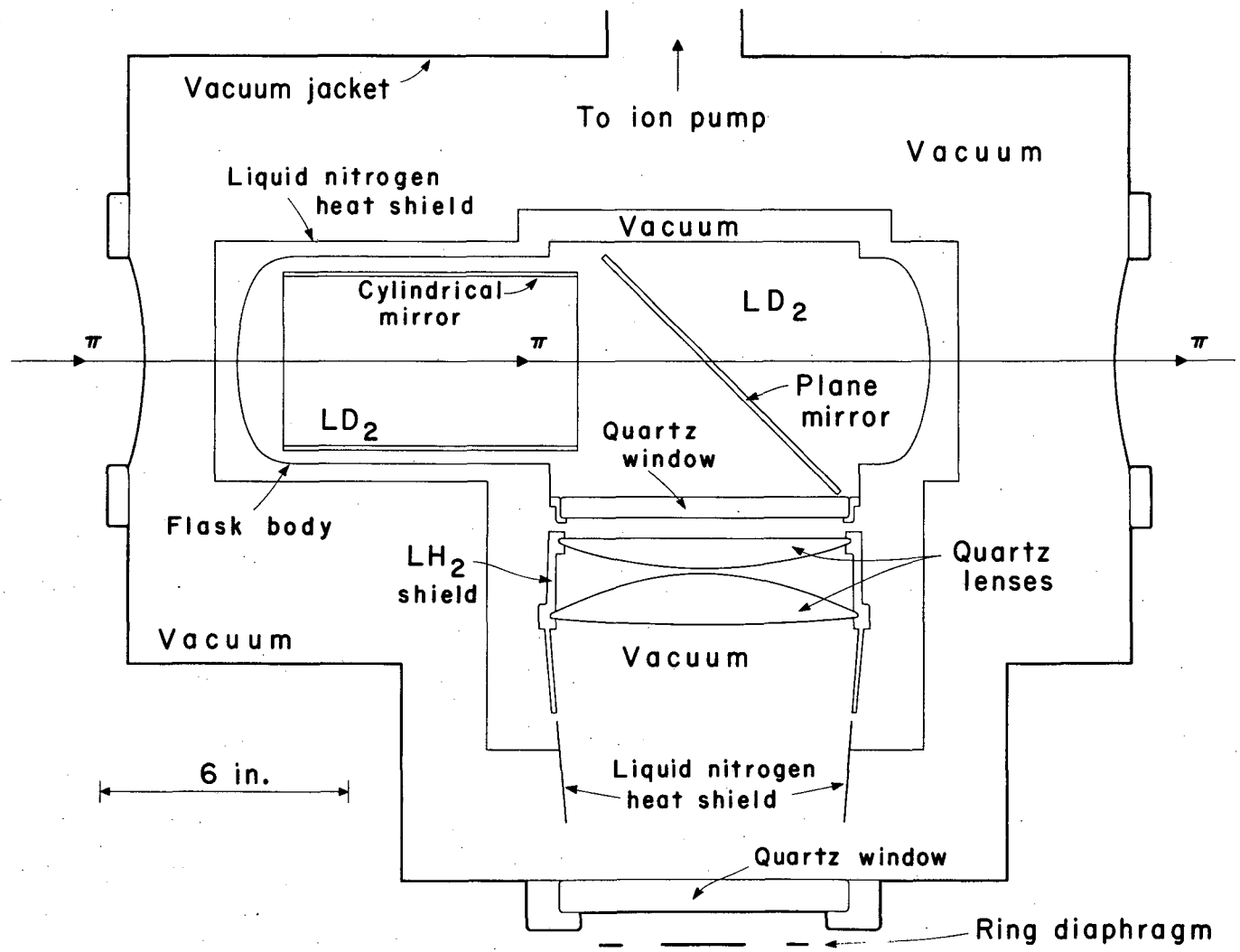

XBL687-3451

Fig. 6. Monitor Cerenkov counter CM (plan view). The 4-in-diameter cylindrical mirror defines the entrance aperture.

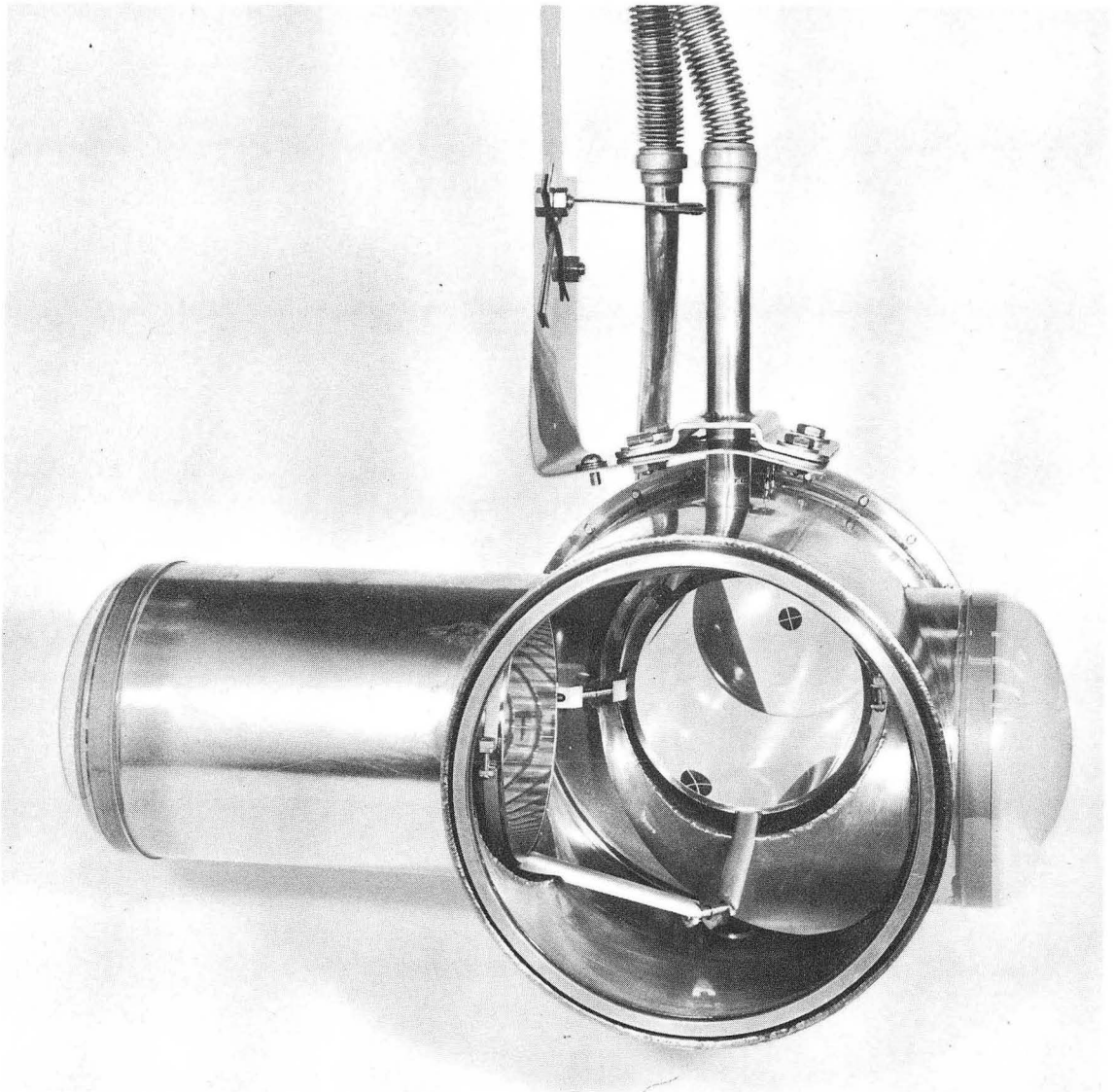

XBB 673-1384

Fig. 7. Photograph of the CM flask. The beam enters from the left. The exit end of the cylindrical mirror and the plane mirror can be seen inside the flask, through the quartz window. The circle with cross hairs seen reflected in the plane mirror was attached to the front of the cylindrical mirror, and was used to align the optics.

in Figs. 8 and 9. The optical systems in these two counters were identical, and were nearly the same as that used in the original Cerenkov counter (Fig. 2), and as that described in Ref. 36. The slight difference in the optical systems of CM and CP from the original design stems from the desire to remove the optical window from the particle beam, since this window was seen to produce some spurious light in the first experiment. Thus, CM and CP have their plane mirrors actually immersed in the radiating medium, with the consequence that the particles have available an extra wedge of Cerenkov medium in which they continue to radiate. This wedge gives rise to the possibility of a variation in counting efficiency across the face of the counter, depending on whether the particle traversed the thick or the thin side of the wedge. Calculations showed that pions should have emitted enough photons (about 250 photons, producing approximately 80 photoelectrons) to be counted before reaching the wedge, and no variation in efficiency from this effect was ever seen experimentally.

The 7-in.-long primary radiating medium was surrounded by a cylindrical mirror to provide uniform efficiency over the entire aperture (4-in.-diameter for CM and 7-in. for CP). The mirror was machined from a tube of stainless steel, honed and polished to a mirror finish, and vacuum plated with aluminum. Since its function was to preserve the angle between the Cerenkov light and the beam axis, the only requirement was that its reflective inner surface be everywhere parallel to the particle axis. Particles which entered off the axis but parallel to it had their Cerenkov light reflected by the cylindrical mirror without change of its angle with respect to the axis. Therefore all the Cerenkov light (including rays which were skew with respect to the cylinder

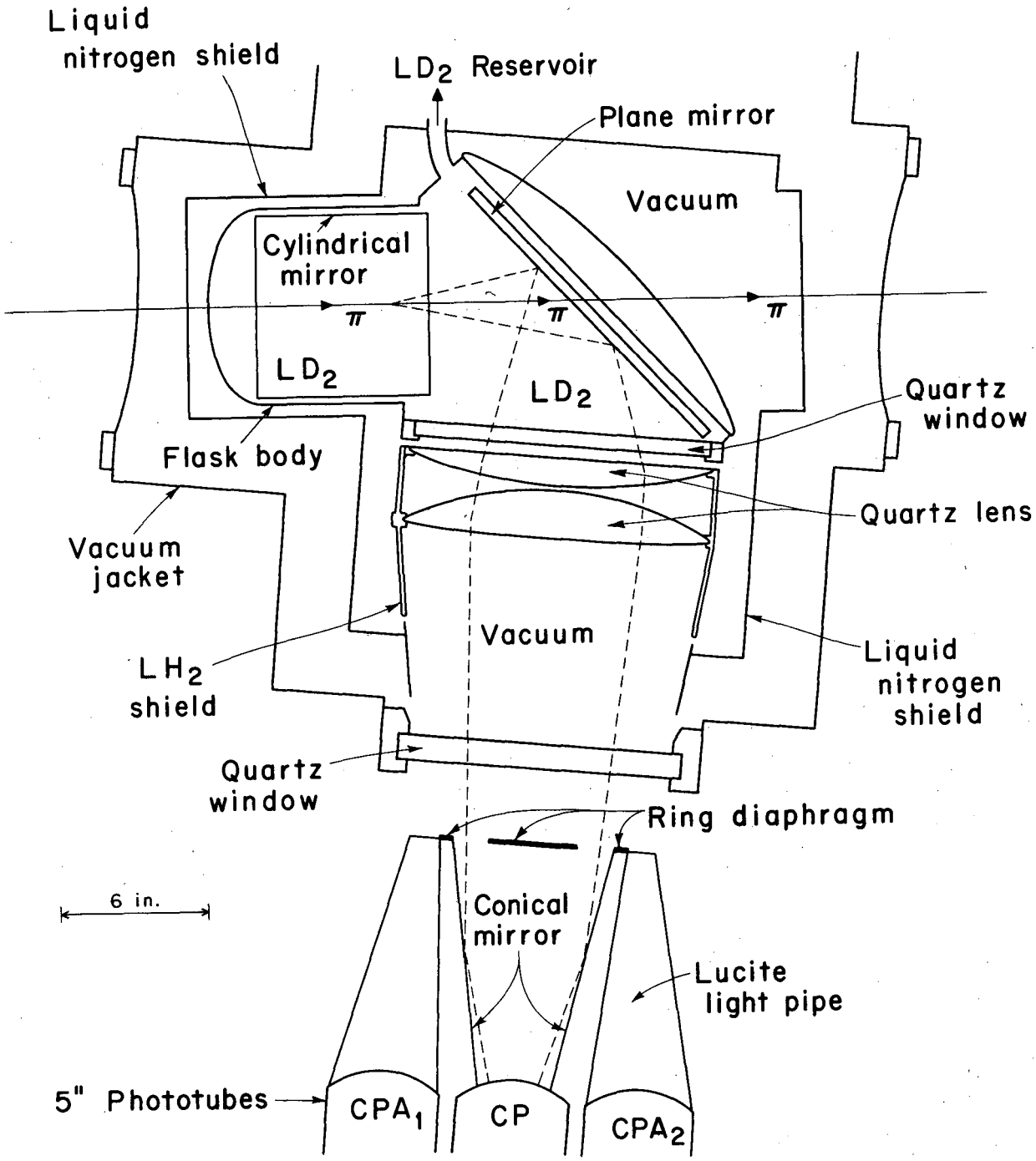

XBL683-2172-A

Fig. 8. Movable Cerenkov counter CP (side view). The optical system is the same as CM's, except that the cylindrical mirror has a 7-in. diameter and the flask optical window is on the bottom. In order to prevent the possible accumulation of material on this window, it (and the entire optical system which follows) is tilted at an angle of 5 deg to the horizontal.

XBB 676-3321

Fig. 9. Photograph of the CP flask. The beam enters from the left. The quartz window is on the bottom and is not visible in this view.

axis) emitted by particles within the cylindrical mirror was usable, and the light-collection efficiency was essentially the same for any particle travelling parallel to the axis, regardless of where it entered the radiating medium. The Cerenkov light was reflected by the plane mirror into the quartz lenses, which brought it to a focus in the plane of the ring diaphragm. Light which passed through the annular aperture in this diaphragm was counted by the central phototube, while light which fell in a ring outside the annulus was counted by the anticoincidence phototubes (see Fig. 8). Cerenkov radiation from particles travelling parallel to the axis was focused to a ring image of radius f tan θ, where f is the focal length of the lens system and θ the Cerenkov angle. The beam momentum was chosen so that pions produced light which fell on the annular aperture, to be counted by the central phototube, while the higher velocity electrons and muons produced light which fell on the anticoincidence ring.

Figure 10 shows a photograph of an optical bench set-up used to test the cylindrical mirror for CP. Eleven-degree Cerenkov light was simulated by a parallel beam of light refracted by a cone of lucite. This light was brought to a focus by the quartz lenses, with or without a reflection from the cylindrical mirror. This arrangement was used for testing the cylindrical mirror shape to insure that reflected light was brought to a ring focus, and also to measure experimentally the focal length of the system.

Particles which had the proper velocity but were travelling at small angles (less than 10 deg) to the axis produced light which was focused to a nearly circular image of the proper radius, but whose center was shifted with respect to the center of the ring diaphragm.

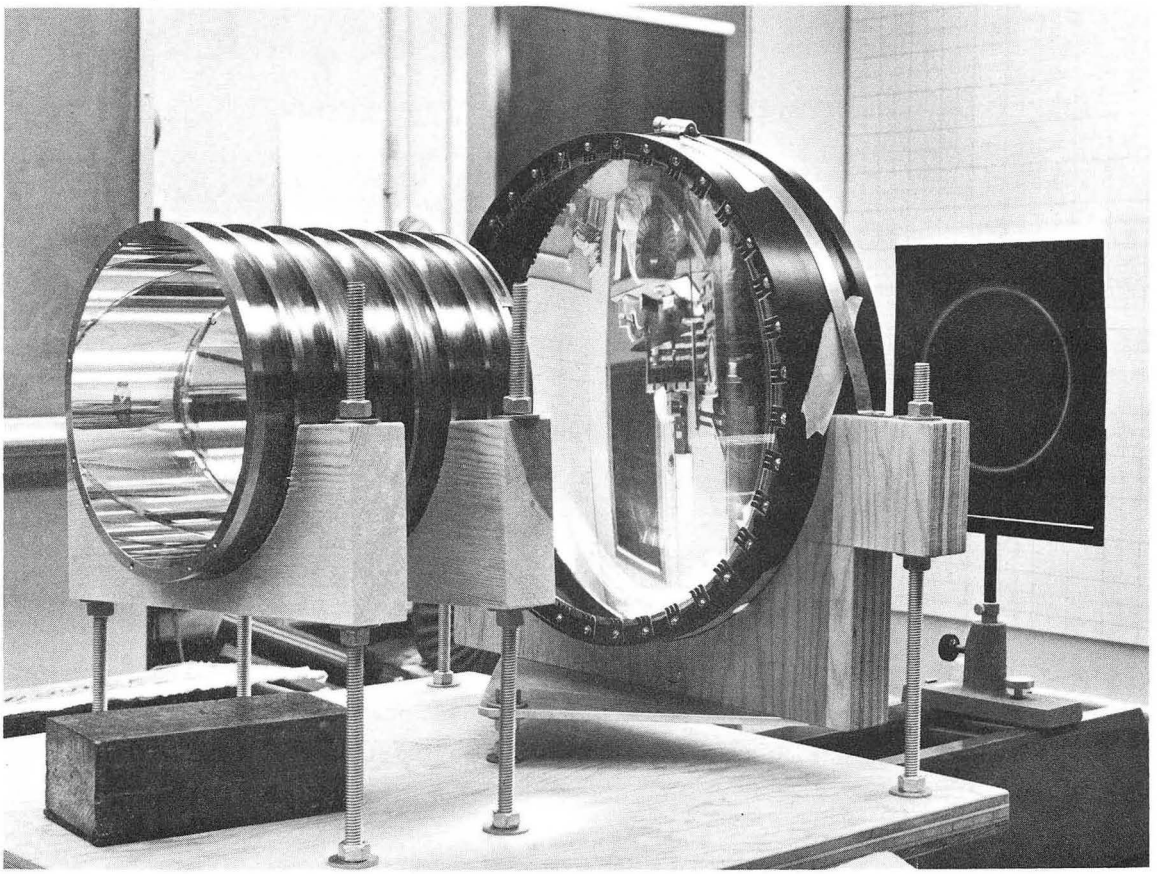

XBB 673-1501

Fig. 10. CP cylindrical mirror and lenses set up on an optical bench, showing simulated Cerenkov light brought to a ring focus.

While such particles put some light into the central phototube, much of their light fell outside the central ring aperture, and was counted by the anticoincidence ring. This property was particularly important in CP, since decay muons produced at 7 deg in the laboratory system had the same velocity as beam pions and would otherwise have been counted as pions. In addition, these decay muons with the proper velocity but the wrong angle soon diverged outside the 7-in.-diameter acceptance aperture of CP, and so were not much of a problem even though they counted with an efficiency of about 1%. Such counting of decay products was not considered serious at the 1% level because it should have been the same on π^+ and π^-, and therefore did not affect the measurement of the lifetime difference.

Cerenkov light from pions was focused to a rather fuzzy ring image in the plane of the aperture, the lack of sharpness being mostly due to multiple Coulomb scattering in the radiating medium (the mean scattering angle was about 1 deg). Other contributing factors were the spread in Cerenkov angle due to energy loss in the medium, spherical aberration in the lenses, and dispersion in the medium. The last effect was partially compensated for by the dispersion of the lens system, and is an important advantage to this type of counter. In spite of this, it was still necessary to limit the acceptance of Cerenkov light to wavelengths longer than 3000 Å, since the dispersion in the medium was much worse in the ultraviolet. The glass phototube face provided a convenient means to limit the counting of shorter wavelengths, which were brought up to this point with high efficiency by the aluminized mirrors, quartz windows and quartz lenses. An idea of the sort of image finally achieved is given by the dimensions of the ring diaphragm

used in CP: the annular aperture had an inner diameter of 3 in. and an outer diameter of 6.75 in. (corresponding to ± 3 deg in Cerenkov angle), while the anticoincidence ring had an inner diameter of 7.5 in. and an outer diameter of 9.75 in.

The light from pions admitted by the central ring aperture was reflected into the central phototube by a conical mirror, while ultraviolet-transmitting lucite light pipes were used to bring the light from the two halves of the anticoincidence ring to the two anticoincidence phototubes. All three photomultipliers were RCA-4522's in CP, and RCA-8575's in CM. In each counter, the output pulses of the two anticoincidence phototubes were added electronically before pulse-height discrimination, since light from off-axis particles was often asymmetrically distributed, producing more light in one side of the annulus than in the other. The collection of light onto the central photomultiplier of CP gave rise to special problems because of our need for uniform efficiency across the entire entrance aperture of the movable counter. Initially the conical mirror was 10-in. high with a 6.75-in.-diameter entrance aperture and a 4.5-in.-diameter exit aperture at the phototube face. Variations in counting efficiency across the face of the counter as large as 3% per inch were eventually traced to a gross nonuniformity of response of the central photomultiplier's photocathode, coupled with a significant correlation between the entrance position of a pion and the portion of the photocathode illuminated by its Cerenkov light. Light-pulser tests of a number of 5-in.-diameter RCA-4522 phototubes helped us to select several tubes which were fairly uniform (± 10%) over the central 3.5-in. of their photocathodes, and the CP conical mirror was rebuilt with a 3.5-in. exit aperture. This produced a much

more uniform efficiency, with variations of less than 0.2% per inch. The larger area reduction of the new conical mirror tended to discriminate against large-angle light, however, with the consequence that the effective aperture of CP was reduced to 5.5-in. diameter. Particles entering the flask outside this aperture were counted with several percent lower efficiency than particles within the central 5.5-in. circle. The effect just described was not a problem with CM because pions were required to traverse CM completely and produce a count in M_4. The relevance of this requirement will be made clear later, when interactions in the Cerenkov medium are discussed.

3. Cryogenic Problems

Although liquid hydrogen and deuterium have the great advantage of lower scattering cross sections than other Cerenkov media, their practical utility can be severely restricted by cryogenic problems. While all of the difficulties were eventually overcome in this experiment, several of them were real limitations to the accuracy attainable in the first experiment. One of the most obvious requirements is that there be very little boiling in the optical path of the Cerenkov light, and it is not at all clear that this condition can be satisfied in a flask of liquid hydrogen which views directly a room-temperature photomultiplier assembly through a large transparent window. The decision to move the optical windows out of the particle beam meant that these windows had to be increased in diameter to allow for the divergence of the Cerenkov light, resulting in a 7-in.-diameter window in CM and an 11.5-in.-diameter window in CP. Boiling was kept to a minimum by surrounding the entire flask with 20 layers of 0.00025-in. aluminized Mylar, and enclosing this in an aluminum heat shield kept at liquid-nitrogen temperature.

This structure was supported by thin insulating rods attached to the outer vacuum jacket, and immersed in an insulating vacuum of 0.5×10^{-8} torr.

One of the greatest difficulties in the first experiment was the slow accumulation of condensate on the outer surface of the flask optical window. This scattered some pion Cerenkov light into the anticoincidence ring, causing a drop in counting efficiency of about 1% per day. Most of the condensate was apparently diffusion-pump oil which had migrated to the flask window (at 20° K) from the warmer liquid-nitrogen shield (at 77° K). In the second experiment this problem was attacked in several ways. The most important was the construction of the lens hydrogen shield (see Figs. 6 and 8) which kept the region in the immediate vicinity of the flask quartz window at liquid-hydrogen temperature. The lens-holding frame, which came to within 1/4 in. of the flask window, was surrounded by tubing filled with liquid hydrogen or deuterium from the deuterium reservoir (see Fig. 11), and this shield cryopumped onto itself condensate which might otherwise have migrated to the flask window. The lens hydrogen shield was always filled with liquid and allowed to stand for several hours before the flask itself was filled. In early trials when the flask and shield were filled simultaneously, condensate was seen on the flask window, but if the proper procedure was used, the flask window remained completely transparent for an entire run (up to two weeks). Additional precautions were taken to limit the amount of material in the main vacuum which could condense on the optical surfaces: the diffusion pump was equipped with a liquid-nitrogen trap to block the migration of diffusion-pump oil into the main vacuum, and after the initial pump-down the diffusion pump

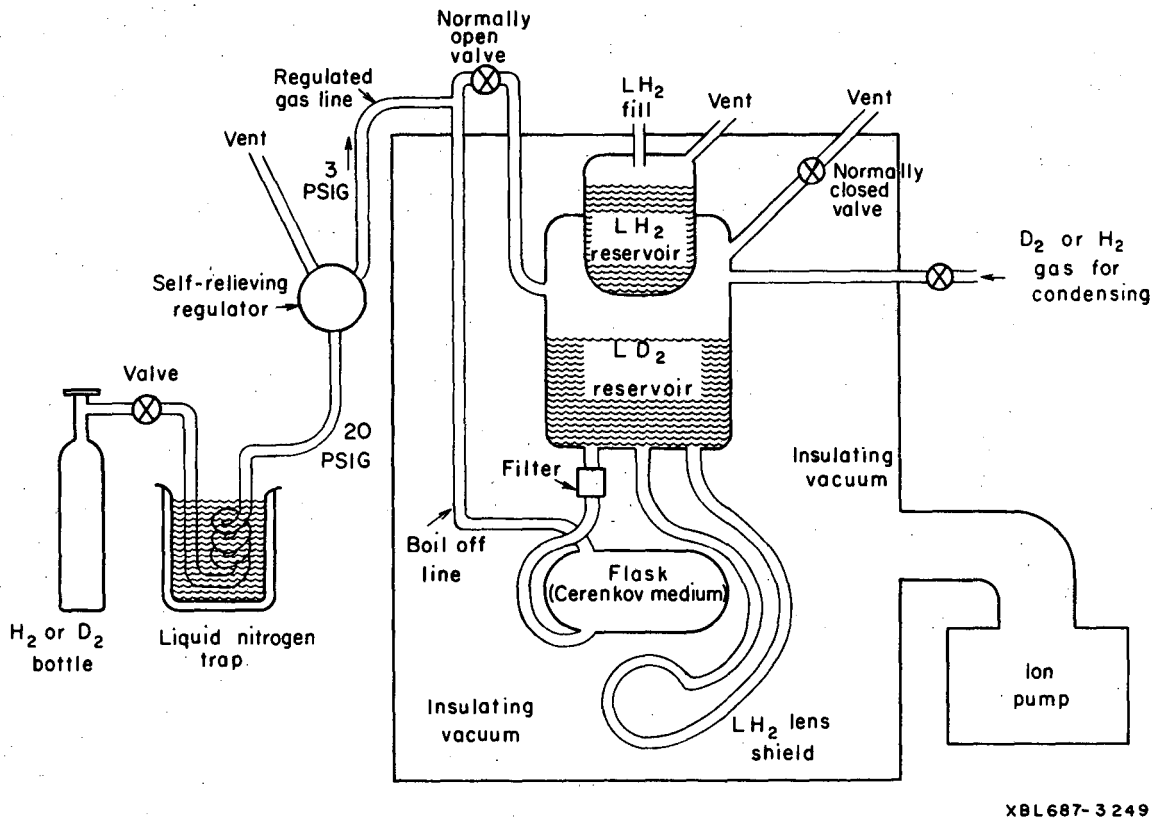

Fig. 11. Simplified schematic drawing of the cryogenic plumbing used to operate CM and CP. All gas fed into the deuterium system was passed through filters containing Linde 5-Å molecular sieves (in 1/16-in. pellets), which were held at liquid-nitrogen temperature. These filters removed water, air, oil, and other contaminants which might otherwise have condensed on the cold optical surfaces inside the flask.

was completely isolated and the vacuum maintained with an ion pump. The lens hydrogen shield had the additional function of reducing heat transfer to the flask, and the boiling rate was observed to be significantly lower when the lenses were in place than it had been during initial tests without the lenses.

A final cryogenic problem concerned the stability of the index of refraction of the Cerenkov medium. It was originally thought that the required stability could be achieved by filling the flask and part of the liquid-deuterium reservoir with liquid (see Fig. 11), and then completely isolating the liquid-deuterium system. By keeping the upper liquid-hydrogen reservoir full, the liquid boiled off in the deuterium reservoir and flask would be recondensed and an equilibrium established at about 3 psig. This is the system used routinely in an ordinary Radiation Laboratory liquid-deuterium target, and is shown in Fig. 11 along with the modification we eventually used to achieve stability. In practical operation the closed-system technique described above did not work very well because small changes in temperature, and hence in index of refraction, caused relatively large changes in the Cerenkov angle and thus the momentum response of the counter. A change of 0.1° K brought about a change in Cerenkov angle of 0.09 deg, and a change in the central momentum accepted by the counter of 0.18%. Since the momentum acceptances of both CM and CP were ± 2.5%, and beam momentum spread was ± 0.5%, such a shift in momentum response did not necessarily result in the rejection of beam pions, but could cause small changes in the efficiency which might be important in a high-precision experiment of this kind. Moreover, changes in temperature of 0.1° K often occurred quite abruptly and irreversibly when the liquid-hydrogen reservoir was

refilled, which had to be done every three hours with CP.

The slight changes in temperature which were of concern to us went largely unnoticed in the first experiment, where the flask temperature was monitored only by a thermocouple. The second experiment used small platinum resistance thermometers,[38] which increased the sensitivity to temperature changes to $\pm$ 0.01°K. Eight of these devices were used in CM and CP, one at the top and one at the bottom of each flask, and in the top and bottom of each liquid-deuterium reservoir. A constant current of 1 mA was maintained through the eight resistors in series, and the potential across each was measured by a potentiometer, through two separate wires which carried no current. During running, measurements were made on each resistor every six minutes by an automatic device, and displayed on a multi-point strip-chart recorder for visual monitoring.

Temperature stability of $\pm$ 0.02° K was obtained by regulating the pressure in the liquid-deuterium system as shown in Fig. 11. A manually-set, self-relieving regulator[39] maintained the pressure in the deuterium reservoir at 3.0 psig, which was slightly higher than the closed-system equilibrium pressure for liquid hydrogen in the deuterium system. For such hydrogen running, hydrogen condensed slowly from the regulating lines until the condensing surfaces of the hydrogen reservoir were partially immersed in the liquid of the deuterium reservoir. This lowered the condensing efficiency to a point which corresponded to an equilibrium pressure of 3 psig, and when this point was reached the condensing stopped. Thereafter, hydrogen gas was bled off into the vent or fed into the deuterium reservoir as needed to maintain constant pressure. The platinum resistance thermometers in the flask showed that the temperature was indeed constant to better than $\pm$ 0.02° K during such operation.

Although much of the early running was done with liquid hydrogen condensed in the deuterium reservoirs and flasks of CM and CP, it soon became obvious that there were systematic errors associated with this radiating medium, and all of the later running and the data-taking was done using liquid deuterium. This posed a new cryogenic problem, due to the fact that liquid deuterium has a slightly higher boiling point than liquid hydrogen at the same pressure (at atmospheric pressure, hydrogen boils at 20.4° K and deuterium at 23.6° K). When the upper hydrogen reservoir was filled with liquid hydrogen at atmospheric pressure, equilibrium pressure for liquid deuterium in the lower reservoir was below atmospheric pressure: about 6 psia. The stability problems encountered by running deuterium as a closed system were even worse than those found with liquid hydrogen, and in the end it was decided to regulate the pressure in the same manner as with liquid hydrogen. The situation was much more delicate in this case however: with liquid hydrogen, the regulated pressures were less than 1 psi above the closed-system equilibrium pressure, whereas with liquid deuterium the regulated pressure was nearly 12 psi above the closed-system equilibrium. Such operation required condensing liquid deuterium to a very high level in the deuterium reservoir, in order to immerse a large fraction of the condensing surface of the hydrogen reservoir in liquid, and thereby reduce the condensing efficiency to a point consistent with an equilibrium pressure of 3 psig. This system turned out to be basically stable, but when the equilibrium was temporarily upset by accident, for instance by overfilling the hydrogen reservoir or by temporary loss of regulating pressure, the system often took 12 hours or longer to return to equilibrium. It was nevertheless possible to run for many weeks in

this delicately balanced equilibrium, with only minor mishaps. The only practical limitation was that each regulating system vented about 100 ft^3 of deuterium gas per day, which was not recovered, and constituted a moderate expense for several weeks of running.

The index of refraction of liquid hydrogen depends on the relative proportions of parahydrogen and orthohydrogen present, and similarly for liquid deuterium. Both liquid hydrogen and liquid deuterium are composed of diatomic molecules which can exist in states which are either symmetric (ortho) or antisymmetric (para) under the interchange of nuclear spins. For a molecule consisting of two identical nuclei of spin I, the numbers of possible spin states are related by:

$$\frac{\text{Number of possible ortho states}}{\text{Number of possible para states}} = \frac{I + 1}{I} .$$

Since I = 1/2 for hydrogen, the ortho-to-para ratio is 3:1 at room temperature because all available states are equally occupied. For deuterium, I = 1, and the ortho-to-para ratio is 2:1 for the gas at room temperature. Since both liquid hydrogen and liquid deuterium were condensed from gases at room temperature, these ratios applied also to the liquid Cerenkov media immediately after condensing.

Since the liquid Cerenkov media were at approximately 20° K, the equilibrium state consisted almost entirely of molecules in their ground states, with total angular momentum J = 0. Hydrogen nuclei are fermions, and the molecular wave function must therefore be antisymmetric under interchange of nuclei. If J = 0, then the space part must be symmetric, which requires the spin part to be antisymmetric. Thus liquid hydrogen at equilibrium is nearly pure parahydrogen (the antisymmetric spin state with nuclear spins antiparallel). The parahydrogen concentration in the Cerenkov medium was 25% initially, and would normally increase to 100%

over a period of weeks. A catalyst[40] was immersed in the liquid hydrogen (contained in the liquid deuterium reservoir) in order to accelerate this process, and the conversion was about 90% complete three days after condensing.

Deuterium molecules, on the other hand, are composed of two identical bosons, and the wave function must be symmetric under interchange of nuclei. Since the space part of the ground-state wave function is symmetric ($J = 0$), the spin part must be symmetric also, and equilibrium liquid deuterium is nearly pure orthodeuterium. Hence the orthodeuterium concentration changed from 66.7% initially to 100% as equilibrium was approached. The same catalyst was used for liquid hydrogen and liquid deuterium, and was equally effective for both. Since the ortho-to-para ratio was much closer to equilibrium initially for liquid deuterium than for liquid hydrogen, conversion was completed more quickly for the former.

The net effect of these ortho-para conversions under our constant-pressure conditions was a slow increase in density (totaling about 0.5% for hydrogen) and decrease in temperature. The change in index of refraction was not entirely due to the density change, however, and at constant pressure the density effect partially compensated the change in index due to the changing ortho-to-para ratio.[41] This compensation appears to be more effective for liquid deuterium than for liquid hydrogen, although existing data does not permit very reliable calculations. For the liquid deuterium the total observed temperature change was about 0.05° K, giving a maximum shift in the central momentum accepted of 0.2%. In any case, changes in index of refraction from this effect are extremely slow compared to the polarity-reversal period (about one hour) used during data taking, and so cannot affect the lifetime-

ratio measurement as long as the change is the same for π^+ and π^-.

4. Performance Tests

A large fraction of the running time was spent checking the operation of CM and CP to prove experimentally that they were performing according to design and to study possible systematic errors. The results of many of our measurements are summarized in Table III, which gives the operating characteristics of CM and CP for both hydrogen and deuterium radiators. Although many techniques were used, the single most useful one was the study of the spectra of pulses from the central phototubes, produced by pions entering the counters. In order that these spectra could be observed continuously during the data taking, the pulses from the last dynodes were used for pulse-height analysis, while the anode pulses could be used simultaneously for the data. The dynode pulses were fed into a linear gate and stretcher, whose stretched output pulse had a voltage which was proportional to the total charge contained in the pulse (i.e. to the integrated "area" of the voltage pulse). These stretched pulses were analyzed by a 1024-channel pulse-height analyzer,[42] producing what will be referred to loosely as a pulse "height" spectrum, although strictly speaking this should be called a pulse-charge spectrum. The linear gate and stretcher could be gated on various coincidence signals from the electronic data-taking logic, and hence provide the spectra of pulses which satisfied a variety of external requirements in addition to producing light in the counter in question. Although pulse-height analysis was used to study the performance of every counter in our system, it was used most frequently to study the performance of CP, and most of what follows concerns this application.

Figure 12 shows schematically a number of possible pulse-height spectra

Table III. Operating characteristics of Cerenkov counters.

Parameter		LH_2	LD_2
No. photoelectrons/particle		80	80
Index of refraction		1.11	1.13
Cerenkov angle*	CP	10.1 deg	10.1 deg
	CM	12.3 deg	12.3 deg
Cerenkov angles accepted		± 3 deg	± 3 deg
Cerenkov angle fluctuation due to temperature changes		± 0.02 deg	± 0.02 deg
Velocity (β)*	CP	0.913	0.898
	CM	0.920	0.915
Velocity acceptance (HWHM)		± 0.009	± 0.009
Usable aperture**	CP	5.5 in.	5.5 in.
	CM	4.0 in.	4.0 in.
Particle angles accepted (HWHM)		± 6 deg	± 6 deg
CM pion efficiency (β = 0.92)		99.7%	99.7%
CM electron efficiency (β = 1.0)		0.5%	1.0%
CM muon efficiency (β = 0.95)		0.02%	0.04%
Empty-counter efficiency (CM and CP)		< 0.01%	< 0.01%
Pions scattered out of beam by CM		43%	51%
<u>Pulse-height spectra P/V ratios</u>			
No back-up counter	π^+	6	4.5
	π^-	18	4.5
With back-up counter (larger than flask)		25	12
With back-up counter (smaller than flask)		500	250

*Since CM preceded CP, it caused an energy loss of about 14 MeV. The ring diaphragm dimensions were adjusted to account for this fact.

**The aperture quoted for CP differs from the 7-in. diameter of the cylindrical mirror because a downstream coincidence counter could not be used with CP.

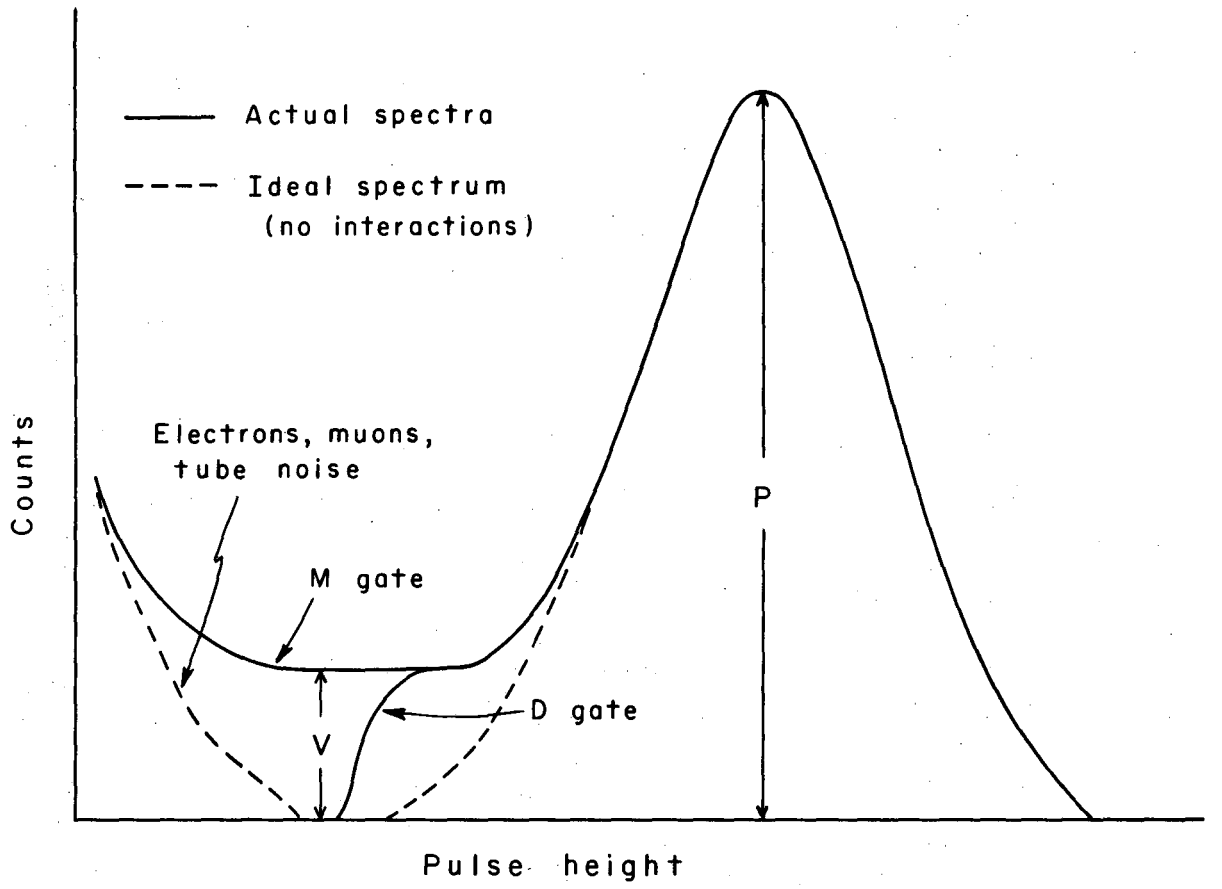

XBL687-3442

Fig. 12. Idealized pulse-height spectra which might be obtained from the CP central photomultiplier under various conditions. The peak-to-valley ratio, P/V, is a measure of the resolution of the counter.

which might be obtained from CP under various conditions. The dashed curve is an ideal spectrum, with all the pulses from pions above a certain level, and all the small pulses from tube noise, electrons, and muons below this level. If this spectrum of pulses were put into a discriminator with a variable threshold, the discrimination level could be set to produce a standardized output pulse whenever a pion entered the counter, but no output when one of the smaller pulses was present. These conditions would correspond to 100% efficiency for pions, 100% rejection of electrons and muons, and no accidentals.

The solid curves show actual spectra obtained from CP under two different conditions: when the linear gate and stretcher was gated on the M coincidence, or alternatively on the D coincidence. The M coincidence signal was produced by a particle which counted in M_1, M_2, M_3, M_4, and CM, but not in any of the anticoincidence counters A_1 to A_6, A_e, or in the CM anticoincidence ring CMA. Such particles were nearly all pions, and if they also produced light in CP it was assumed that they had not decayed. Thus, the curve labelled "M gate" is the spectrum obtained from <u>all</u> particles entering CP which were pions when they left CM. The curve labelled "D gate" imposed the additional restriction that these same particles produce enough light to exceed the CP discriminator threshold and yet not produce light in the CP anticoincidence ring CPA. It can be seen that none of the particles which produced low pulse heights in the CP phototube exceeded the discriminator level, and that the effect of the discriminator was to cut off all particle pulses below some minimum height. A pair of such spectra, on M and D gates, was often used to obtain a preliminary setting for the CP discrimination level.

Figure 13 shows some actual CP pulse-height spectra obtained using the M gate under various conditions. It can be seen that the counter was operating in a manner which was far from ideal: the peak-to-valley ratio, defined in Fig. 12, was typically about 4.5 with liquid deuterium in the counter (curve A, Fig. 13), to be compared with an ideal value of infinity. The continuous spectrum of small pulses which "filled up" the valley was due to pions which entered the counter and penetrated only a short distance before undergoing a nuclear interaction. Since beam pions ($\beta = 0.92$) were not very far above threshold ($\beta = 0.89$), most interacting particles stopped emitting Cerenkov light, or at least no longer emitted light at the proper angle. Thus they produced only a small pulse in the CP photomultiplier, proportional to the distance travelled before the interaction. This conclusion was reached by comparing the pulse-height spectra obtained under conditions characterized by different interaction cross sections. Curve A in Fig. 13 was obtained with liquid deuterium in CP, had a peak-to-valley ratio P/V = 4.5, and was exactly the same on both π^+ and π^-. Curves B and C were obtained with liquid hydrogen as the radiating medium, on π^+ (P/V = 6) and π^- (P/V = 18) respectively. It can be seen that the peak-to-valley ratio increased with decreasing interaction cross section, and that the use of liquid hydrogen as the radiating medium created a potentially dangerous difference between π^+ and π^-.

One way to improve the operation of the counter significantly was to require that particles travel all the way through the radiating medium without deflection, for instance by requiring a coincidence with a scintillation counter behind the Cerenkov counter. Figure 14 shows three pulse height spectra, all taken with liquid hydrogen in CP and

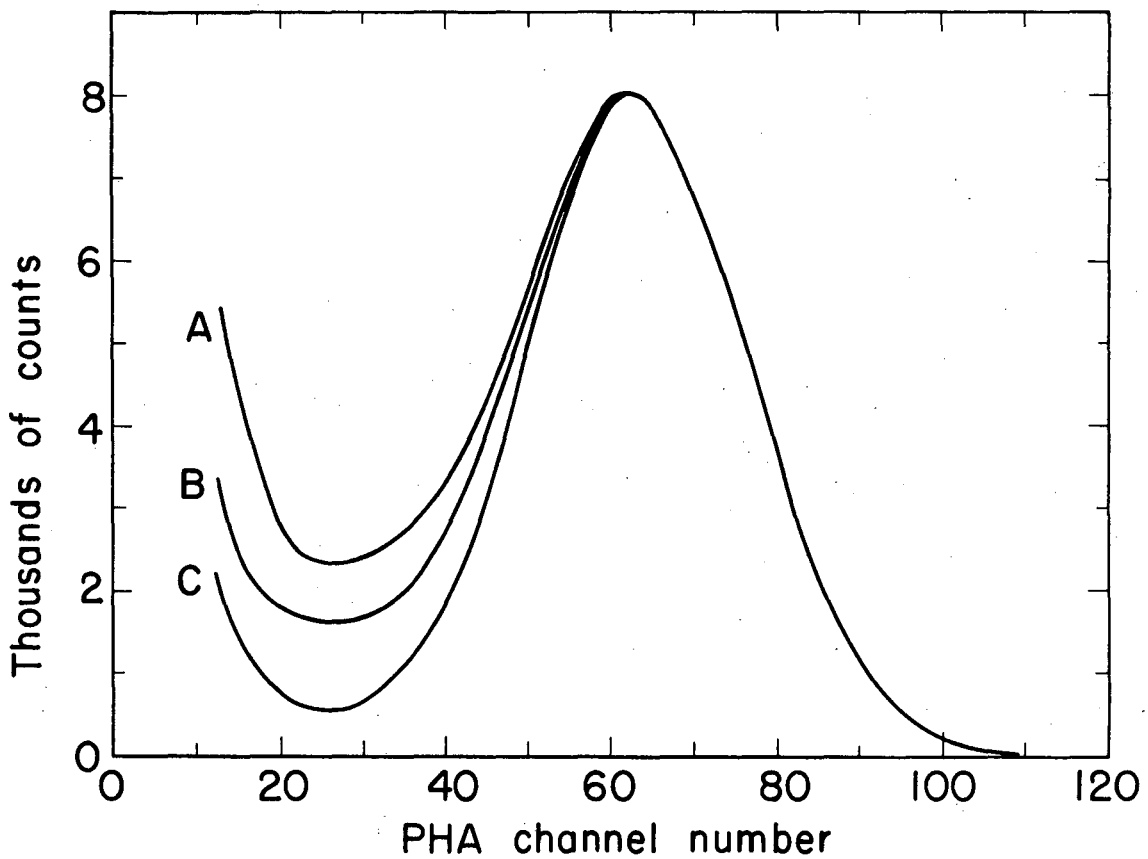

XBL685-2677

Fig. 13. Some actual CP pulse-height spectra, gated on the M coincidence. Curve A was obtained with liquid deuterium in the counter, and was the same for π^+ and π^-. Curves B and C were obtained with liquid hydrogen in the counter, for π^+ and π^- respectively.

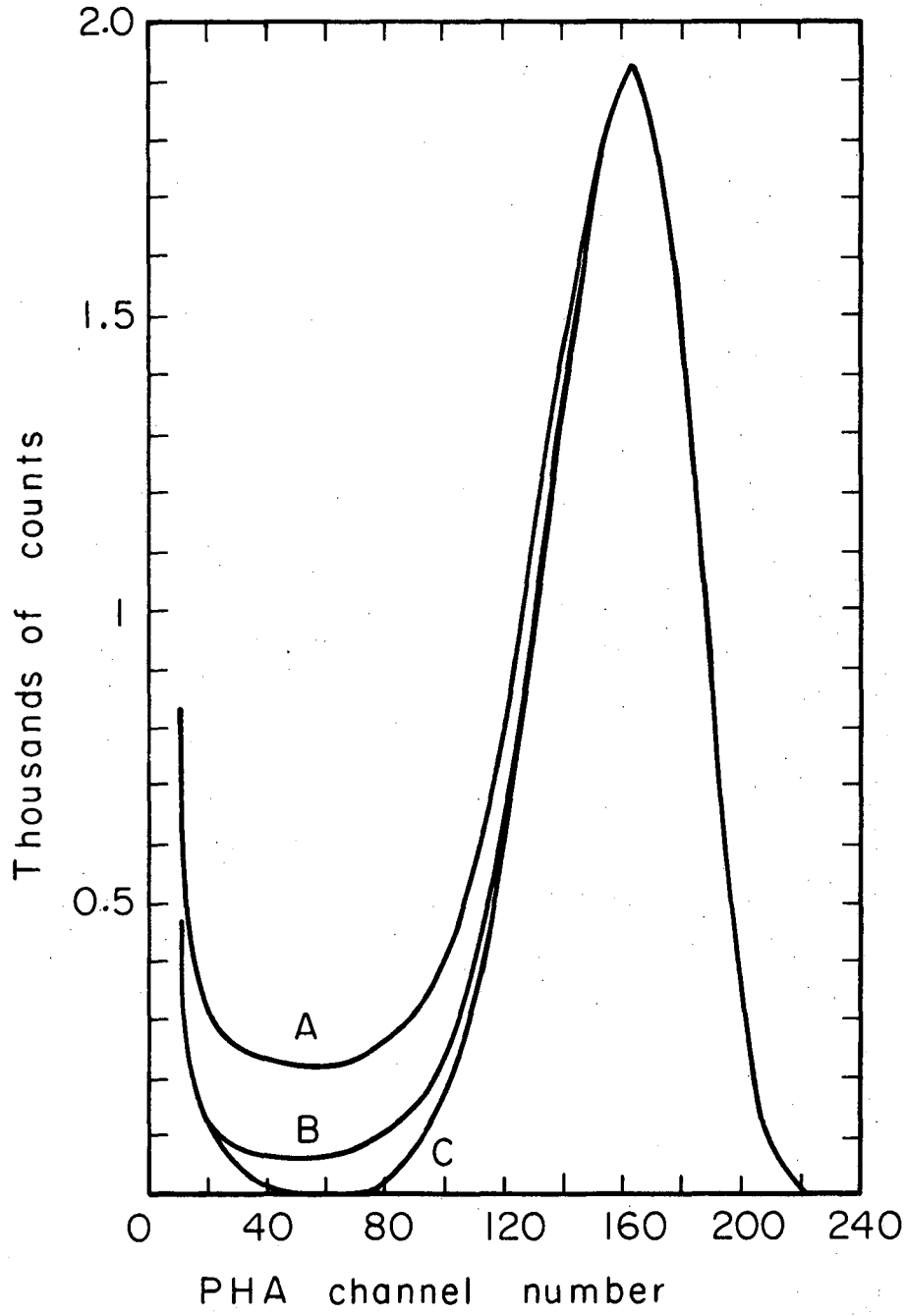

XBL687-3191

Fig. 14. Pulse-height spectra of CP, all taken with liquid hydrogen and π^+ particles. Curve A was obtained using the M gate (and is the same as curve B in Fig. 13; note the difference in scales). Curve B was obtained using the MM_5 gate, when M_5 was a 1-ft-square scintillator behind CP. Curve C was also obtained using the MM_5 gate, but here M_5 was a 3-in.-diameter counter behind CP.

positive particles. Curve A is thus the same as curve B of the previous figure, and was obtained by analyzing pulses from all pions entering the counter (M gate). Curves B and C were obtained with the gate MM_5, where M_5 was a scintillation counter placed immediately behind CP. In curve B, this counter was 12-in. square and gave P/V = 25, while curve C shows the spectrum with a 3-in.-diameter M_5 giving P/V = 500. Tests showed, however, that no improvement resulted by requiring coincidence with a small thin counter in front of CP, again consistent with the interpretation that the bad peak-to-valley ratio was due to interactions. It seems at this point that it would always be desirable to run CP in coincidence with a scintillator just behind it. In fact, this is exactly how CM was operated, since it was in coincidence with M_4. CM gave pulse-height distributions with P/V = 500 with liquid hydrogen and P/V = 250 with liquid deuterium. However, there were serious problems associated with operating CP in this manner.

The difficult arose because of our requirement that the Cerenkov-counter aperture be larger than the pion beam, thus making the detector's efficiency independent of small changes in beam position. A downstream coincidence counter improves the pulse-height distribution because it does not intercept most of the "halo" of pions scattered by the Cerenkov medium, and this very fact makes the efficiency sensitive to beam position within the counter. Even if such effects could be made small, the construction of CP (Fig. 8), which had its beam-exit window parallel to the 45-deg mirror, posed another problem. The amount of deuterium radiator (an absorber) encountered by a pion trajectory depended on its vertical position in the flask, and the efficiency was therefore very sensitive to this position when a downstream coincidence counter required

a particle to traverse the entire deuterium radiator. Furthermore, the aluminized-Mylar plane mirror was supported by a cross piece of stainless-steel tubing which was directly in the beam path. The varying amounts of absorber gave rise to a variation in efficiency with vertical position of about 2% per inch, when coincidence was required between CP and the 12-in.-square M_5 counter behind it. This situation makes the lifetime-ratio measurement very sensitive to small spatial differences between the π^+ and π^- beams: for instance, if the vertical separation between the beams were to gradually increase along the decay path due to a small horizontal magnetic field, the efficiencies on π^+ and π^- would change in different ways, giving rise to an apparent lifetime difference. During the data taking the 12-in.-square M_5 counter was actually in place behind CP, and data with it in coincidence was scaled independently of the data without it. The information thus obtained was very useful in pointing up certain difficulties with normal CP operation, but was not usable for the lifetime ratio analysis.

Another performance check which was repeated at the start of each data run was the measurement of the CP efficiency as it was moved across the pion beam (see Fig. 15). This was usually done near the middle of the decay path where the beam was the smallest, about 2.5-in. wide and 3-in. high. As already mentioned, these profiles showed a considerable variation in efficiency until the aperture of the CP central phototube was restricted to 3.5-in. diameter, and a tube with fairly uniform photocathode efficiency was found. Such variations in efficiency were initially seen to be much worse on π^+ than on π^- when liquid hydrogen was the radiating medium, and very much worse than either of these when liquid deuterium was used.

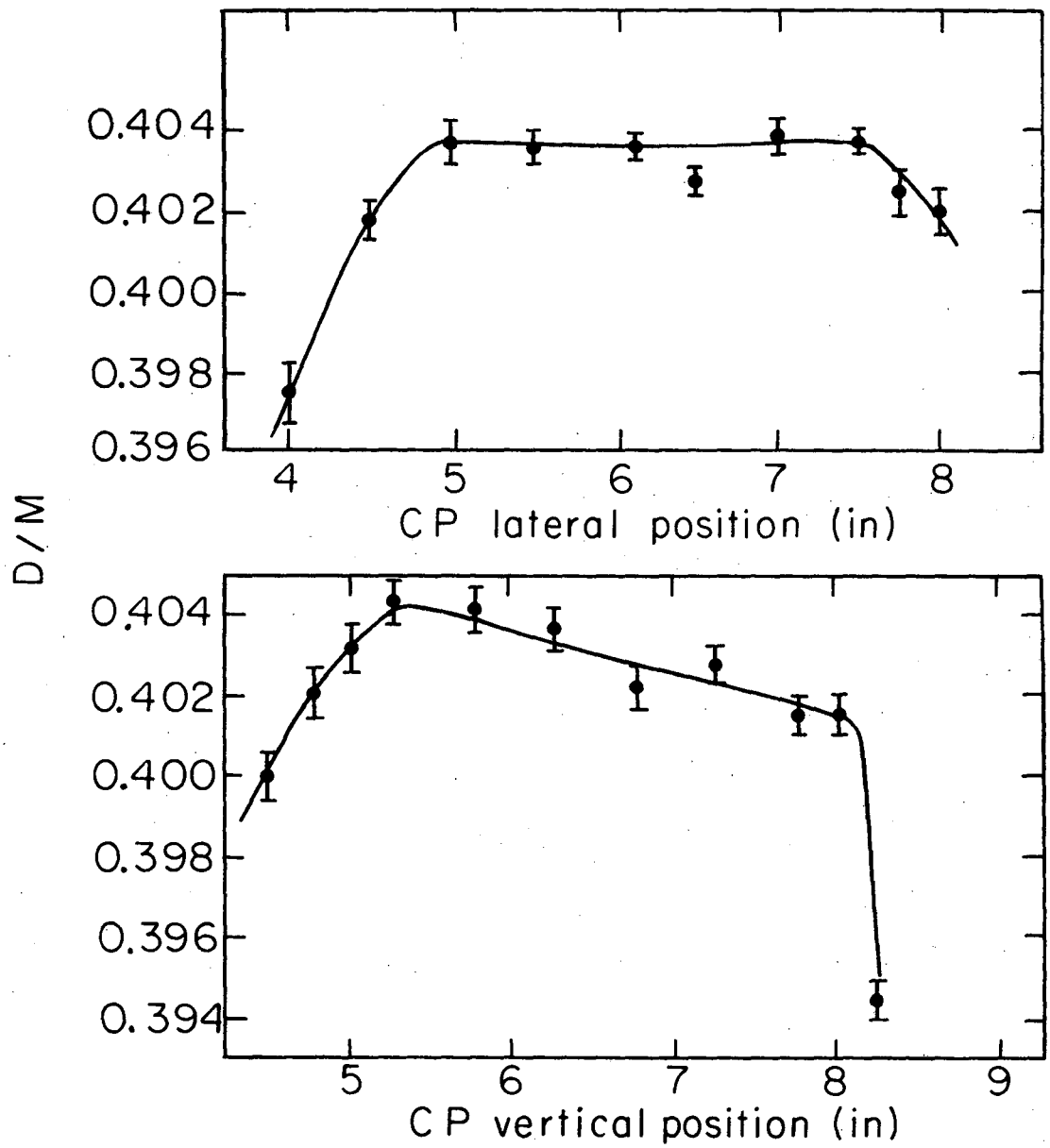

XBL687-3192

Fig. 15. Lateral and vertical profiles of CP. These were obtained by moving CP laterally and vertically across the pion beam at a point where it was 2.5-in. wide by 3-in. high. D/M is the fraction of monitor coincidences which were counted by CP. The ratio was less than unity because more than half the pions had decayed before reaching this position on the decay path.

These differences can be understood in terms of the pulse-height distributions from the CP photomultiplier. Differences in photocathode efficiency across the face of the tube caused the entire pulse-height spectrum to shift by several channels as the counter was moved across the beam. For an ideal counter, the discrimination threshold is set in the middle of an infinitely deep valley, and small shifts in the pion-peak position do not change the counting efficiency as long as the tail of the distribution does not extend beyond the discriminator cut. For the actual CP pulse-height distributions shown in Fig. 13, however, shifts of the spectrum clearly caused the efficiency of the counter to change considerably, although the effect was smaller for larger peak-to-valley ratios. The effect was also diminished slightly if the discriminator was set in the very lowest point of the valley, and in fact this was one of the criteria for setting the CP discrimination level. The high voltage was set at a value which gave a reasonable separation between the noise spectrum and the pion peak, although if it were set too high the gain of the photomultiplier was found to be somewhat less stable with time than for lower voltages. (The phototube was normally operated at a gain of about 10^7.) Then pulse height spectra were observed using the D gate for a number of different CP discriminator levels, and a level tentatively chosen which put the discriminator cut in the middle of the valley. Finally, the lateral and vertical efficiencies were measured as the counter was moved across the pion beam. If these curves (see Fig. 15) were not wide enough, corresponding to an effective aperture of at least 5.5 in., then the CP discriminator was lowered, and this also tended to make the response more uniform. Other means used to achieve the desired width and flatness of these curves were to change the exit aperture of

the conical mirror (a major undertaking) or to change the potential of the photomultiplier's focusing grid.

Another criterion for setting the CP discriminator level was that the counter not respond to electrons or muons with high efficiency. While electrons were removed from the monitor coincidence by A_e and CM, a high efficiency for counting them was considered to be symptomatic of generally poor discrimination against decay muons. The CP efficiency for counting electrons was measured by comparing the number of CP coincidences with counts in A_e to the total number of counts in A_e; this ratio was typically around 7%. The CP efficiency for counting beam muons was measured by looking at the fraction of particles which counted in CP and did <u>not</u> count in CM, since most of the particles which did not count in the CM central photomultiplier were muons. The CMA anticoincidence ring was not used in this comparison, because it vetoed some good pions as well as electrons and muons. Typically, CP counted 0.5% of the beam muons when filled with liquid hydrogen and 1% of the muons when filled with liquid deuterium. Thus, the final criteria for setting the CP discrimination level were lateral and vertical profiles which were wide and flat, and low counting efficiency for beam electrons and muons. The CM high voltage and discriminator level were set in the same way, although proper operation was much less sensitive to the values chosen because of the very wide and deep valley of the pulse-height distribution. As might be expected, CM lateral and vertical profiles were absolutely flat to 0.1% accuracy, and the effective entrance aperture was close to 4-in.

One of the classic methods of checking the operation of a pressurized-gas differential Cerenkov counter is to measure the response as a function of pressure, i.e. as a function of the index of refraction of the radiating

medium. In a momentum-analyzed beam containing several different types of particles with well-defined velocities, this pressure curve shows sharp peaks in the response when the index of refraction corresponds to one of the particle velocities. The depth of the valley between two adjacent peaks gives a good measure of the ability of the counter to discriminate against one type of particle when it is adjusted to count only the other type. Unfortunately it is not possible to vary the index of refraction of liquid hydrogen or deuterium over any significant range, so this check was not available to us. But a similar test of performance consisted of measuring the counter efficiency as a function of beam momentum. The momentum varied linearly with the magnet currents, and so could be changed by a known amount simply by changing all magnet currents by the same factor. The Cerenkov counters showed sharp peaks in response whenever one of the particle components had $\beta = 0.92$, and the depth of the valleys between these peaks gave a measure of the counter resolution. Pions and muons were the only particles in our beam which were accessible for this test, and the resulting momentum-response curve is shown in Fig. 16. While the interpretation is not quite as straightforward as for an index-of-refraction curve, clearly a great deal of information can be gained from it. Notice for instance the sloping top on the muon peak: this was not due to a momentum-dependent efficiency of the counter, but rather was caused by the fact that the fraction of muons in the beam decreased with increasing momentum. The beam muons came from pion decay upstream of the first bending magnet, and at higher momentum the pion lifetime in the laboratory is longer and fewer muons are produced. A similar slope, in the opposite sense, was seen on the pion peak, although this is not discernible in Fig. 16 because of the

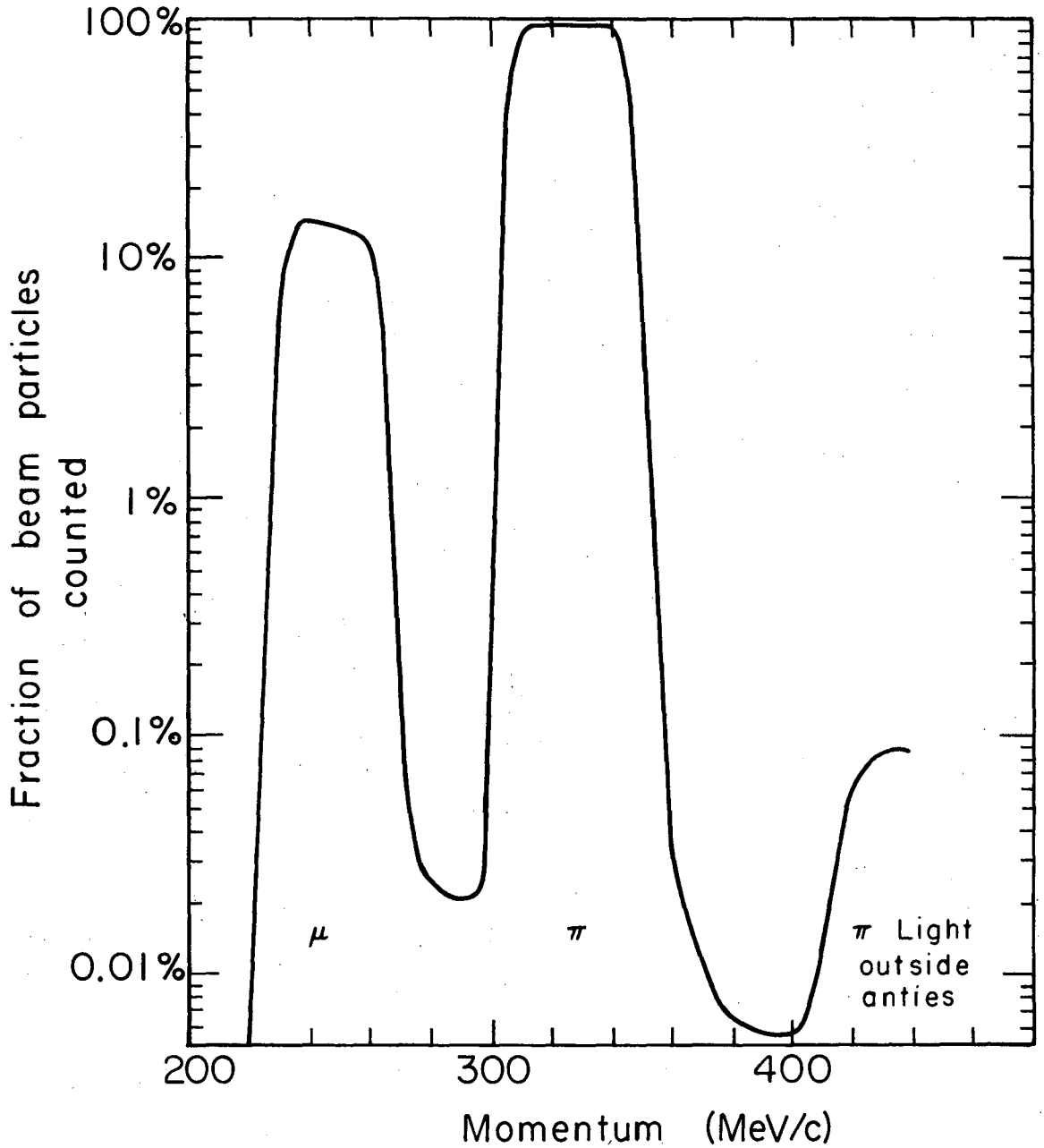

XBL687-3161

Fig. 16. Momentum-response curve for CM when filled with liquid hydrogen. It was obtained by measuring the CM counting rate as a function of beam momentum, and was the same for positive and negative particles. The momentum scale refers to beam momentum at the first bending magnet.

logarithmic scale. In fact, the height of the pion peak increased nearly linearly with momentum, showing that the counter response was approximately independent of momentum within the central 15 MeV/c.

The pion peak did not rise to 100% because the beam contained 10% muons: in fact, careful analysis of the CM pulse-height distribution, not taking into account the fraction of particles vetoed by CMA, showed that the efficiency of CM for pions was 99.9%. The valley between the pion and muon peaks in Fig. 16 falls to about 0.02% of the pion peak counting rate, showing extremely good discrimination against muons when the beam momentum was set for pions to count in CM. In fact, the situation was even better than this! When the beam momentum was set in the valley, about 290 MeV/c, the entire pion beam was off-velocity, and was counted with 0.02% efficiency, whereas during normal operation only 10% of the beam (muons) was off-velocity and it was this smaller fraction which was counted with 0.02% efficiency. It is evident that CM did an extremely good job of discriminating between pions and muons. Unfortunately CP was much worse than CM because of interactions and the presence of off-angle decay muons: the valley between pions and muons fell only to the 1% level with liquid deuterium in the counter.

It will be noticed that the valley on the high-momentum side of the pion peak is even deeper than on the low-momentum side. When the beam momentum was around 400 MeV/c, the ring of pion Cerenkov light fell directly on the anticoincidence ring and was vetoed with high efficiency. The situation was somewhat less clean when the momentum was further increased and the ring of pion light spread outside the anticoincidence ring. Actually, for such high velocities, the Cerenkov angle became too large for the light to be fully accepted by the optics, and there was no

clear image produced in the focal plane. This was presumably one of the reasons why CP counted electrons with 7% efficiency.

Momentum-response curves were useful in three additional applications. By looking in detail at the sloping top of the pion peak (with a linear efficiency scale), the best momentum for data taking was chosen to be in the center of the linear portion of this curve. This turned out to be the same "momentum," i.e. magnet current setting, for both CM and CP because the radius of the ring aperture of CP had been reduced to take into account the energy loss in CM (about 14 MeV). The top of the pion peak was also used to set the discrimination threshold for the anti-coincidence rings, CMA and CPA. First the beam momentum was set at 400 MeV/c to place the ring of pion light directly on the anticoincidence ring, and the two (e.g. CPA_1 and CPA_2) photomultiplier high voltages adjusted to give identical pulse-height distributions for the two halves of the ring. These two halves of the anticoincidence signal were added linearly before being fed into a pulse-height discriminator. The top of the pion peak of the momentum-response curve was then measured for several different values of this anticoincidence-discriminator threshold. If the threshold was set too low, pions on the high-momentum side were vetoed, and the pion peak had no linear region, but instead was round-topped. If the discrimination level was set too high, there was a broad linear region, but the muons and electrons were counted with rather high efficiency. A compromise between these two effects allowed us to set the CPA discriminator at a level consistent with a short linear region and counting efficiencies of 1% for muons, and 7% for electrons. Under these conditions, CPA vetoed about 1% of the particles counted by the CP central photomultiplier. The CMA discrimination level was set in the same way.

In addition to their usefulness in choosing the central momentum and in setting the anticoincidence discrimination levels, momentum-response curves were also used for comparing the momenta of the positive and negative beams. The same magnet settings (the "momentum" scale reading on the momentum-response curve) might conceivably produce beams which have different momenta for the two magnet polarities. In this event, a comparison of the positive and negative momentum-response curves would show the positive and negative pion peaks to be centered about different momenta (magnet currents). Because these peaks had such steep sides, with a change of 1% in momentum resulting in a 30% change in counting efficiency, it was possible to compare their positions with great accuracy. Although momentum differences as small as 0.03% could have been detected, none was ever found. This check was made periodically using both CM and CP, with liquid-hydrogen and liquid-deuterium radiators.

C. Electronics

A block diagram of the electronics used during the data taking is shown in Fig. 17. A list of the important coincidences which were scaled simultaneously is given in Table IV, and some typical values in Table V. While this basic arrangement was modified temporarily from time to time in order to make a particular test, most of these changes were minor. It is seen that many more quantities were scaled than were actually needed to measure the lifetime ratio, for which only two coincidences were used directly. The "monitor" coincidence M, consisting of particles which counted in M_1, M_2, M_3, M_4, and CM, but not in A_1 to A_6, A_e, or CMA, was nearly 100% pions, containing less than 0.04% muons and less than 0.01% electrons. The anticoincidence ring CMA vetoed about 0.2% of the particles which satisfied all other requirements of the M coincidence, but CP indicated that most of these vetoed particles were actually pions. Analysis of the shape of the central-photomultiplier pulse-height spectrum showed it to be 99.9% efficient, so that the monitor signature M represented 99.7% of the pions physically present in the beam. The "data" coincidence D, consisting of particles which counted in M and also in CP (the central photomultiplier) but not in CPA, was the number of pions which had not decayed before reaching the movable Cerenkov counter. Only the ratios D/M were actually used in obtaining the lifetime difference, and all other coincidences listed in Table IV were recorded to help pinpoint malfunctioning equipment, to form part of the basis for data selection, and to have a record of systematic effects present during data taking.

The logic elements represented as blocks in Fig. 17 were standard E. G. G. 100-MHz modules,[43] with the exception of some of the coincidence units which had been modified to have four outputs instead of two. All of

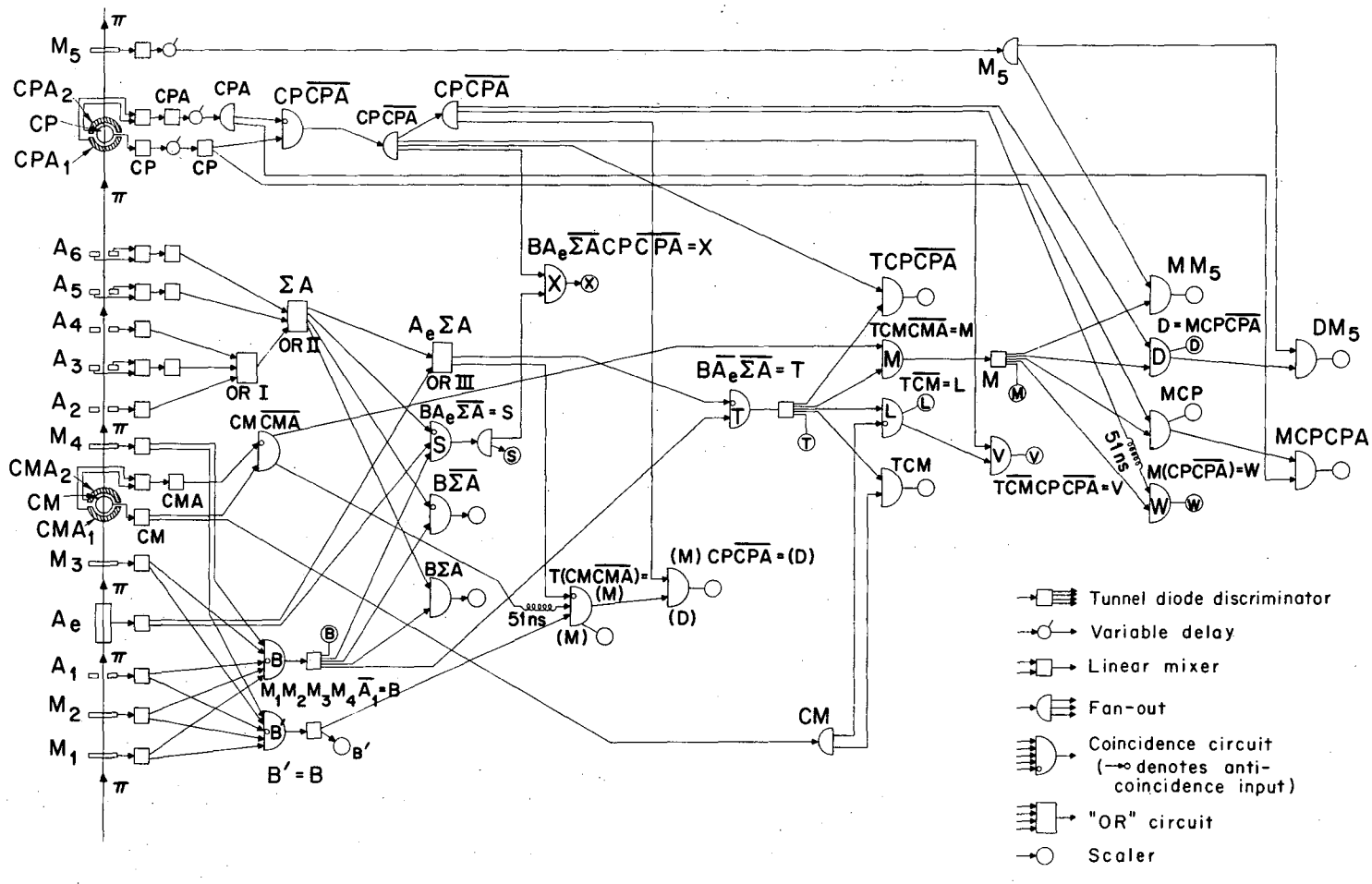

Fig. 17. Block diagram of the electronics used during data taking. All components were E.G.G. 100-MHz fast logic modules.

Table IV. Particle coincidence scaled during data taking.

Coincidence	Scaler	Comments
$M_1M_2M_3M_4\overline{A}_1 = B$	TSI	all beam particles
$B\overline{\Sigma A}$	J(12)	beam particles not vetoed
$B\Sigma A$	J(12)	beam particles vetoed
$BA_e\overline{\Sigma A} = S$	J(2)	beam electrons
$B\overline{A}_e\overline{\Sigma A} = T$	TSI	beam particles, not electrons and not vetoed
$TCM\overline{CMA} = M$	TSI	pion monitor
TCM	TSI	pion monitor without CMA vetoes
$T\overline{CM} = L$	J(2)	not electrons, not pions (mostly muons)
$T(CM\overline{CMA}) = (M)$	J(2)	monitor accidentals: CM delayed
$MCP\overline{CPA} = D$	TSI	surviving pions: "data"
MCP	TSI	data without CPA vetoes
MCPCPA	J(12)	particles vetoed by CPA
$M(CP\overline{CPA}) = W$	J(2)	data accidentals: CP delayed
$(M)CP\overline{CPA} = (D)$	J(2)	data accidentals: CM delayed
$TCP\overline{CPA}$	TSI	data without $CM\overline{CMA}$
$T\overline{CM}CP\overline{CPA} = V$	J(2)	muons counted by CP
$BA_e\overline{\Sigma A}CP\overline{CPA} = X$	J(2)	electrons counted by CP
MM_5	J(12)	monitor particles through M_5 counter
DM_5	J(12)	data with M_5 in coincidence

Key

$\Sigma A = A_2A_3A_4A_5A_6$

A bar over a symbol means anticoincidence. Parentheses indicate an extra delay of 51 nsec to measure accidental coincidences.

Scalers

TSI = 100 MHz, Transistor Specialties, Inc.
J(2) = 10 MHz 2-channel "Jackson" (LRL).
J(12) = 25 MHz 12-channel "Jackson" (LRL).

Table V. Typical values of quantities scaled.

Quantity	Description	Liquid deuterium π^+	Liquid deuterium π^-	Liquid hydrogen π^+	Liquid hydrogen π^-
$S/B\overline{\Sigma A}$	Electrons in monitor	.0755	.349	.043	.207
$B\overline{\Sigma A}/B$	All particles not vetoed	.243	.242	.258	.258
L/T	Muons in monitor	.091	.076	.062	.044
M/T	Pions in monitor	.907	.922	.935	.953
M/second	Pion rate	640	580	1000	960
D/M^*	Surviving pions	.560	.572	.628	.678
DM_5/M^*	Pions traversing CP	.390	.390	.490	.610
V/L^*	Muons counting in CP	.012	.012	.0016	.0016
X/S^*	Electrons counting in CP	.072	.072	.098	.100
(M)/M	Monitor accidentals	.0006	.0005	.0007	.0006
(D)/D	CM-delayed data accidentals	.0004	.0003	.0004	.0004
W/D	CP-delayed data accidentals	.0001	.0001	.0002	.0002

*Ratios depend on CP position along decay path. Values given are those obtained with CP just after A_6.

the photomultiplier signals were "clipped" at the phototube bases in order to have short pulses which would not trigger the discriminators more than once. Discriminator output pulses used for coincidence were 8-nsec long, while those used for vetoing were typically 16 nsec. The anticoincidence counters A_1 to A_6 were an exception to this: their pulses were 40-nsec wide to insure 100% efficiency. All veto counters were run in a "no dead-time" mode; i.e., the output pulses were lengthened to cover the discriminator recovery time. This was particularly important in the case of A_2 to A_6, where any inefficiency or dead time could result in a "halo" of pions outside of the main beam and outside the aperture of CP.

Coincidences were scaled on standard Radiation Laboratory 10-MHz dual Jackson scalers, on a 12-channel, 25-MHz Jackson scaler, and on 100-MHz dual TSI scalers. Table IV indicates the type of scaler used for each coincidence. The contents of all the scalers were read out periodically during data taking onto an on-line IBM automatic typewriter and simultaneously onto an incremental magnetic tape recorder. The latter facility made it possible to punch each printout automatically onto a set of four IBM cards using the CDC-6600 computer, and thus large quantities of data could be analyzed completely within a few hours after acquisition. The ability to do this proved invaluable for pointing out subtle systematic errors while a run was in progress and corrective measures could still be taken.

Table V gives typical values of ratios between the scaled quantities. Notice that the B coincidence involved only scintillation counters and hence included pions, muons, and electrons; the T coincidence had A_e and A_2 through A_6 in anticoincidence, and therefore involved only pions and muons travelling through the central holes of the veto counters; the M coincidence required in addition a count in CM with none in CMA, and hence was pure pions. The fraction of all beam particles counting in A_e was monitored by $S/B\overline{\Sigma A}$, and the fraction of all beam particles which were not vetoed in A_2 through A_6 was measured by $B\overline{\Sigma A}/B$. The T coincidence was composed of both pions and muons, the pion fraction being given by M/T and the muon fraction by L/T. The latter ratio was the fraction of pions and muons <u>not</u> counting in the central photomultiplier of CM, which was mostly muons since CM had 99.9% efficiency for pions (not including the 0.2% of pions vetoed by CMA). Actually, L/T contained small unknown amounts of pions and electrons as well. A measure of the performance of

CM was the quantity M/T, which was equal to the efficiency of CM multiplied by the fraction of pions in T; in the same way, D/M was proportional to the efficiency of CP.

Some of the differences between liquid-hydrogen and liquid-deuterium Cerenkov media in CM and CP which are shown in Table V were due to the difference in beam momenta. Because of the difference in the indices of refraction of liquid hydrogen and liquid deuterium, the pion beam momentum at CP had to be 285 MeV/c when liquid deuterium was used, and 311 MeV/c for liquid hydrogen. Since the electron and muon contaminations increased at lower momenta, this explains the differences in $S/B\overline{\Sigma A}$ and L/T for the two cases. The lower pion rate when liquid deuterium was used was caused by the lower pion production rate and by the increased absorption in CM. Notice that D/M was nearly 8% different on π^+ and π^- when liquid hydrogen was used, but only 2% different when liquid deuterium was used. The 2% difference can be understood in terms of the false M coincidences caused by charged reaction products produced upstream of M_4, and producing counts in M_4. But π^- can produce neutral reaction products and π^+ cannot, making more false monitor coincidences on π^+ than on π^-. Since none of the reaction products could count in CP, this made D/M larger for π^- than for π^+.

The ratios V/L and X/S monitored the fractions of muons and electrons counted by CP, assuming that L and S were purely muons and electrons respectively. These ratios were extremely sensitive to the CP discrimination level (see Fig. 12), providing not only a criterion for setting this threshold, but also serving as good indicators of gain changes in the CP photomultiplier. Of historical interest are the quantities TCM/T and MCP/M, involving only the central phototubes of CM and CP, without

the anticoincidence rings. The two quantities were constructed on the basis of the first experiment, when slow accumulation of diffusion-pump oil on the flask window caused the anticoincidence ring to veto larger and larger fractions of good pions, but not affecting the data taken without the anticoincidence ring. The coincidences without CMA and CPA served to assure us that no such problem existed in this experiment.

The DM_5 coincidences kept track of the data with the 12-in.-square M_5 counter behind the CP to require that the particles counted by CP had not undergone a large deflection in the Cerenkov medium. This greatly reduced the number of interacting particles counted, and gave a ratio DM_5/M which was relatively insensitive to fluctuations in the CP photomultiplier gain. Such gain variations were a problem during parts of the running, and were characterized by values of D/M well outside of allowed statistical fluctuations, but by normal values of DM_5/M. This was a particularly good indicator of gain fluctuations since DM_5/M was formed from the very same particles as D/M, with the exception of roughly 30% which interacted in the Cerenkov medium and produced pulses in the valley of the pulse-height spectrum of CP. As already mentioned, this coincidence was not suitable for the lifetime ratio measurement since it was very sensitive to the vertical position of the pion beam in CP.

Three different types of accidental coincidences were scaled, all of them utilizing a delay of 51 nsec added to one input of a coincidence which would otherwise be properly timed for pions. This delay corresponded to the radio-frequency fine structure period of the cyclotron beam. Thus, (M) was the same as the usual M coincidence except that $CM\overline{CMA}$ was out of time by 51 nsec: any counts in (M) resulted from accidental coincidences between a beam pion or muon (T coincidence) in one radio-frequency bunch

and a count in $CM\overline{CMA}$ from the previous bunch. The accidental coincidences monitored in this way were (M)/M = $CM\overline{CMA}$-delayed accidentals in the monitor, (D)/D = $CM\overline{CMA}$-delayed accidentals in the data, and W/D = $CP\overline{CPA}$-delayed accidentals in the data. The small differences in accidental rates on positive and negative particles were largely caused by a systematic tendency to run with the π^+ rate slightly higher than the π^- rate. Since the accidental rates are extremely small, and nearly the same on the two polarities, no correction has been made for them in the data analysis.

D. Data-Taking Procedure

The experiment was performed by measuring the fraction of surviving pions at each of seven data positions along the 35-ft decay path. These data positions were roughly 6-ft apart and were labelled DP1 through DP7, in order of increasing distance downstream. The beam polarity was alternated frequently between positive and negative particles to cancel the effects of any slow changes in counter efficiencies. CP was usually kept at one position for 6 to 12 hours, and during this time the beam polarity was changed at approximately one-hour intervals. When running on π^+ the proton beam intensity was reduced to 20% of the intensity used for π^- data, to compensate for the difference in production cross sections and keep the pion rates equal on the two polarities. Polarity changes typically took about 10 minutes, which allowed time for the bending magnet fields to reach equilibrium. Each magnet was reversed by switching off the current, changing the polarity of the solid-state power supply, and turning the current back on. The quadrupole currents were set to the same values on both polarities using a potentiometer, while the bending magnet currents were set to give the same central fields using NMR. At the start of each run all the magnet currents were set, and then polarities were reversed twice to establish the standard hysteresis cycle.

In order to achieve approximately the same statistical accuracies on the D/M ratios at different CP positions, we usually counted for equal numbers of D coincidences at all data positions, which required spending about twice as long at DP7 as at DP1. At a particular data position, the scalers were typically read out onto the typewriter and incremental tape recorder every 2×10^5 D coincidences in the following sequence: $/2 \times 10^5\ \pi^+,\ 2 \times 10^5\ \pi^-/2 \times 10^5\ \pi^-,\ 2 \times 10^5\ \pi^+/$etc. Commas denote polarity

changes and the data between two slashes was used to form the ratios f_+/f_-, where f = D/M. The sequence above was normally continued for six polarity reversals, giving a total of six measurements of f_+/f_-, which were the numbers ultimately used to compute the lifetime difference. When CP was at upstream data positions where the rates were higher, scaler readouts were made after 4×10^5 D coincidences, and polarity reversed after two of these printouts: this maintained the time between printouts at roughly one hour, although it gave fewer measurements of f_+/f_-.

Whenever CP was moved to a new data position, vacuum pipe had to be put up or taken down to maintain continuous vacuum between M_4 and CP. This was accomplished without disturbing the veto counters A_2 through A_6 (which were in the vacuum without light-proof wrappings) by closing an 8-in. diameter gate valve just downstream of A_6, allowing the veto counters to be kept under vacuum while air was let into the pipe along the decay path. After CP had been moved and sections of pipe changed, the decay-path pipe was evacuated up to the gate valve using a mechanical pump. During all of this activity, the vacuum was maintained on the veto counters using a mechanical pump, which was cold-trapped with liquid nitrogen to reduce the migration of pump oil onto the scintillator and light-pipe surfaces. After the decay-path vacuum had been established up to the gate valve, the roughing pump was valved off and the gate valve opened, the entire vacuum then being maintained by the cold-trapped pump.

One of the most important checks of systematic errors was the measurement of the absolute lifetime. While the absolute value of the lifetime could not be measured any more accurately than the beam velocity was known, the decay curve (D/M plotted against distance) should have been a pure exponential, and this could be checked very accurately using the

lifetime ratio data. For this reason we chose to spend a large fraction of the data-taking time at data positions other than DP1 and DP7, even though there is a great statistical advantage to spending most of the time at these two end points. Ideally, one would like to visit various data positions at random in order to detect any possible change in CP efficiency with time, and we tried to adhere to this philosophy as much as possible. When CP was moved downstream, however, the new sections of pipe which were installed had to be carefully aligned, making it more efficient to move CP downstream in large jumps, and then move back upstream in smaller steps. A typical sequence of data positions during a one-week run might start at DP4, where the beam was smallest, for systematic studies, followed by data at the following positions: DP4-DP7-DP5-DP3-DP1-DP6-DP4-DP2-DP1-DP7. This type of schedule tended to shuffle the order of data positions without spending too much time moving CP. An effort was made to spend some time at all seven positions, and to return to as many as possible to check reproducibility directly.

Although the data analysis will be discussed in detail later, the essential idea behind the lifetime-difference measurement can be introduced at this point. The data consisted of the experimental values f_+/f_- at a number of distances along the decay path. These numbers were essentially the ratios of the fraction of π^+ in the beam to the fraction of π^- in the beam. If the lifetimes of π^+ and π^- were the same, the ratio ought to have remained constant all along the decay path, but if for instance π^+ were longer-lived than π^-, then f_+/f_- would increase at larger distances downstream. By keeping track of this ratio during the data taking, it was possible to check the consistency and repeatability of the data, as well as to observe preliminary indications of any lifetime difference.

IV. SYSTEMATIC ERRORS

A. Equality of Momenta of the Positive and Negative Beams

If the π^+ and π^- beams had slightly different momenta, then a lifetime difference would have been detected in the laboratory system and attributed to an actual lifetime difference in the pion rest frame. A number of precautions were taken to insure that the positive and negative beams did have the same momentum: magnetic shielding reduced the nonreversing cyclotron fringe field to less than 0.2 gauss along the beam line, and nuclear magnetic resonance devices in the two bending magnets guaranteed long-term stability and equality of the central fields on π^+ and π^- to 0.005%. In addition to these precautions, three types of measurements were made on the positive and negative beams themselves, and none of these indicated any momentum difference.

The first test involved a direct measurement of the momentum distributions and mean momenta of the positive and negative beams. An auxiliary bending magnet was placed in the beam after A_6, as shown in Fig. 18. The asymptotic entrance and exit trajectories of individual pions were recorded by four wire spark chambers, SC1 through SC4. The vertical component of the H-magnet's field had been previously measured at points along the beam path so that a unique momentum could be assigned to each set of pion entrance and exit trajectories. The bending magnet's field was mapped at several currents, and at each of five different elevations at points on 1-in. square grids. These field maps were made on both magnet polarities, and with the magnet actually in place so as to take into account the effects of the cyclotron fringing field and various ferromagnetic structures in the area.

The first three spark chambers were each 1-ft square, while SC4 was

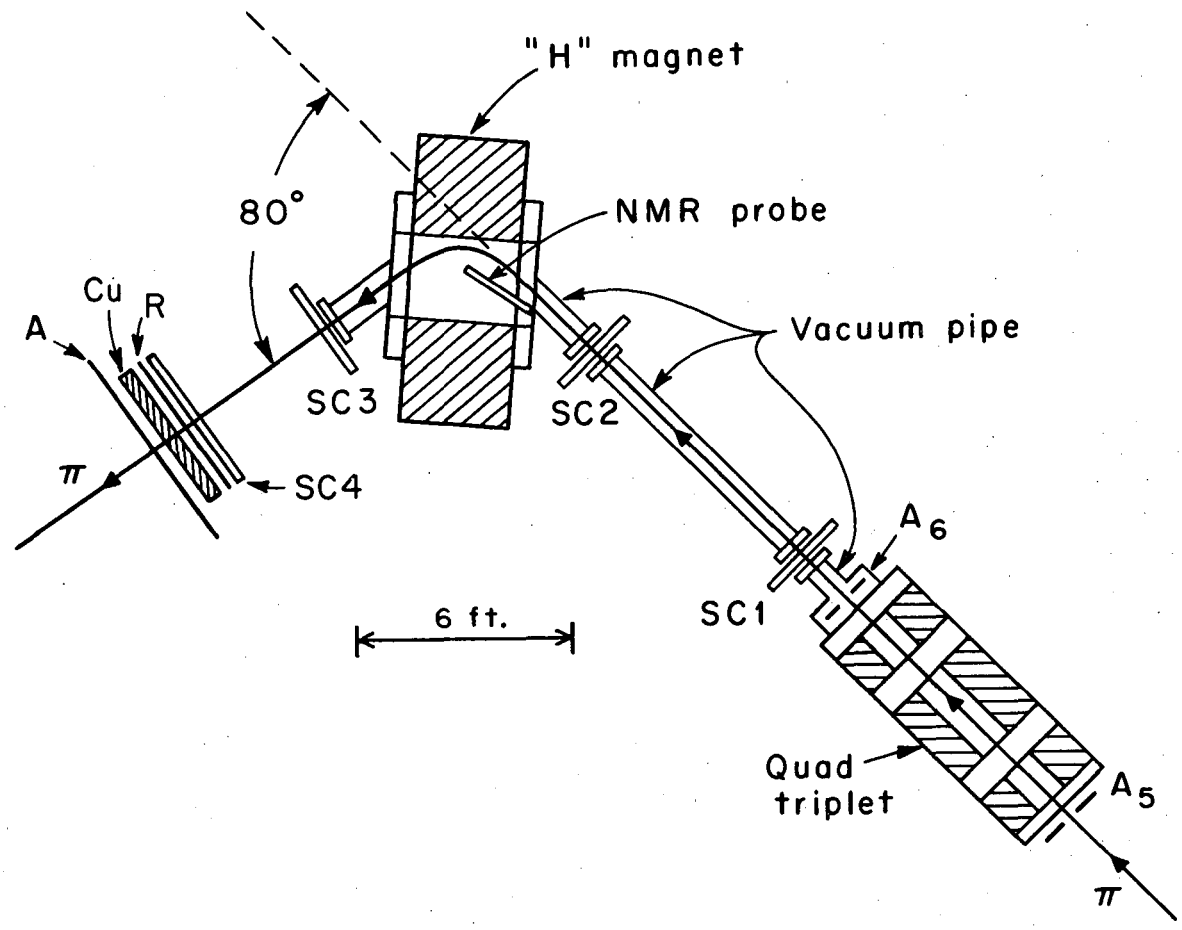

XBL687-3445

Fig. 18. Experimental arrangement used during the spark-chamber momentum analysis. R and A were 0.5-in.-thick scintillation counters which were sometimes used to trigger the chambers on particles that stopped in the 0.5-in.-thick copper block, Cu.

1-ft high by 2-ft wide. Each chamber had four planes of parallel 0.006-in.-diameter aluminum wires with 26 wires per inch. The wires in each of the four planes of a chamber were oriented at 0 deg, 60 deg, 90 deg, and 120 deg to the horizontal. When a particle passed through a chamber and the high-voltage pulse was applied, two sparks were produced: one between the 0-deg and 60-deg planes, and one between the 90-deg and 120-deg planes. The coordinates of each spark could be reconstructed from the timing of the pulses produced in the magnetostrictive wands which passed over the ends of the wires of each plane. Multiple sparks could be detected since two pulses from each wand were recorded. Particle tracks produced two sparks at the same position in a particular chamber, eliminating ambiguities due to spurious sparking. Only those events which had two coincident sparks in each of the four chambers were accepted for analysis. Figure 19 shows typical distributions of particles in SC2, SC3, and SC4.

The spark-chamber momentum analysis was beset by several serious difficulties. First of all, the measurements were made just before the installation of CP, when it was still believed that most of the running would be done with liquid hydrogen as the radiating medium. Only one set of measurements was taken with liquid deuterium in CM. These gave quite unreasonable results, probably because they were the first measurements taken with the system, before the operation of the chambers was fully understood. Later measurements taken with liquid hydrogen in CM gave believable results, but even these were open to question in light of our inability to explain the earlier poor results. Part of the difficulty was that a reliable identification of pions was hard to devise. If the chambers were triggered on the pion monitor M in coincidence with a count in a 1-ft by 2-ft scintillation counter R behind SC4, a considerable

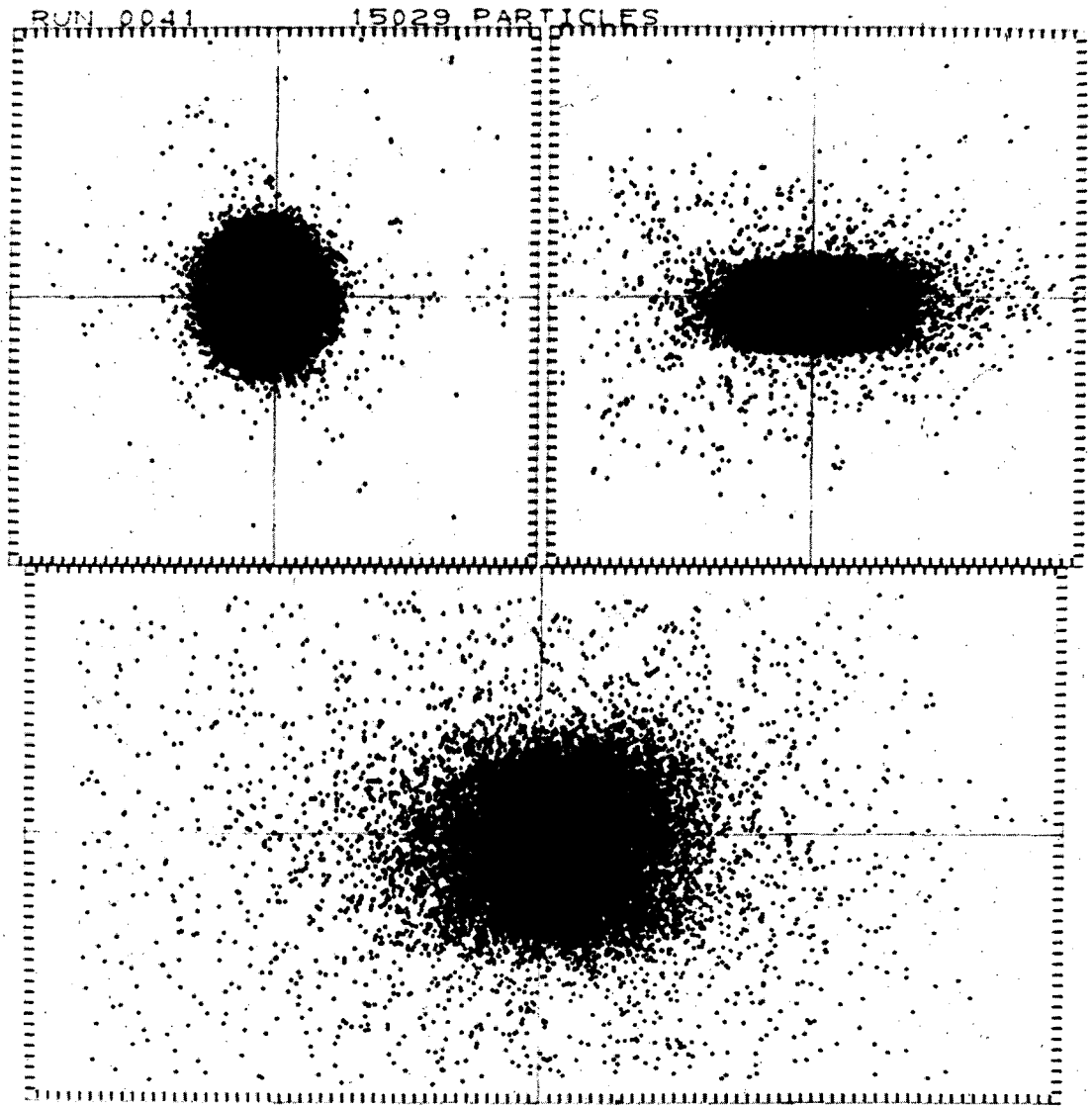

XBB 687-4583

Fig. 19. Beam profiles obtained during the spark-chamber momentum-analysis. Profiles shown are for SC2 (top left), SC3 (top right), and SC4 (bottom). Each dot represents the position at which a particle passed through the chamber. Note the effect of the bending-magnet fringe-field focusing in the SC3 profile. Scale: 1 division = 1/4 in.

number of decay muons were included. A system which seemed to work fairly well was to trigger the chambers on those particles which counted in M and which stopped in a 1/2-in.-thick block of copper behind SC4. The trigger required a count in R(in front of the copper) but no count in a scintillator A (behind the copper); this arrangement is shown in Fig. 18. Only pions stopped in the copper, by virtue of their strong interactions, while decay muons continued on through. Even this scheme was not entirely effective, although it gave reasonable results.

The worst problem was the long sensitive time of the chambers, which was found to be about 25 μsec. Thus, when the chambers were pulsed to look at the track of a particle satisfying some coincidence criterion, sparks were formed not only along the path of the desired particle but also along the path of any other particle which had passed through the chamber during the previous 25 μsec. The spurious track could be due to any particle whatsoever, regardless of whether it was a good pion, a scattered pion, an electron, or a muon. Furthermore, it was even possible that the sparks from the spurious particle could inhibit the formation of sparks along the desired particle's path. This problem could be solved completely only by running at such low rates that the accuracy of the results would have been severely limited by statistics.

The results of the spark-chamber momentum analysis are shown in Table VI. The nominal momentum ("Nom. p") given in the table is the momentum at the first bending magnet, as determined from the wire-orbit measurements. The "No. pions" column gives the number of particles which were momentum analyzed for the particular measurement. The momenta p_1 and p_2 are the computed means of the momentum distributions, using particle

Table VI. Results of the spark-chamber momentum analysis

Pol.	Nom. p (MeV/c)	No. pions ($\times 10^{-3}$)	S.C. Trig.	$\bar{p}=(p_1+p_2)/2$ (MeV/c)	$(p_1-p_2)/\bar{p}$	$(p_+-p_-)/\bar{p}_+$
			Liquid hydrogen in CM			
+	330	12	M	312.66	0.26%	- 0.004%
-	330	11	M	312.67	0.25%	
+	330	22	MR$\bar{A}$	312.69	0.27%	- 0.03%
-	330	15	MRA	312.80	0.27%	
+	330	17	TR$\bar{A}$	312.56	0.36%	+ 0.05%
-	330	20	TRA	312.41	0.35%	
+	330	19	MR$\bar{A}$	312.52	0.37%	+ 0.02%
-	330	23	MRA	312.45	0.35%	
+	320	5	MR	302.65	0.22%	+ 0.05%
-	320	5	MR	302.21	0.23%	
+	320	17	MR$\bar{A}$	302.58	0.36%	+ 0.19%
-	320	22	MRA	302.01	0.17%	
+	320	20	MR	302.59	0.33%	+ 0.20%
-	320	20	MR	302.00	0.31%	
			Liquid deuterium in CM			
+	300	6	TR	280.31	0.26%	+ 0.68%
-	300	5	TR	278.46	0.23%	
			CM moved out of beam			
+	330	17	TR$\bar{A}$	326.62	0.38%	- 0.17%
-	330	19	TRA	327.17	0.36%	

positions in SC1, SC2, and SC3 to find p_1 and in SC2, SC3, and SC4 to find p_2. The agreement between the two results gives a measure of the reliability of the method. The averages for positive and negative particles, p_+ and p_-, were compared to find the momentum difference between the two beams. The momentum distributions had identical shapes for π^+ and π^-, but their higher moments were probably due to multiple scattering in the chambers rather than to the momentum populations of the beams. Taking the difference between p_1 and p_2 as an indication of the error on the plus-minus momentum difference, it can be concluded that the π^+ and π^- beams had the same momentum but only to an accuracy of 0.3%. Even if the measurement made with liquid deuterium in CM is ignored, the result is not nearly precise enough for our purposes. Because of the unreasonable and yet unexplained momentum difference obtained with liquid deuterium in CM, and the generally low precision finally obtained for other configurations, any meaningful statement about the equality of momenta of the positive and negative beams must be based on the other two measurements, described below.

The second method used to compare the momenta of the positive and negative beams was to measure the efficiency of CP as a function of momentum in the region of the pion peak (see Fig. 16). By comparing the steeply sloping sides of the π^+ and π^- peaks, it was possible to detect momentum differences as small at 0.02%, as already discussed under Cerenkov-counter performance tests. When these curves were measured, care was taken to use the same hysteresis cycle on the two polarities, and some points were repeated at the end of the measurement as a check on reproducibility of the points. The results of six different determinations made under a variety of conditions are shown in Table VII, including measurements made during two of the three runs in which usable data was taken.

Table VII. Summary of the momentum-response-curve measurements of the π^+-π^- momentum difference.

Counter used	Cerenkov medium	$(p_+ - p_-)/\bar{p}$	Comments
CM	hydrogen	$-0.01 \pm 0.02\%$	measured before CP installation
CP	hydrogen	$-0.02 \pm 0.02\%$	
CP*	deuterium	$+0.02 \pm 0.04\%$	two measurements made during the same run
CP*	deuterium	$-0.02 \pm 0.01\%$	
CP*	deuterium	$-0.02 \pm 0.005\%$	
CP	deuterium	$-0.045 \pm 0.010\%$	measured with CM moved out of the beam

*Data taken during the runs in which these measurements were made was used in the final lifetime-ratio computation.

The third method used to compare the π^+ and π^- momenta involved a comparison of the flight times of pions from M_4 to the end of the decay path. In order to have the longest possible flight path, the measurement was made after all the data running had been completed and CP had been removed, giving a total distance of 87 ft between the two time-of-flight counters. The systematic errors involved in this method were considerably smaller than those which entered into the spark-chamber momentum analysis, because we were able to use the electrons in the beam as a velocity reference (310-MeV/c electrons had exactly the velocity of light for all practical purposes). By comparing the time-of-flight of π^+ to e^+ and of π^- to e^-, it was possible to compare π^+ with π^- to very high precision.

The electronic arrangement used is shown schematically in Fig. 20. T_1 and T_2 were 2.25-in.-square, 1/2-in.-thick scintillation counters viewed by RCA-8575 photomultipliers through short lucite light-pipes, designed to reduce the time jitter in the light collection as much as possible. T_1 was placed just after CM and T_2 was 87-ft downstream, at the end of the

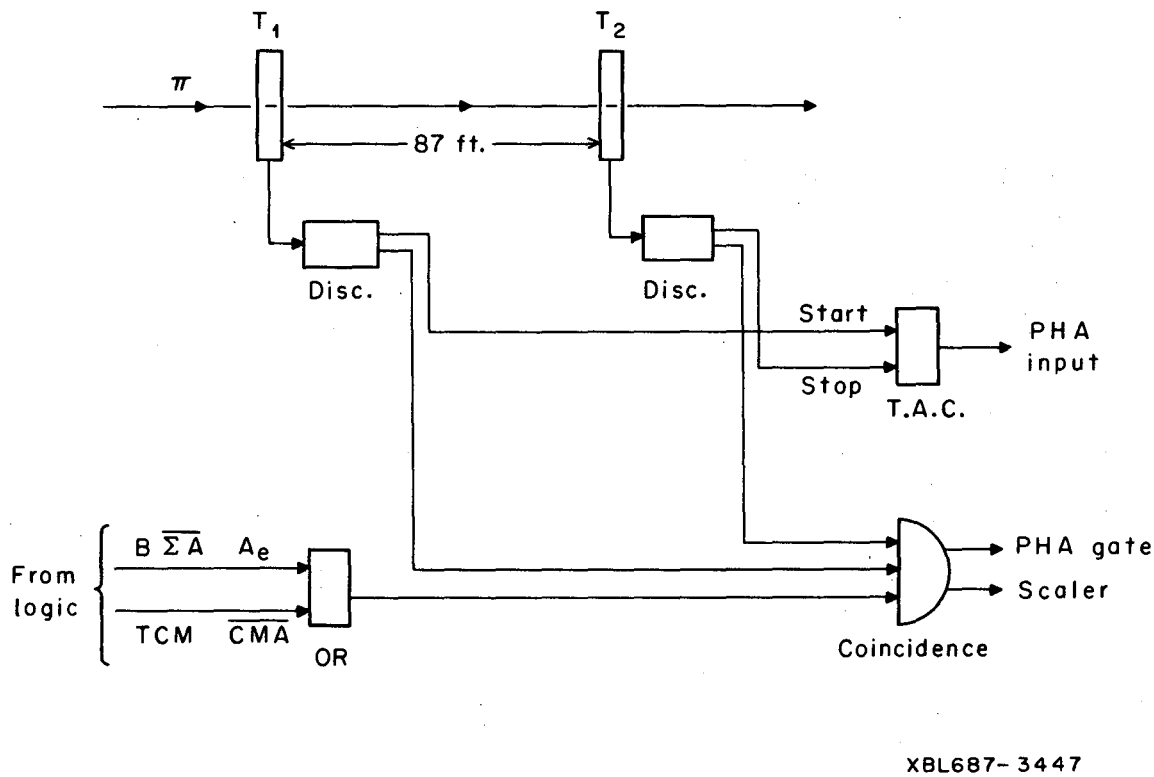

Fig. 20. Electronic arrangement used for the time-of-flight measurements. T_1 was located between M_4 and CM, while T_2 was at the end of the decay path. Disc. = tunnel-diode discriminator, T. A. C. = time-to-amplitude converter, PHA = pulse-height analyzer.

decay path. The time-of-flight between the two counters was changed to a voltage pulse suitable for pulse-height analysis by an E. G. G. time-to-amplitude converter (TAC), whose output pulse had an amplitude proportional to the delay between the input START and STOP pulses. The output of the TAC was analyzed by a pulse-height analyzer (PHA),[42] which was gated on coincidences between T_1 and T_2, and either an electron (S coincidence) or a pion (M coincidence) signature from the logic. In this way, the time-of-flight spectra of electrons and pions were accumulated simultaneously, and small drifts in the TAC or the PHA gains affected both spectra equally without changing their mean separation. A typical time-of-flight spectrum, with the analyzer gated on all beam particles, is shown in Fig. 21. The shoulder on the high-velocity side of the pion peak was due to muons from pion decay between T_1 and T_2, but since most of the muons did not stay in the beam, they constituted only a very small background which was the same on π^+ and π^-.

In order to calibrate the gain of the analyzer, and to insure that this calibration remained valid during the time-of-flight measurements, the arrangement shown in Fig. 22 was used as an alternative input to the TAC. The START pulse was supplied directly by a pulse generator, while the STOP pulse was generated indirectly from the START signal, through a diode light pulser and a photomultiplier. The photomultiplier output pulse was used instead of the pulse generator directly to introduce time jitter into the delay, so that the calibration pulses would fall into more than one analyzer channel. The arrangement shown produced a Gaussian distribution whose center could be found quite accurately from the PHA output. The center of this distribution was then shifted by a known time delay by inserting a precisely calibrated cable in the START side, and thus the number of channels/nsec could be measured. The calibration peaks

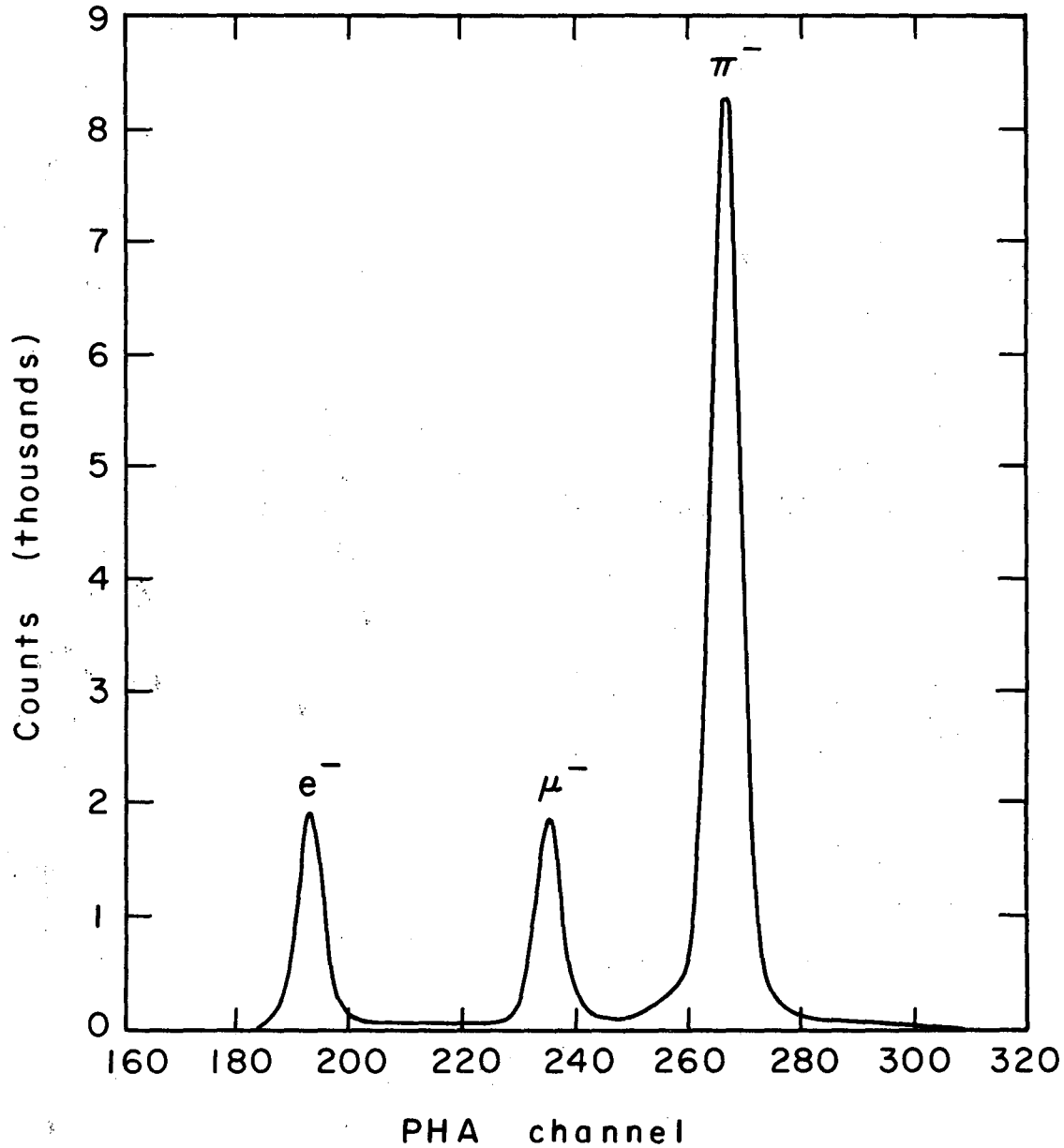

XBL687-3443

Fig. 21. Typical time-of-flight spectrum, obtained with T_2 near DP7 (and not at the full distance downstream).

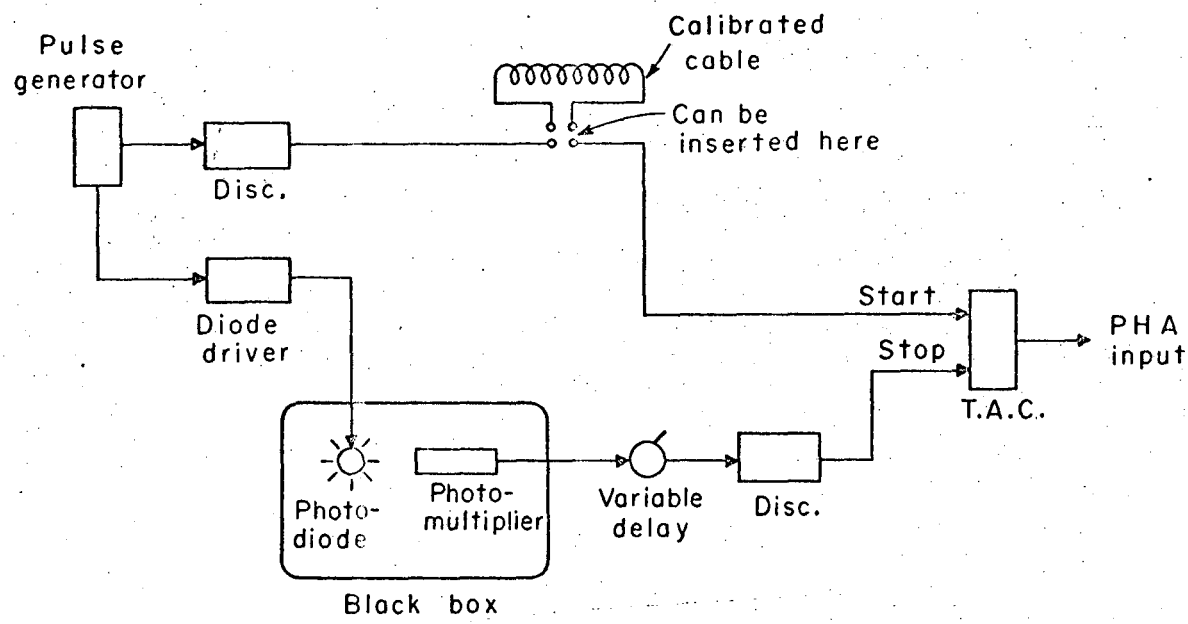

XBL687-3448

Fig. 22. Electronic arrangement used to calibrate the T.A.C. - PHA system during running. The variable delay could be adjusted to place the calibration peaks in the region of interest on the PHA.

were made to occupy the same regions of the TAC and the analyzer as the pion and electron peaks, and calibration runs were interspersed with particle runs to monitor the overall gain of the system. While small drifts were actually observed, these were all of the sort which would change the absolute positions of the pion and electron peaks, but not the number of channels between them.

Three measurements of the time-of-flight difference between pions and electrons of both polarities were made, giving an average of 107.55 channels between π^+ and e^+, and 107.58 channels between π^- and e^-. Since one channel was equivalent to a momentum difference of 0.455%, the final result was

$$\frac{p_+ - p_-}{\bar{p}} = +0.014\% \pm 0.019\%,$$

where the uncertainty is the standard deviation of the mean for the three determinations.

Some mention should be made about the relative merits of measurements on the beam momenta versus those on the beam velocities. All of the results above are stated in terms of momentum differences because a given percentage difference in plus and minus momenta would produce the same percentage difference in the lifetimes, e.g. if the π^+ momentum were 1% higher than the π^- momentum, the π^+ lifetime would be observed to be exactly 1% longer than the π^- lifetime. But it is important to recognize that what was actually checked in the last two types of measurement was the equality of π^+ and π^- <u>velocities</u>. This is obvious for the time-of-flight method, but is also true for the momentum-response-curve comparison, since the Cerenkov angle depends on the pion velocity (not the momentum). Consequently, our measurement of the lifetime ratio was independent of any possible difference in the π^+ and π^- masses, although in fact, the masses are known

to be equal to 0.036%, which would be sufficient for our purposes.[21] The experiment measured the lifetime ratio in the laboratory system, and if the velocity difference between the π^+ and π^- beams was known, the lifetime ratio could be found in the pion rest frame. But if the <u>momentum</u> difference were measured, then an assumption about the equality of masses would be needed to obtain the velocity difference required to find the lifetime ratio in the pion rest system.

B. Beam Containment Along the Decay Path

It was important that the pion beam be fully contained within the aperture of CP, in order that small spatial differences between the π^+ and π^- beams not bias the lifetime-ratio measurement. The effective aperture of CP was obtained at the beginning of every data run by measuring the widths of the flat regions of the lateral and vertical profiles (see Fig. 15) at DP4, where the beam was smallest. Furthermore, the centering of the Cerenkov counter on the beam was checked by similar profiles at other data positions, particularly at the last one where the beam was largest. In fact, for a few runs, DP7 was not used at all because the profiles showed that the effective aperture of CP was not large enough to contain the beam with certainty. Such conditions changed from run to run depending on the central photomultiplier being used in CP at the time.

The most direct method of measuring beam sizes and positions was to employ one of the 12-in.-square magnetostrictive spark chambers used for the momentum analysis. This was a particularly effective means for comparing the π^+ and π^- beams, since the chamber was not moved during the polarity change, and the relative positions and shapes of the two spatial distributions could be measured very accurately. Typical profiles obtained on a single polarity are shown in Figs. 23, 24, and 25, for DP1, DP4, and DP7 respectively. The background of particles outside the main beam was due to accidental detection of unwanted particles along with the desired particle, due to the long (25-μsec) sensitive time of the chambers, and in some cases was due to serious spurious sparking not associated with real particles. Evidence for this interpretation can be seen in Fig. 23, the beam profile just downstream of A_6. Since A_6 was in anticoincidence

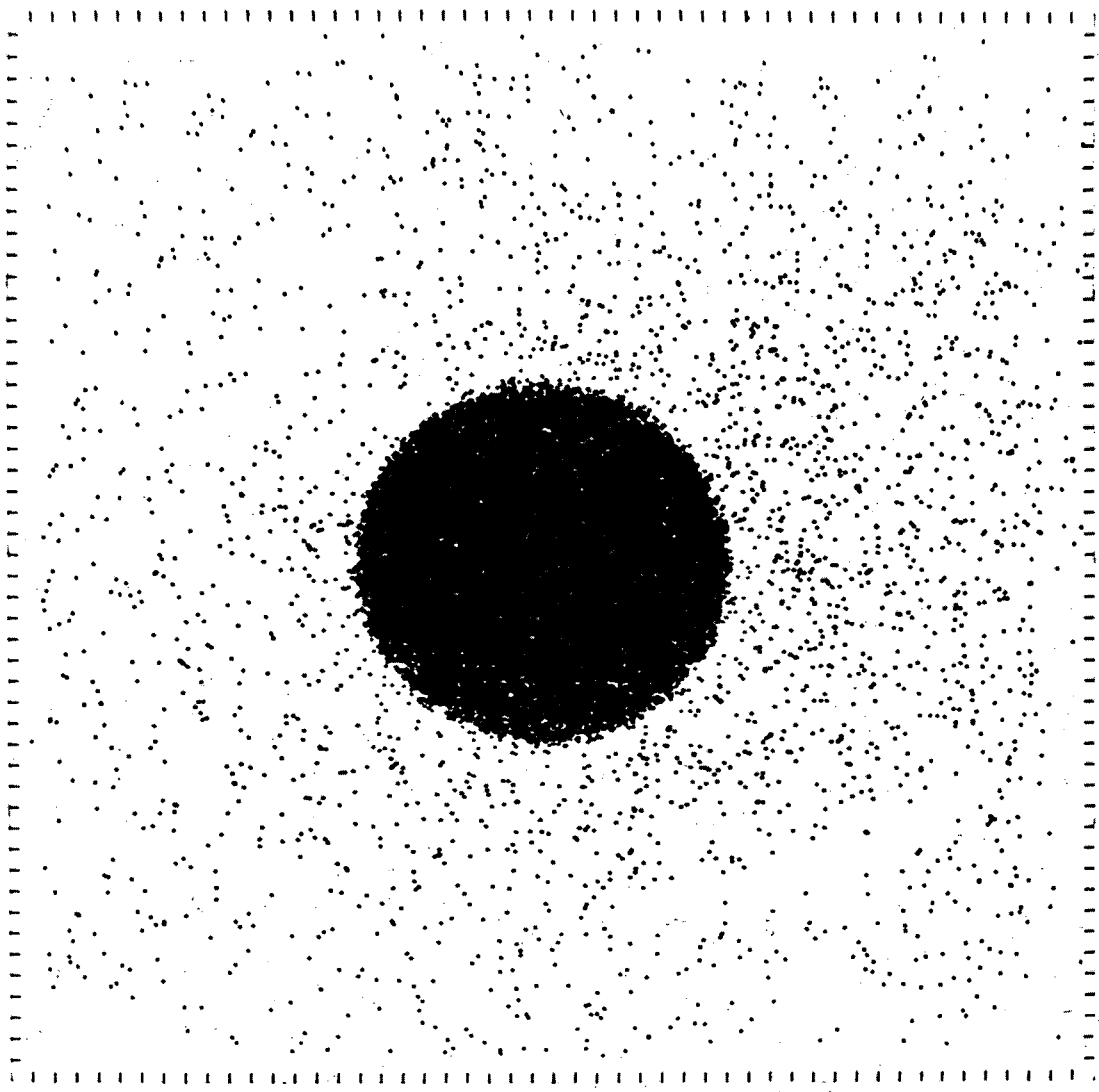

XBB 687-4584

Fig. 23. Spark-chamber beam profile at DP1, consisting of 27,882 particles. The sharp cut-off of the main beam was due to beam definition by A_6, which was about 1-ft upstream. Background counts outside the main beam were caused by accidental inclusion of additional particles within the long sensitive time of the chamber. Scale: 1 division = 1/4 in.

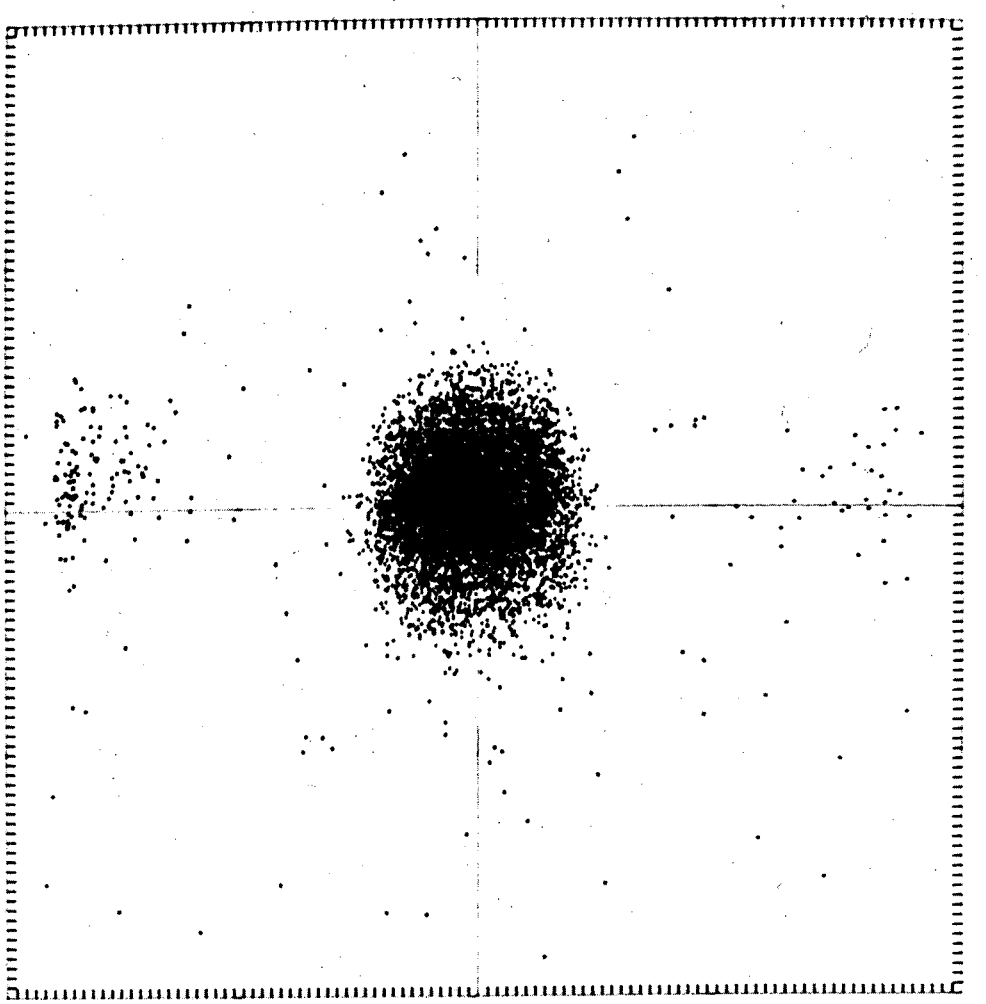

RUN 0116 7135 PARTICLES

XBB 687-4585

Fig. 24. Spark-chamber beam profile at DP4 (210-in. downstream of DP1), consisting of 7,135 particles. The clusters of particles outside the main beam were caused by spurious sparks. Scale: 1 division = 1/8 in.

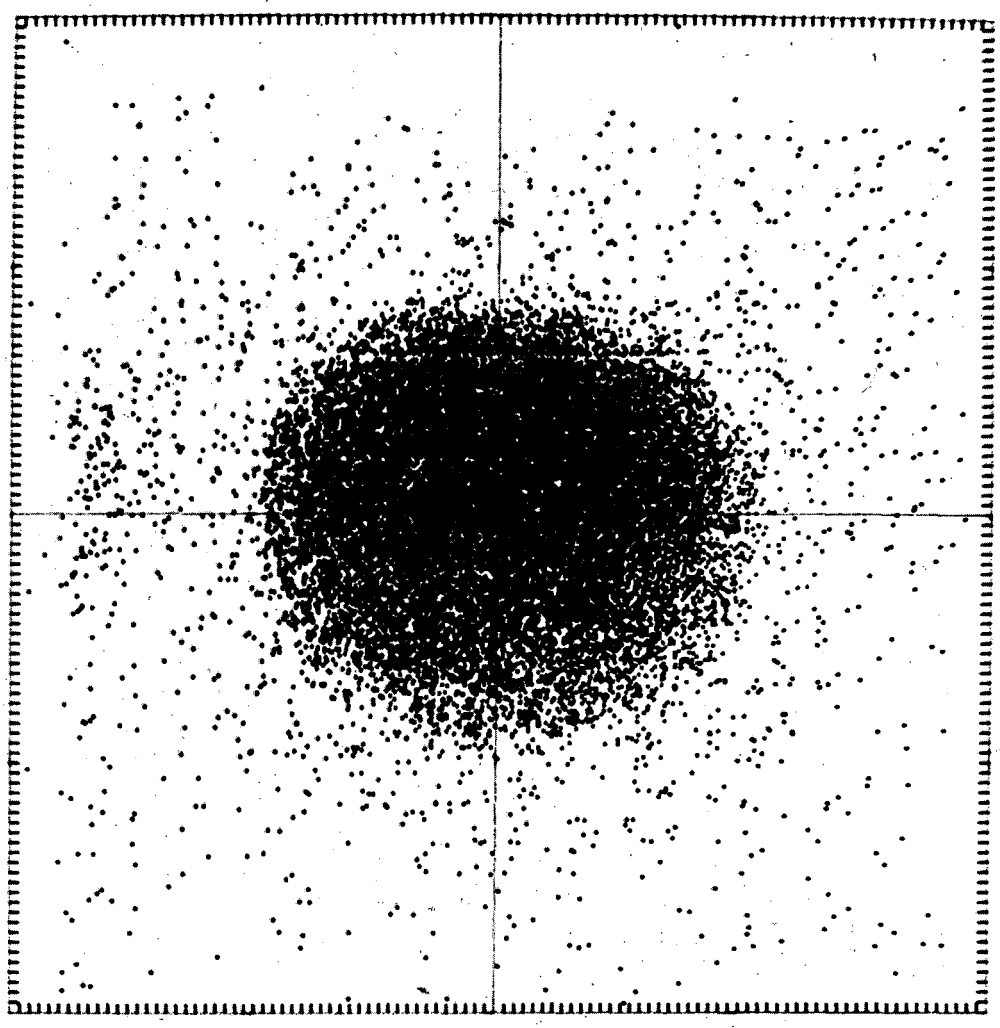

RUN 0121 20672 PARTICLES

XBB 687-4582

Fig. 25. Spark-chamber beam profile at DP7 (427-in. downstream of DP1), consisting of 20,672 particles. Scale: 1 division = 1/8 in.

in the spark-chamber trigger, there should have been no particles outside the 4.5-in. diameter of the A_6 hole. Further tests were made with a small, thin scintillator behind the chamber and in the trigger, and they also showed a uniform distribution of background particles outside the allowed area. This effect made the spark chamber unsuitable for any determination of beam containment, but it was still the best way to compare the π^+ and π^- beams.

The spark-chamber profiles showed the positive and negative beams to have identical spatial distributions, and also measured the gradual horizontal separation of the centers of the two beams with increasing distance along the decay path. This separation was due to the remaining cyclotron fringe field, which was not completely eliminated by the magnetic shielding used around the decay-path vacuum pipe. The horizontal separation of the two beams reached a maximum of 0.154 ± 0.065 in. at DP7, while no evidence for significant vertical separation was seen, the maximum of 0.034 ± 0.051 in. occuring at DP7.

Figure 25 shows that the beam was approximately 6.5-in. wide by 5.75-in. high at DP7, and therefore somewhat wider than the horizontal aperture of CP. To correct the situation, the diamter of the hole in A_3 was reduced to its final value of 2.00 in., as given in Table II. The beam at DP7 was then found to be roughly circular with a diameter of 5.5 in.

Another way in which the beam size and containment was checked was to mount a thin 1-in.-square counter in front of CP, and use it in coincidence with CP to survey the horizontal and lateral intensity distributions of the beam. Profiles obtained in this way gave beam sizes, distributions, and plus-minus displacements which agreed with the spark-chamber results. While the profiles were very steep-sided, they fell only

to the 0.1% level outside the main pion beam, an effect which was due to the low-efficiency counting of decay muons by CP. The decay muons were emitted at angles up to 7 deg in the laboratory, and hence produced a halo of muons outside the main pion beam. The tails on the CP beam profiles were identified as muons by placing varying amounts of lead absorber in front of the 1-in.-square counter; the range of the particles in the tails corresponded to decay muons and not to beam pions. The distribution of particles in the muon tails was found to be identical on π^+ and π^-.

Before the tails of the beam profiles were recognized as decay muons, they were attributed to poor containment of the pion beam. The magnitude of the tails was completely insensitive to relatively drastic changes in the high voltages of A_2 through A_6, and did not change when the A_3 counter was rebuilt with a smaller hole. The possibility that the tails were caused by pions counting in the thin lucite light-pipe of M_4 by Cerenkov light was considered, and eliminated by replacing M_4 with two overlapping scintillation counters whose light pipes did not overlap. A coincidence between these two counters (M_{4A} and M_{4B}) was required, and the output of the coincidence unit used in place of the old M_4 discriminator output. While the change had no effect whatever on the magnitude of the tails, it was regarded as a useful precaution and the arrangement was used throughout all of the data taking.

A final check on beam containment was the calculated value of the pion absolute lifetime, and the shape of the decay curve. The test required that the efficiency of CP remain constant over long periods of time, and hence was best performed with π^- and liquid hydrogen as the radiating medium, which gave the cleanest pulse-height spectrum and made the counter least sensitive to changes in photomultiplier gain.

Unfortunately, slow changes in phototube gain coupled with the poor pulse-height distribution when liquid deuterium was used, made this test less than definitive for the runs during which the lifetime ratio was actually measured. However, the π^- data taken with liquid hydrogen gave a good fit to a pure exponential decay curve, and an absolute lifetime of 25.97 ± 0.04 nsec, to be compared with the most accurate π^+ lifetime value[44] of 26.02 ± 0.04 nsec. The value of the pion velocity used for our determination was measured by a time-of-flight method similar to that already described. The determination is treated in detail in reference 45.

C. CP Performance

The single most important source of systematic errors turned out to be the movable Cerenkov counter. While many biases were eliminated by using liquid deuterium instead of liquid hydrogen as the radiating medium, there were a number of undesirable aspects of the movable counter's performance which had to be considered as possible sources of systematic bias. The three worst problems with CP to be discussed here were (1) the counting of electrons and muons by CP, (2) the central photomultiplier's nonuniformity of response, and (3) the erratic gain fluctuations observed in some photomultipliers which were tried in CP. Some aspects of these difficulties have already been discussed in detail in the section on Cerenkov counter operation and will only be summarized here.

The relatively large efficiency of CP for counting electrons and muons resulted from the fact that this counter could not be operated like CM, which counted only particles which had traversed the entire Cerenkov medium and produced a count in M_4. The very fact that CM worked so well, however, reduced the seriousness of this shortcoming in CP. The monitor coincidence M was more than 99.95% pions, containing less than 0.01% electrons and less than 0.04% beam muons. Thus, the only particles which were eligible to count in CP were pions and the muons from pion decay between CM and CP. Most of these muons left the beam physically because they were produced at relatively large angles in the laboratory, and the remainder counted with 1% efficiency in CP. Furthermore, the counting of decay products was the same for π^+ and π^- (see Table V), and could not bias the measurement of the lifetime difference, which was already known to be quite small. At the beginning of every

data run, the CP discriminator level was adjusted to reduce the efficiency for counting beam muons and electrons to about 1% and 7% respectively, and these counting rates were monitored continuously during the data taking. It should be emphasized again that these electrons and muons counted by CP were not included in the D coincidence, since they had been eliminated from the monitor by A_e and CM. These counting efficiencies can only be regarded as an indication of the actual efficiencies for counting decay products.

The most serious difficulties with CP were caused by the characteristics of the central photomultiplier, an RCA-4522 with a 4.5-in. diameter, high quantum efficiency, bialkali photocathode. Our efforts to find a phototube with a uniform response have already been mentioned; the correlation between the position of a pion entering the CP flask and the portion of the photocathode illuminated by its Cerenkov light, translated the nonuniformity of response of the photocathode directly into a nonuniformity of efficiency across the face of the counter. The magnitude of the effect was directly related to the peak-to-valley ratio of the pulse-height spectrum, making the problem worst when liquid deuterium was the radiating medium. Curves like those shown in Fig. 15 were typical of the efficiency variations seen during data taking. Although the curves shown indicate a fairly uniform lateral response, this was not always the case. A lateral variation in efficiency was particularly serious because of the gradually increasing horizontal separation of the positive and negative beams along the decay path. For example, if CP were moved downstream, one sign of pion would be counted with gradually increasing efficiency, and the other with decreasing efficiency. The second type of particle would then appear to have a shorter lifetime. If

a lifetime comparison were to be based on data taken only at DP1 and DP7, with a plus-minus beam separation of 0.25 in. at DP7 and a linear change in efficiency of 1%/inch, then an apparent lifetime difference of 0.25% would be found! For all the data runs used in the final analysis, corrections to the lifetime ratio due to the lateral efficiency variation across the face of CP were less than 0.03%.

A second and more serious problem with the CP central photomultiplier was that particular phototubes exhibited significant gain variations over periods of time shorter than one-half hour. This sort of fluctuation could easily affect π^+ and π^- in different ways, since polarity was changed only once an hour on the average. Although the net effect of the fluctuations ought to have been the same on the two polarities over long enough periods of time, data taken under such conditions was not used in the analysis. Such data was characterized by values of χ^2 per degree-of-freedom (χ^2/D) significantly larger than unity for the least-squares fit used to find the lifetime ratio. The blame could be traced to the CP central photomultiplier in such cases because observed fluctuations in various monitor quantities (such as M/T, $S/B\overline{\Sigma A}$, etc.) were no larger than expected from statistics. Furthermore, χ^2/D was almost always unity for the fit to the DM_5 data, which was characterized by a pulse-height distribution with a much deeper valley and was therefore less sensitive to fluctuations in CP gain. Selecting data on this basis turned out to be very simple, since runs characterized by bad χ^2/D could not be "saved" by throwing out the points with the largest fluctuations. Such a procedure resulted in an improved χ^2/D, but it was never improved to the point of being usable (less than 1.2) until more than half of the data had been thrown out. Thus, a run was either good or bad from the start,

and either all the data was usable or none of it was. By keeping close watch on the data as it was acquired, and by making full use of the fast data analysis made possible by the incremental tape recorder, it was possible to detect runs with bad fluctuations before too much time had been wasted. In such cases, the CP phototube could often be exchanged for another one, although this usually meant at least a 12-hour delay while the gain of the new tube came to equilibrium.

Data taken with liquid hydrogen provides a good example of the effect of the different peak-to-valley ratios for π^+ and π^- (see Fig. 13), and of the importance of changing polarities frequently. A typical hydrogen run with a "bad" photomultiplier had χ^2/D values of 2.99 for the π^+ absolute-lifetime fit, 1.54 for the π^- absolute-lifetime fit, and 1.80 for the lifetime-ratio fit. Even with relatively stable photomultipliers, there were slow gain fluctuations which cancelled out of the lifetime-ratio data if polarities were reversed often enough, but led to χ^2/D values considerably higher than unity for the absolute-lifetime fit.

A number of tests were made to insure that the various shortcomings of CP were at least the same on positive and negative particles. The pulse-height spectra from the central photomultiplier were identical on the two polarities providing liquid deuterium was the radiating medium (Fig. 13). The momentum response curves (Fig. 16) were measured on both polarities and found to be identical; in this connection, the comparison of the steep sides of the pion peaks as a check on the equality of velocities in the two beams can also be regarded as a test of the similarity of CP response to π^+ and π^-. Any difference in the response of CP caused by rate dependencies was minimized by running π^+ and π^- at the same rates ($\pm$ 10%; see Table V) during data taking. The efficiency of CP was measured

with the flask emptied of liquid and found to be less than 0.01% of the flask-full efficiency, on both π^+ and π^-; this test was also performed on CM with the same result.

D. Biases Related to the Use of Liquid Hydrogen

Up to this point it has been inferred that liquid deuterium was used as the Cerenkov medium only as a precaution against unknown systematic effects which might have been associated with the use of liquid hydrogen, without knowledge of any specific mechanisms. In fact, this was not the case. Liquid deuterium was extremely difficult to handle even after the regulating system had been perfected: both CM and CP had to be maintained in a precarious equilibrium, and a single mistake often cost 12 hours of running time. The greater number of interactions in liquid deuterium made it very difficult to achieve flat lateral and vertical profiles, and also made the CP efficiency much more sensitive to gain fluctuations. For these reasons, much of the early running was done only with liquid hydrogen, and several complete data runs were taken. After several data runs, it became increasingly obvious that π^- had a lifetime which was consistently about 0.25% longer than π^+, even for runs taken with a stable CP photomultiplier giving χ^2/D of unity for both the lifetime-ratio fit and the π^- absolute-lifetime fit.

An understanding of the reason for this result came only after several data runs using liquid deuterium showed any difference in the lifetimes to be less than 0.1%. It had been observed for some time that the pion peak of the CP pulse-height spectrum shifted gradually to lower channels of the PHA as CP was moved downstream. This was initially attributed to a "beam-size" effect, with the idea that CP had a lower efficiency at the end of the decay path due to the larger beam cross section, although the peak was shifted down from the DP1 position even at DP4, where the beam was actually smaller than at DP1. The effect was eventually identified with a rate-dependent gain of the CP photomultiplier: pions produced larger

pulses at upstream data positions because of the higher beam rate, and the average size of the pulses decreased as CP was moved downstream where the the rate was lower. This is just the sort of systematic bias which could completely invalidate a measurement of the absolute lifetime. But how could it lead to an apparent lifetime difference between π^+ and π^-? A look at curves B and C of Fig. 13 show the answer: for a given change in gain (shift in the pulse-height spectrum), the change in efficiency for counting pions depends on the depth of the valley of the pulse-height spectrum. For a distribution with a deep valley, few pion pulses move across the discriminator cut (Fig. 12) as the curve is shifted to lower pulse heights. But for a counter with many pulses in the valley, there would be a large change in efficiency as the distribution shifted and many pion pulses moved across the discriminator cut. Thus, with liquid hydrogen in the Cerenkov counter, the efficiency drop as CP was moved downstream would be much greater for π^+ than for π^-, due to the very different pulse-height distributions. It would then appear that the fraction of π^+ in the beam was dropping off faster than the fraction of π^-, and that π^+ had a shorter lifetime than π^-! The differences between π^+ and π^- disappear if liquid deuterium is used, however, and the method should then give a true measure of the lifetime difference, even though the absolute lifetimes of both could be expected to appear anomalously short.

Another systematic effect related to the use of liquid hydrogen had turned up earlier, and although it was solved by less drastic means than changing to liquid-deuterium Cerenkov media, it was a larger effect and particularly interesting because it was also present during the first experiment. As CP was moved downstream to a new data position, the cable

delay had to be changed for the CP and CPA photomultiplier pulses so that the $CP\overline{CPA}$ pulse would still arrive at the D coincidence at the same time as the M-coincidence pulse (see Fig. 17). Specifically, the pion associated with a particular M-coincidence pulse took longer to get to DP7 than to DP1. This longer flight-time delay had to be compensated for by using a shorter cable delay between the CP photomultiplier and the CP discriminator when the counter was at DP7 (and similarly for CPA and M_5, which also moved with CP). The mistake which was made during the first experiment and during the first part of this experiment, was to remove the needed cable delay from a signal <u>before</u> the discriminator. Since cables attenuate pulses, this meant that pulses reaching the CP discriminator were larger on the average when the counter was at DP7 than when it was at DP1. In terms of pulse-height spectra, this meant that the entire spectrum shifted to higher PHA channels as CP was moved downstream. But again, when liquid hydrogen was used as the radiating medium, the resultant increase in <u>efficiency</u> was more on π^+ than on π^-, which meant that the fraction of π^+ seemed to be dropping off more slowly than the fraction of π^-, i.e. the effect gave π^+ an apparently longer lifetime than π^-!

When the existence of the effect was recognized, the variable cable delays in CP, CPA, and M_5 were placed <u>after</u> the pulse-height discriminators, so that the length of cable between the photomultipliers and the discriminators was constant, independent of the position of CP along the decay path. The standardized output pulses of the discriminators were now subject to variable attenuation, but this was not a problem because these pulses were all well above the threshold of the next logic module, which restandardized the pulses before they were used for coincidences, as shown in Fig. 17.

A less elegant way of solving the problem was to use liquid deuterium in the Cerenkov counters, making the increase in efficiency with distance along the decay path the same for π^+ and π^-. The lifetime-ratio measurement ought to be valid under these conditions, although both absolute lifetimes can be expected to appear anomalously long. In fact, one liquid-deuterium data run was actually made before the error in the placement of the variable delay was corrected, and these data were included in the final analysis.

The significance of the results of the first experiment now are clear: an anomalously long π^+ absolute lifetime, with π^+ longer lived than π^- are precisely what are expected to result from the variable-delay placement mistake, coupled with the use of liquid hydrogen as the radiating medium. Furthermore, measurements showed that the effects would create an apparent lifetime difference of about 0.5%. It is doubtful that the rate effect was present in the first experiment, since the original Cerenkov counter used an RCA-8575 as the central photomultiplier. Search for a rate effect in CM, which also used RCA-8575 photomultipliers, failed to reveal any rate dependence of the pulse-height spectrum. Furthermore, a single data run made with liquid hydrogen and an RCA-8575 in CP (after the delay problem had been corrected) showed no lifetime difference. Unfortunately the new conical mirror which was built to reduce the 6.75-in.-diameter ring aperture down to the 1.8-in.-diameter photocathode diminished the effective entrance aperture of CP to about 5-in., and DP7 could not be used.

E. Changes in the Experimental Method

Two important checks of possible systematic bias were done by measuring the lifetime ratio under conditions signficantly different from the normal data-taking arrangement. One of these modifications was to remove CM physically from the beam, to test whether the scattering of pions in its liquid-deuterium radiator was causing any systematic bias. The monitor for this data run was the T coincidence, which contained both pions and muons. This in itself should have caused no problem, since the fraction of pions in T was constant with time, but there were other potential dangers involved. CM contributed significantly to the rejection of electrons, although electrons were mostly removed by A_e. Because of the 7% efficiency of CP for counting electrons, and the very different electron contaminations in the positive and negative beams (see Table V), the small fraction of electrons present in the T coincidence could have caused problems. Therefore, the absolute efficiency of A_e was measured by examining time-of-flight spectra taken with and without A_e in anticoincidence (see Fig. 21). The number of counts under the electron peak when A_e had supposedly vetoed all the electrons, gave a conservative measure of its absolute efficiency. The results of two measurements were consistent with an absolute A_e efficiency of 99.24%. The 0.76% electron contamination in T, combined with the 7% efficiency of CP for electrons, showed that a determination of the lifetime ratio ought to be valid at the 0.1% level without CM in the beam.

In addition to the measurement of the efficiency of A_e, the precaution had been taken during earlier data runs to record "data" coincidences without CM in the electronic monitor, although it was still physically in the beam. The resulting $TCP\overline{CPA}/T$ ratios were analyzed in the same way as

the D/M ratios acquired simultaneously, and the resulting lifetime differences compared. In all cases, the data without CM gave essentially the same result as the D/M data. The result for the data run with CM physically removed from the beam was

$$\tau_{\pi^+}/\tau_{\pi^-} = 0.99961 \pm 0.00071,$$

where the error is purely statistical. Unfortunately, $\chi^2/D = 1.44$ for the lifetime ratio fit, and while every indication was that the trouble was due to gain fluctuations of the CP central phototube, the real uncertainty on the result was probably at least $\pm$ 0.001.

A second and more drastic modification of the experimental method involved replacing the movable Cerenkov counter with an alternative pion detector. The detector selected pions on the basis of their strong interactions in a block of aluminum absorber, and is shown schematically in Fig. 26. R_1 was an 8-in.-square, 1/2-in.-thick scintillation counter which identified pions entering the absorber, a 2.8-in.-thick block of aluminum. About 20% of the beam pions stopped in the aluminum, while electrons and muons continued on through and were vetoed by the 14-in.-square, 1/2-in.-thick scintillation counter RA which was viewed by two photomultipliers, RA_1 and RA_2. The total absorber in front of RA was considerably less than the range of any of the beam particles, and the only pions which stopped in the block (or were scattered at wide enough angles not to count in RA) did so because of their strong interactions. The electronic arrangement used was the same as that shown in Fig. 17, with R_1 replacing CP, and RA_1 and RA_2 replacing CPA_1 and CPA_2. The veto pulse which was the sum of RA_1 and RA_2 was made 40-nsec long to insure 100% efficiency, since RA was required to veto 80% of the beam particles:

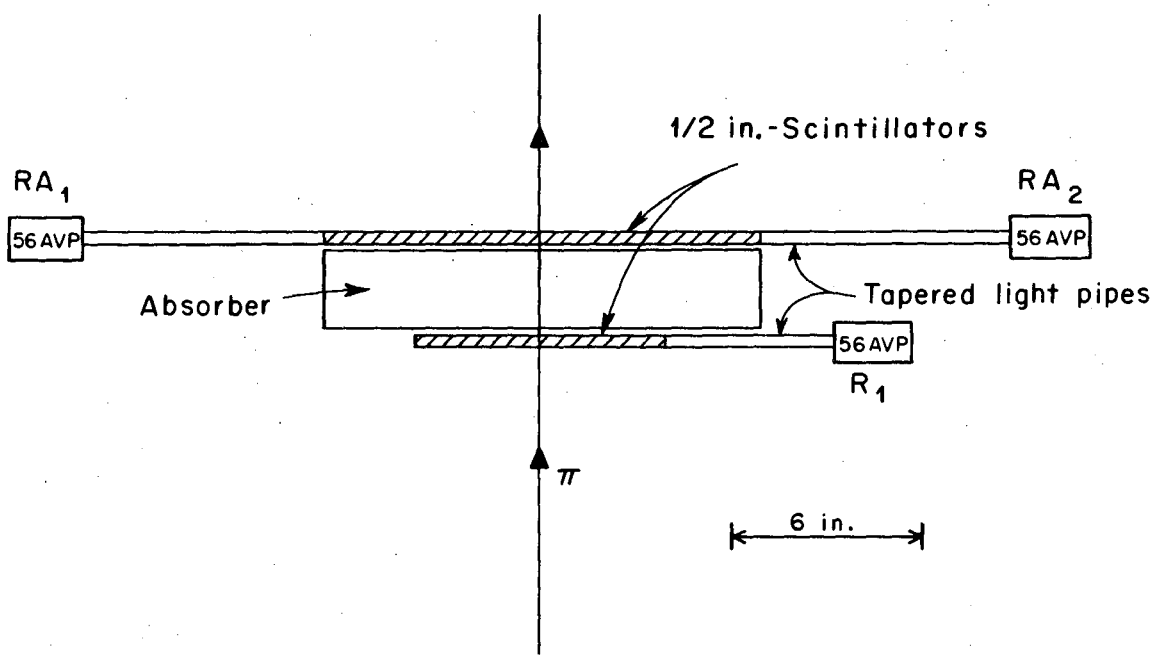

XBL687-3446

Fig. 26. Schematic diagram of the absorption device, viewed from above. The absorber used was a 2.8-in.-thick block of aluminum. Its thickness, as well as that of R_1 and of the counter wrappings, was made as uniform as possible to insure uniform efficiency across the face of the device.

the fraction of beam particles not vetoed by RA constituted the data. The greatest disadvantage was the low efficiency of the absorption device, approximately 20% of the CP efficiency, which meant that runs had to be five times as long as those with CP to achieve the same statistical accuracy.

Several systematic checks were made of the performance of the absorption device before it was used to measure the lifetime ratio. The efficiencies for counting electrons and beam muons were continuously monitored as always, and were about 5% and 0.08% respectively. The counting of slow decay muons, emitted backwards in the center-of-mass system, was checked by lowering the beam momentum until beam muons had $\beta = 0.92$ and counted in CM, making the M coincidence a muon monitor. This muon beam was degraded by a 5-in.-thick aluminum block in front of R_1, so that the emerging muons had the velocity of backward muons from pion decay. These counted in the absorption device with only 0.4% efficiency. The efficiency for pions was measured as a function of momentum in the region of the data-taking momentum, and found to have essentially the same shape for π^+ and π^-. One disturbing feature was that the efficiency for counting π^- was 20% larger than that for counting π^+. This difference arose because neutral final states were accessible to π^- reaction products and would not be vetoed by RA, while π^+ reaction products could never be neutral.

Just as with CP, the variation of counting efficiency was measured as the absorption device was moved laterally and vertically across the beam, to about 0.15% accuracy. While RA seemed to have slightly higher efficiency for vetoing particles which passed through the center of the counter than for those near the edges, the effect was at most 0.2% and

did not seem to be serious. The absolute-lifetime analysis of the data acquired later showed that there was a serious problem here, however. The value found for the π^+ lifetime was 26.74 ± 0.03 nsec, to be compared with the accepted value of 26.02 ± 0.04 nsec. Furthermore, χ^2/D for the fit was about 1.5, with most of the contribution coming from the central data positions (DP3 and DP4) where the beam was smallest. The effect was consistent with a higher vetoing efficiency where the beam was small, showing that a considerable fraction of the "stopping" pions actually were scattered at large angles, missing RA.

The anomalously long value of the absolute lifetime obtained with the absorption device can be partially understood on the basis of measurements made after the data taking. R_1 was replaced by the smaller time-of-flight counter T_2, and the time-of-flight spectra examined with and without RA in anticoincidence. The results are shown in Fig. 27, with the two curves normalized to the same number of counts in the pion peak. It is seen that the high-velocity shoulder on the pion peak was enhanced by using $\overline{RA}$ in the gate, i.e. some decay muons seem to have been counted as pions, leading to a net lifetime longer than that of pions alone. The problem seems to have been that the device counted all particles with such low efficiency that even an inefficient counting of decay products, which constituted a small fraction of the beam, enhanced the relative contamination of these particles in the data. Figure 28 shows the comparable time-of-flight spectra for CP, with the expected suppression of decay products.

All of the difficulties described above seemed at least to be the same for π^+ and π^- and there was no reason to doubt the validity of the lifetime comparison. The result of that analysis was

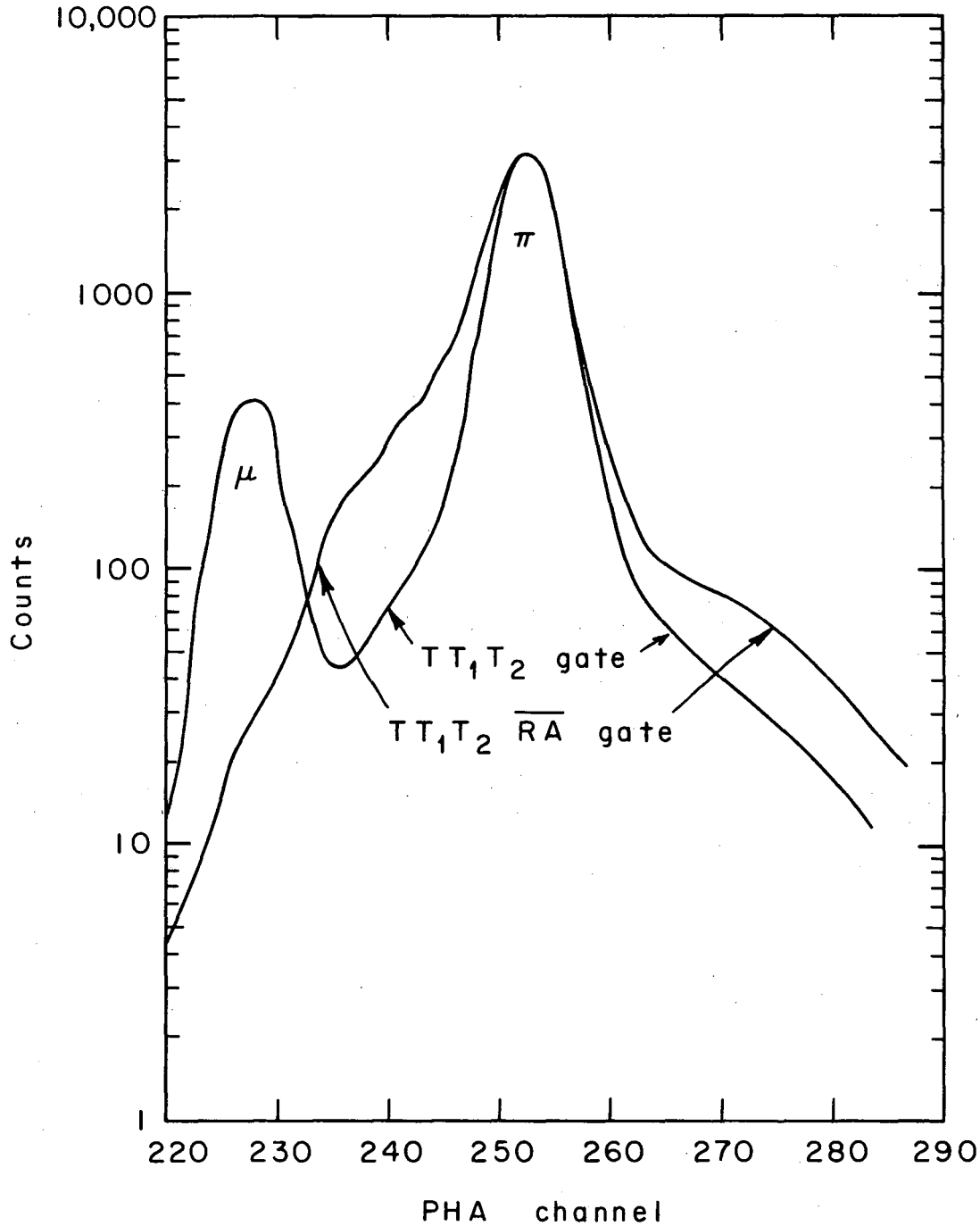

XBL687-3441

Fig. 27. Comparison of time-of-flight spectra with and without RA in anticoincidence. The two spectra have been normalized to the same number of pion counts in the peak. Notice that the inclusion of $\overline{RA}$ in the gate increased the relative contamination of decay products counted.

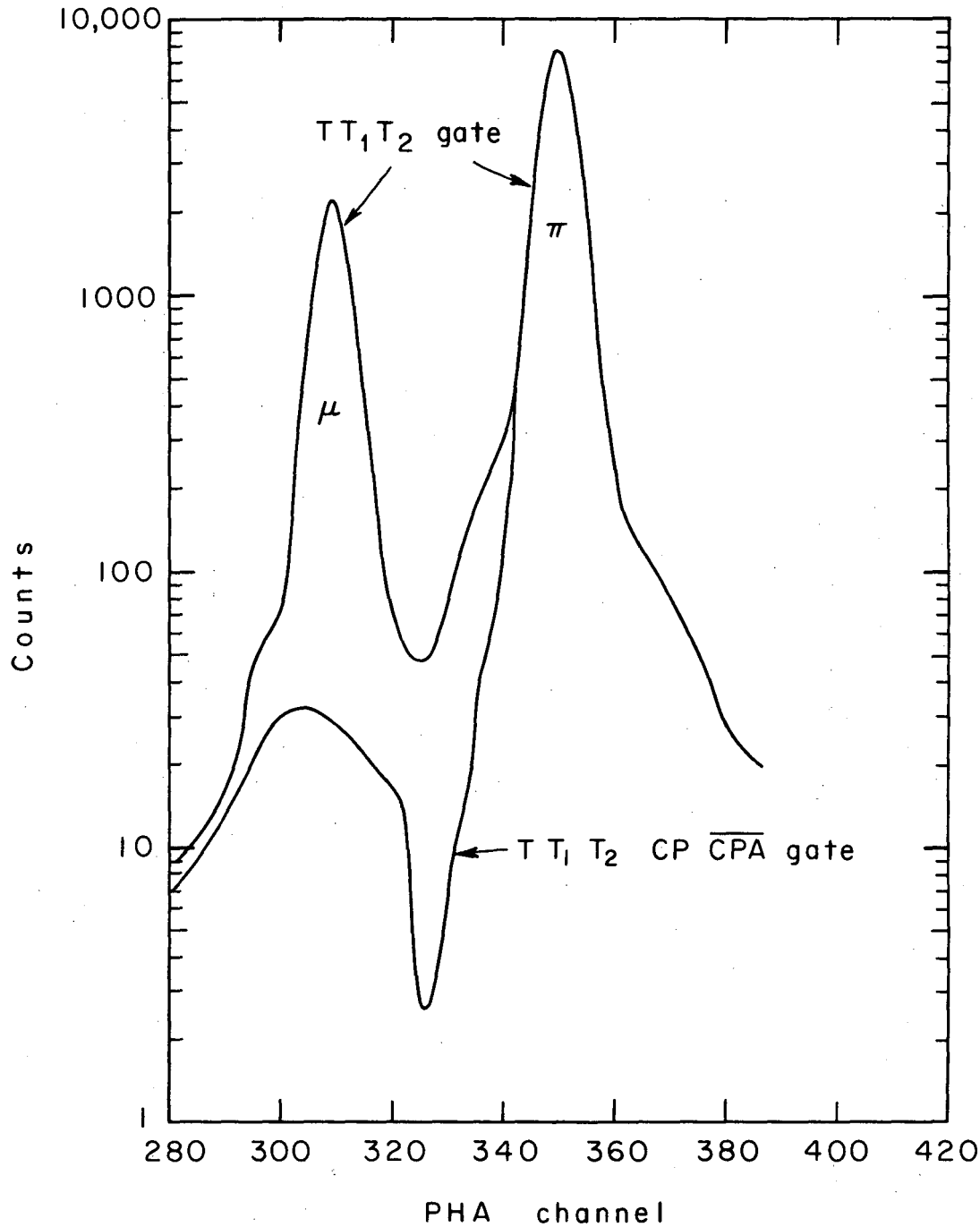

XBL687-3440

Fig. 28. Comparison of time-of-flight spectra with and without CPCPA in the coincidence. CP was filled with liquid deuterium for the test. Notice that the high-velocity shoulder on the pion peak was due to decay muons, and was removed by CPCPA.

$$\tau_{\pi^+}/\tau_{\pi^-} = 1.0006 \pm 0.0011,$$

where the uncertainty is purely statistical. Furthermore, $\chi^2/D = 0.90$ for the fit, involving 106 π^+-π^- groups at six different positions along the decay path. Both this absorption-device measurement, and the measurement made using CP with CM moved out of the beam, were regarded as tests of possible systematic bias, and were not included in the calculation of the final quoted lifetime ratio.

V. DATA ANALYSIS

A. Derivation of Formulae Used

The experimentally-determined quantities used to calculate the lifetime difference are the ratios f_+/f_-, where $f = D/M$. These quantities were measured repeatedly at seven different distances x along the decay path. If the velocity of light is taken to be unity, then the number of pions at a distance x from the start of the decay path is

$$N(x) = N(0)e^{-mx/p\tau} \quad , \tag{1}$$

where m is the pion rest mass, p is the momentum in the laboratory, and τ is the lifetime in the pion rest system. Notice that the exponent is actually independent of the mass, since $p = \beta\gamma m$, and is written in the above manner because the momentum enters into the equations for the lifetime in a simpler way than does the velocity.

The quantities measured experimentally are the numbers of M and D coincidences, which are related to the numbers of actual pions by

$$M = \epsilon_{mon}N(0), \text{ and } D = \epsilon_{mon}\epsilon N(x) \ . \tag{2}$$

The efficiency of the monitor for counting pions at $x = 0$ is given by ϵ_{mon}, and includes a factor to account for the fact that the monitor measures the pion intensity at some fixed distance from $x = 0$. The quantity ϵ is the efficiency of CP for counting pions, and is assumed to be independent of distance. D contains a factor ϵ_{mon} because pions which do not count in the monitor are not eligible to count in the D coincidence. Equations (1) and (2) can now be used to relate the experimentally-measured numbers to the fraction of pions present as a function of distance:

$$f = D/M = \epsilon_{mon}\epsilon N(x)/\epsilon_{mon}N(0) = \epsilon e^{-mx/p\tau} \quad ,$$

which is independent of the efficiency of the monitor. Taking the natural logarithm of this expression, we get the formula from which the absolute pion lifetime can be calculated:

$$\ell n(D/M) = \ell n(\epsilon) - (m/p\tau)x. \qquad (3)$$

The measured numbers $\ell n(D/M)$ at distances x are fitted by the method of least squares[46] to an expression of the form A - Bx, where A and B are constants to be determined by the fit. $B = m/p\tau = 1/\beta\gamma\tau$, and hence gives the absolute lifetime if either the velocity, or the mass and momentum, are known. The measurement requires that the efficiency ϵ of the movable Cerenkov counter be independent of x, and remain constant during the data taking, although its value does not have to be known. The latter requirement makes an absolute-lifetime measurement difficult if liquid deuterium is used in the counter, for then the efficiency is sensitively dependent on the gain of the central photomultiplier. If the efficiency is to be independent of x, then it must be independent of the beam size and shape (which vary along the decay path). The position of the beam within the counter may also change with distance due to small differences in the positioning of CP at different data positions, so the efficiency must be unaffected by these differences also.

The basic formula for the lifetime difference can be obtained by considering the quantities $\ell n(f) = \ell n(D/M)$ measured on both π^+ and π^-, and applying (3) to each. Denoting quantities referring to π^+ and π^- by subscripts + and - respectively, and subtracting logarithms in (3) we obtain:

$$\ell n(f_+/f_-) = \ell n(\epsilon_+/\epsilon_-) + \left(\frac{1}{\tau_-} - \frac{1}{\tau_+}\right) \frac{x}{\beta\gamma}$$

or

$$\ell n(f_+/f_-) = \ell n(\epsilon_+/\epsilon_-) + \left(\frac{\tau_+ - \tau_-}{\bar{\tau}}\right) \frac{x}{\beta\gamma\bar{\tau}}$$

and finally:

$$\ell n(f_+/f_-) = \ell n(\epsilon_+/\epsilon_-) + \frac{\Delta\tau}{\tau} X, \qquad (4)$$

where

$\frac{\Delta\tau}{\tau} = (\tau_+ - \tau_-)/\bar{\tau}$, $\bar{\tau} = (\tau_+ + \tau_-)/2$, and X is the distance x measured in mean decay lengths. The assumption has been made in deriving (4) that the <u>velocities</u> of the π^+ and π^- beams are equal, but no assumption about the equality of the π^+ and π^- masses is needed.

Equation (4) can be used to find the lifetime difference $\Delta\tau/\tau$ from the measured quantities, $\ell n(f_+/f_-)$. These numbers, obtained at distances X, are fitted by the method of least squares[46] to an expression of the form C + EX, where C and E are constants to be determined from the fit, and E is just equal to the lifetime difference $\Delta\tau/\tau$. The χ^2 distribution for the fit gives a measure of the consistency of the data, and hence of reliability. The usual criterion is that χ^2 per degree of freedom (χ^2/D) should be close to unity, where the number of degrees of freedom is the number of points fitted minus two.

Several important consequences of (4) should be discussed. The validity of the measurement does not require that the CP efficiency be known, or even that it remain constant. It is only necessary that the <u>ratio</u> of the efficiencies for π^+ and π^- remain constant. This is not hard to achieve if the changes in absolute efficiency with time occur slowly compared to the time interval between the taking of positive and negative data which are used to form the ratio f_+/f_-. While random fluctuations in the efficiency ratio show up as an improbable χ^2 distribution for the fit, systematic errors like those caused by the rate effect, and by the gradual separation of the positive and negative beams along the decay path, give rise to smooth changes in the efficiency ratio

with distance. Notice that the beam velocity does not have to be known very accurately for the lifetime ratio measurement, since it is required only to express the distance x in terms of mean decay lengths.

If the π^+ and π^- velocities are <u>not</u> assumed to be equal, then it is convenient to rederive Eq. (4) in terms of the mean momenta of the positive and negative beams, p_+ and p_- respectively. We assume that the π^+ and π^- masses are both equal to m. Thus:

$$\ell n(f_+/f_-) = \ell n(\epsilon_+/\epsilon_-) + \left(\frac{1}{\beta_-\gamma_-\tau_-} - \frac{1}{\beta_+\gamma_+\tau_+}\right) x$$

$$= \ell n(\epsilon_+/\epsilon_-) + \left(\frac{m}{p_-\tau_-} - \frac{m}{p_+\tau_+}\right) x$$

$$= \ell n(\epsilon_+/\epsilon_-) + \left(\frac{p_+\tau_+ - p_-\tau_-}{\overline{p}\overline{\tau}}\right) \frac{m\,x}{\overline{p}\,\overline{\tau}}$$

$$= \ell n(\epsilon_+/\epsilon_-) + \frac{\Delta(p\tau)}{p\tau} X ,$$

where $\overline{p} = (p_+ + p_-)/2$. Hence:

$$\ell n(f_+/f_-) = \ell n(\epsilon_+/\epsilon_-) + \left(\frac{\Delta p}{p} + \frac{\Delta\tau}{\tau}\right) X \qquad (5)$$

where $\Delta p/p = (p_+ - p_-)/\overline{p}$. Equation (5) illustrates two points. If the <u>momentum</u> difference between the π^+ and π^- beams is measured, the additional assumption of equality of masses is needed for the lifetime-ratio determination. In this experiment, the <u>velocities</u> were compared by both the momentum-response-curve method and by the time-of-flight method, so that the validity of our result does not depend on the equality of π^+ and π^- masses. Second, it can now be seen that the error in $\Delta\tau/\tau$ caused by a velocity difference is just equal to the equivalent momentum difference, $\Delta p/p$. This is the reason why the results of the velocity-difference measurements were always expressed in terms of the corresponding momentum

difference.

The raw data taken during each run had to be corrected for the roughly linear change in CP efficiency as the beam moved laterally across the CP entrance aperture. This effect was coupled with a lateral separation of the positive and negative beams which gradually increased along the decay path, and thus gave rise to an efficiency ratio ϵ_+/ϵ_- which changed with x. Although Eqs. (4) and (5) are still valid, the least-squares fitting procedure used is not, because it assumes the efficiency ratio to be constant. Thus, the full analysis of the data had to account explicitly for this effect. In fact, only one of the three runs used in the final data analysis involved a CP lateral efficiency which was not constant within the 0.1% measurement of the effect; however, the uncertainties on the results of all three runs were increased to account for the possible existance of the effect below the 0.1% level. The relation between the measured quantities and the lifetime difference will now be derived quantitatively.

We assume that the π^+ and π^- beams coincide at DP1 ($x = 0$), and that each travels along a circular trajectory with very large radius of curvature R. The experimentally-measured parameter is the separation D between the two beams at distance $x = L$ drom DP1, where L is the maximum decay length used during a particular data run. If y measures the lateral displacement of the positive beam center from the average position of the centers of the positive and negative beams, then $y = 0$ at $x = 0$, and increases to $y = + D/2$ for the positive beam and to $y = - D/2$ for the negative beam at $x = L$. Since the center of curvature of the positive trajectory is at $y = R$, the equation of trajectory is

$$(R - y)^2 + x^2 = R^2 \quad \text{or} \quad y = R - R\sqrt{1 - x^2/R^2} \quad .$$

But, since $x \ll R$, this reduces to:

$$y = x^2/2R.$$

We can find R in terms of measured quantities by recalling that $y = D/2$ at $x = L$, so that $D/2 = L^2/2R$ or

$$R = L^2/D, \tag{6}$$

giving the final equation for positive particle trajectories:

$$y = (x/L)^2\ D/2 = \frac{X^2}{(L/\lambda)^2}\ D/2 = \delta X^2 \tag{7}$$

where

$$\delta = \frac{D/2}{(L/\lambda)^2}\ ,$$

λ = the mean decay length for pions and $X = x/\lambda$ as before.

Equation (6) confirms that x/R is small; since the maximum value of x is L, $x/R < L/R = D/L \approx (0.2\text{-in.})/(400\text{-in.}) = 5 \times 10^{-4}$.

The other experimentally-measured quantity was the fractional change in CP efficiency ϵ per inch of CP lateral displacement perpendicular to the beam. If $\epsilon(y) = \epsilon(0) + sy$ describes this variation, then $y = +\delta X^2$ for π^+ and $y = -\delta X^2$ for π^-, from (7). Hence:

$$\frac{\epsilon_+(X)}{\epsilon_-(X)} = \frac{\epsilon_+ + s\delta X^2}{\epsilon_- - s\delta X^2} = \frac{\epsilon_+}{\epsilon_-}\,(1 + 2s\delta X^2/\epsilon), \tag{8}$$

where $\epsilon_\pm$ without an argument refers to the value at $x = 0$, and ϵ is the average value of ϵ_+ and ϵ_-, which are nearly equal to each other and to unity. Terms of order $(s\delta)^2$ have been neglected, since $s\delta = \frac{(D/2)s}{(L/\lambda)^2} = \frac{(0.1\text{-in.})(0.2 \times 10^{-2}/\text{in.})}{(0.5)^2} \approx 1 \times 10^{-3}$. Thus we obtain, by substituting (8) into (4)

$$\ell n(f_+/f_-) = \ell n\left[\frac{\epsilon_+}{\epsilon_-}\ (1 + 2s\delta X^2/\epsilon)\right] + \frac{\Delta\tau}{\tau}\ X$$

$$\approx \ell n(\epsilon_+/\epsilon_-) + 2s\delta X^2/\epsilon + \frac{\Delta\tau}{\tau}\ X.$$

This last expression is of the form:

$$\ell n(f_+/f_-) - FX^2 = C + \frac{\Delta\tau}{\tau}\ X \tag{9}$$

where $F = 2s\delta/\epsilon = \dfrac{2sD}{2\epsilon(L/\lambda)^2} = \dfrac{SD}{(L/\lambda)^2}$. (10)

The parameter S is defined as $S = s/\epsilon = \dfrac{\Delta\epsilon/\epsilon}{y}$ = the fractional change in CP efficiency per unit displacement. Therefore, all the factors appearing in (10) can be measured, and F is a known number. Thus, in order to correct for the slope of the CP lateral profile, the least-squares fit to the data can be performed using Eq. (9) instead of Eq. (4). The measured numbers are now $\ell n(f_+/f_-) - FX^2$, and these are to be fitted to an expression of the form C + EX, where the coefficient E is determined by the fit and is equal to the lifetime difference $\Delta\tau/\tau$.

The uncertainty on the value of $\Delta\tau/\tau$ obtained is derived from the uncertainties of the input data, and is thus a combination of the statistical error on $\ell n(f_+/f_-)$ and the measurement error of the number F. The former is obtained from the statistical uncertainty of the ratios $f = D/M$. We must recognize however, that D and M are not independent: M may be thought of as a fixed number of pions out of which a certain number D (to be measured) survive. The uncertainty on D is then

$$\Delta D = \sqrt{f(1 - f)M}, \text{ and } \Delta f = \Delta D/M = \sqrt{f(1 - f)/M}.$$

The relative uncertainty of f is then

$$\Delta f/f = \sqrt{f(1 - f)/f^2M} = \sqrt{\frac{1}{D} - \frac{1}{M}}\ .$$

Hence, the relative uncertainty in f_+/f_- is

$$\frac{\Delta(f_+/f_-)}{f_+/f_-} = \sqrt{\left(\frac{\Delta f_+}{f_+}\right)^2 + \left(\frac{\Delta f_-}{f_-}\right)^2} = \sqrt{\frac{1}{D_+} - \frac{1}{M_+} + \frac{1}{D_-} - \frac{1}{M_-}} \quad .$$

But the quantities actually used in the fit are the numbers $\ell n(f_+/f_-)$, so it is the absolute error on these which must be found. Since the absolute uncertainty on $\ell n(R)$ is just the relative uncertainty on R (= $\Delta R/R$), the input data quantities are:

$$\ell n(f_+/f_-) \pm \sqrt{\frac{1}{D_+} - \frac{1}{M_+} + \frac{1}{D_-} - \frac{1}{M_-}} \quad . \tag{11}$$

These statistical uncertainties must be combined with the measurement errors for the quantity F, computed from (10). The largest of these are associated with the beam separation D and the slope S of the CP lateral profile.

B. Data Analysis for a Particular Run

Data runs usually lasted about a week, and consisted of measurements made from a single filling of the Cerenkov counters. More than 24 hours were required from the start of condensing to attainment of the cryogenic equilibrium necessary for operation of the Cerenkov counters, and the recovery of the deuterium at the end of a run took another 16 hours. These time factors, combined with maintenance which was necessary between runs to insure clean optics for the next run, meant that a shutdown of at least five days was needed between the end of one run and the start of the next. Such long delays made it impractical to fit data from different runs simultaneously. Rather, each run was treated as an independent determination of the lifetime ratio, and the final number quoted represents the weighted average of the results of several runs. Another reason for treating the data in this way is that the CP central photomultiplier or conical mirror or both were often changed between runs in an attempt to achieve greater stability, more uniform response across the face of the counter, and a wider effective aperture. Thus, there was often a complete change in the operating conditions from run to run, making the different measurements of $\Delta\tau/\tau$ quite independent. The statistical accuracy achieved during a single run was usually about 0.1%, although some measurements were better than this.

The data from a particular run was treated by three computer programs, which performed numerous checks on the consistency of the data, and calculated the absolute lifetimes for π^+ and π^-, and the lifetime ratio. Partial analyses were often done on the data available two or three times during a run, in order to detect the more subtle equipment malfunctions while there was still time to correct them. The most useful program for

the last purpose was called SUMHIS. This program calculated the ratios shown in Table V, as well as many quantities not shown there, for each scaler readout. Histograms were then made for each of the ratios, making it easy to detect departures from normal operation and fluctuations larger than those expected from statistics. SUMHIS was also used to check the data for internal consistency by utilizing the considerable redundancy inherent in the large number of quantities scaled. For instance, $(B\Sigma A + B\overline{\Sigma A})/B = 1$ and $(T + S)/B\overline{\Sigma A} = 1$ should always be satisfied; also, several important coincidences such as M and D were scaled on two independent scalers, and the program readily detected any disagreement between the two.

The program PILIFE fitted the measured numbers $\ell n(D/M)$ to an expression of the form $A - Bx$ (see Eq. (3) of the previous section), and used the relation $B = m/p\tau$ to calculate the absolute lifetimes of π^+ and π^-. The same procedure was carried out using, instead of D/M, the following ratios:

(a) MCP/M, which detected any anomalous bias produced by CPA,

(b) $TCP\overline{CPA}/T$, which was the same as D/M without $CM\overline{CMA}$,

(c) DM_5/M, which was useful in detecting fluctuations in CP efficiency,

(d) V/L, which would have given the muon lifetime if L were pure muons,

(e) X/S, which would have given the electron lifetime if S were pure electrons.

Calculations (a) and (b) generally gave the same result as the D/M analysis, although χ^2 distribution for the MCP/M fit was usually a little worse than that for the D/M data. The DM_5/M data typically had a χ^2

distribution better than that for the D/M fit, but resulted in a longer absolute lifetime. This was probably because of the CP efficiency's extreme sensitivity to the vertical position of the beam, coupled with a gradual change in beam height with distance. The X/S and V/L fits gave values of the absolute lifetime on the order of 70 nsec, but with $\chi^2/D = 50$ or even more. Closer examination of the data revealed that the decrease in these ratios was roughly exponential with very long lifetimes up to DP4, but further downstream the attenuation became much faster than exponential because both muons and electrons were getting farther and farther out of time with the pions.

The program PIRATIO fitted the quantities $\ell n(f_+/f_-) - FX^2$ to an expression of the form C + EX (see Eq. (9) of the previous section), where X is the distance in mean decay lengths, $E = \Delta\tau/\tau$, and F is the correction factor for the CP lateral efficiency slope. In order to apply the χ^2 test to the f_+/f_- ratios, the uncertainty in F was taken to be zero. This was done because the value of F was actually constant throughout a particular run, and the uncertainty attached to it was meant to estimate the <u>systematic</u> error in its measurement. By way of contrast, the uncertainty in $\ell n(f_+/f_-)$, given by Eq. (11) of the previous section, was purely statistical, so that the χ^2 test provides a criterion for comparing the actual fluctuations observed to those expected from the statistics. Thus, the test loses its validity if the statistical uncertainties are inflated by the additional measurement error in F, and these systematic uncertainties were included only after the statistical fluctuations of the data had been investigated. Figure 29 is a plot of the lifetime-ratio data from one of the successful runs used in the final analysis.

Just as with the PILIFE program, the PIRATIO analysis was done using the ratios MCP/M, $TCP\overline{CPA}/T$, DM_5/M, V/L, and X/S in addition to the ratio

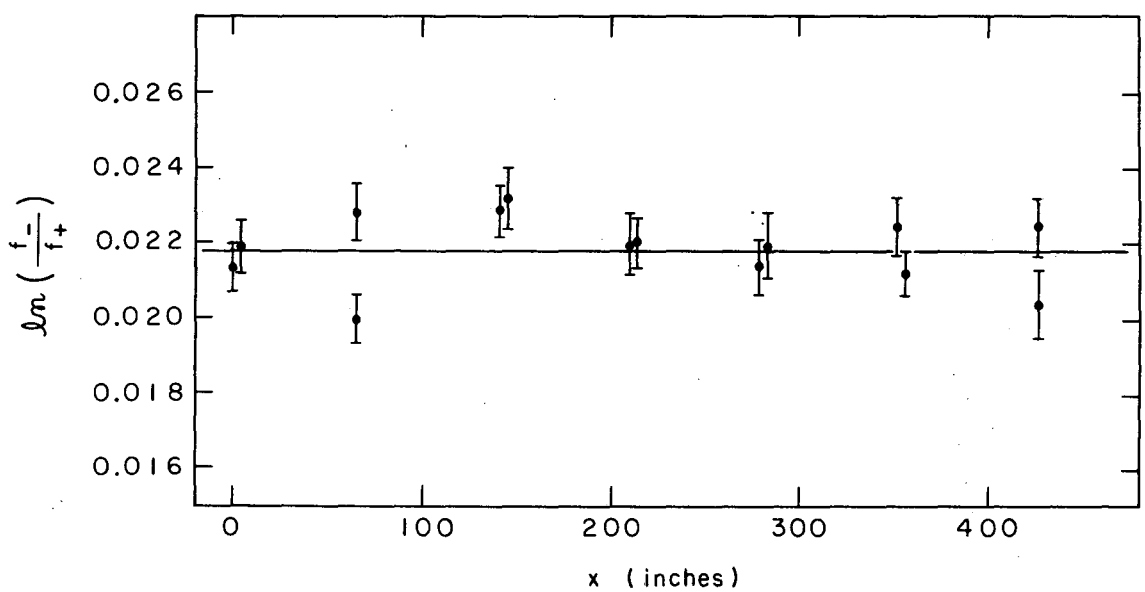

XBL687-3444

Fig. 29. Plot of the lifetime-ratio data for one of the three data runs (Run 28) used in the final analysis. Each of the points plotted is an average of several measurements made with the counter at a single data position. The line drawn through the points is the least-squares computer fit to the individual points (and not to the averages plotted), giving

$$\tau_{\pi^+}/\tau_{\pi^-} = 0.99989 \pm 0.00086, \text{ with } \chi^2/D = 1.09.$$

D/M. As before, the first two gave the same answer for the lifetime ratio as the D/M data. The DM_5/M data nearly always had $\chi^2/D = 1.0$, but often gave lifetime ratios significantly different from unity due to systematic effects. Despite the poor timing of the V and X coincidences at large distances, the V/L and X/S analyses generally gave the result of equal lifetimes for positive and negative particles, with considerably better χ^2 distributions than the absolute-lifetime fit. For example, a typical run had $\chi^2/D = 20$ for the X/S absolute lifetime, but $\chi^2/D = 1.5$ for the lifetime ratio. This is an experimental demonstration that the validity of the lifetime-ratio measurement requires only that the ratio of positive to negative efficiencies be constant, while the absolute-lifetime determination requires that the absolute value of the CP efficiency be fixed.

In the event that the lifetime-ratio analysis gave a poor fit, characterized by χ^2/D significantly greater than unity, a number of techniques were used to locate the source of the difficulty. The χ^2 contributions of the individual fitted points were examined, and correlations sought between bad points and fluctuations in other quantities in the same scaler readout, using the SUMHIS-calculated ratios. Large blocks of data with anomalously large χ^2 contributions were thrown out, and portions of the data were fitted separately. Points with particularly bad fluctuations were thrown out and the remainder refitted, in the hope that the poor fit had been due to just a few large fluctuations. Without exception, the results of these attempts to improve the fit for a bad run led to a single conclusion: the fluctuations responsible for the unreasonable χ^2 distributions occurred on a time scale which was short compared to the polarity-reversal period, and consisted of a whole

spectrum of fluctuations outside of statistics rather than a few large ones. Furthermore, no correlation was ever seen between fluctuations in D/M and fluctuations in monitor quantities such as absolute rate, accidental rate, electron contamination, CM efficiency, and many others. The trouble was not in the CPA vetoes (which were only 1% of the data), because the MCP/M fits were essentially identical to the D/M fits. The fact that the DM_5/M data did not exhibit the unreasonable fluctuations of the D/M data was the final piece of evidence which identified the source of the trouble as the gain of the central CP photomultiplier in every instance. Fortunately, several photomultipliers were eventually found which were stable enough for our purposes, and these allowed meaningful measurements to be made.

C. Data Selection and Final Compilation

Table VIII outlines the history of the data taking. Runs are numbered in chronological order, and major changes in the experimental arrangement are indicated as they occurred. The Cerenkov medium specified was used in both CM and CP, except in Run 36 when CM was moved physically out of the beam. The lifetime differences with their statistical uncertainties are those computed from the D/M data by the PIRATIO program, with no correction included for the lateral slope of the CP efficiency. No data selection was made for the results quoted, except for Run 36 where a few points which had fluctuations of more than six standard deviations from the expected value were omitted. The selection of the data to be used in the final computation of the lifetime difference was done on the basis of systematic errors present during particular runs, and on the internal consistency as indicated by the χ^2 distribution for the fit. Because of the rate-dependent efficiency of the CP central photomultiplier, and the very different pulse-height distributions for π^+ and π^-, none of the data taken with liquid hydrogen as the Cerenkov medium were used. This leaves only the four runs taken with liquid deuterium and of those only Runs 24, 28, and 34B had χ^2/D values indicating reliable fits. Analysis of the first half of the Run 34 data showed serious CP gain fluctuations, and the pulse-height spectrum showed that the CP discriminator was not set at the very lowest point in the valley. Therefore, the discriminator threshold was lowered as much as possible, still keeping the efficiency for counting electrons under 8% and the beam-muon efficiency under 1%. The data taken after this change were treated separately, and gave a much-improved χ^2 distribution, thus making it useful in the final compilation. Aside from the fact that Run 36 (with CM out) can be regarded as a check on systematic

Table VIII. Chronology of the data taking.

Run No.	Cerenkov medium	$(\tau_+ - \tau_-)/\bar{\tau}$	χ^2/D	Comments
24*	deuterium	+0.25±0.14%	1.04	old A_3; variable-delay error
---	Variable delays placed after discriminators for CP, CPA, and M_5.			
25A	hydrogen	-1.04±0.16%	5.1	bad CP central phototube (RCA-4522, 5-in. diam.)
25B	hydrogen	+0.04±0.15%	1.29	CP central phototube was an RCA-8575 (2-in. diam.)
---	A_3 changed to a double-ended, thinner counter with a smaller hole.			
27	hydrogen	-0.288±0.076%	0.94	good π^- lifetime measurement
28*	deuterium	-0.011±0.086%	1.09	
---	CP flask ruptured. New flask being installed is black inside to reduce scattering of unwanted light.			
29, 30, 31	Absorption device	+0.06±0.11%	0.90	result is a weighted average of three runs
33	hydrogen	-0.360±0.065%	1.80	first run with new CP flask; noisy CP photomultiplier
34A	deuterium	-0.43±0.14%	1.68	CP discriminator threshold too high
34B*	deuterium	+0.048±0.118%	1.18	CP discriminator reset
35	Time-of-flight studies			
36	deuterium	-0.039±0.071	1.44	CM moved out of beam
37-41	Time-of-flight measurements with CP removed			

*These runs were used for the final calculation of the lifetime ratio.

biases rather than data, the bad X^2/D for the fit makes it unusable in the final computation.

Table IX summarizes the calculation of the final weighted average of the fractional lifetime difference $\Delta\tau/\tau$. The "No. Points" entry gives the total number of values of $\ell n(f_+/f_-) - FX^2$ fitted for each run, and is therefore equal to the number of polarity reversals during that run. The lifetime differences given under the "raw data" entry have F = 0, and thus involve no correction for the slope of the CP efficiency. These are to be compared with the"corrected" lifetime differences which were computed using the measured values of F. The only run where F differed significantly from zero was Run 24, and it can be seen that the effect of the correction here was quite small. The statistical uncertainties of the three individual results were each increased by a factor $\sqrt{X^2/D}$, to account for the fact that the fluctuations were slightly larger than expected on the basis of statistics alone. No correction was made for the existence of a possible momentum difference between the positive and negative beams, but an uncertainty of 0.03% was included in the final error assigned to each measurement, to account for the fact that individual determinations of the momentum difference were no more accurate than this.

The last entry in Table IX gives the corrected lifetime difference obtained from each run, and is the result of fitting $\ell n(f_+/f_-) - FX^2$ to the form $C + \frac{\Delta t}{\tau} X$. The uncertainty on the corrected result is a combination of the statistical error (augmented by $\sqrt{X^2/D}$), uncertainty in the equality of momenta, and uncertainty in the correction for the lateral-efficiency variation of CP. The last uncertainty was obtained in the following way. Fits to the data, including the lateral-slope

Table IX. Final calculation of the lifetime ratio.

Run Number:	24	28	34B
No. Points:	78	88	62
$(\tau_+-\tau_-)/\bar{\tau}$ $(\times 10^3)$: (raw data)	+2.45±1.40	-0.11±0.86	+0.48±1.18
χ^2/D for above fit:	1.04	1.09	1.18
Uncert. $\times\sqrt{\chi^2/D}$ $(\times 10^3)$:	±1.43	±0.90	±1.29
Mom. uncert. $(\times 10^3)$:	±0.30	±0.30	±0.30
Lat. slope uncert. $(\times 10^3)$:	±0.33	±0.28	±0.41
$(\tau_+-\tau_-)/\bar{\tau}$ $(\times 10^3)$: (corrected)	+2.16±1.50	-0.11±0.99	+0.48±1.39

The weighted average* of the three corrected results is:

$$(\tau_+ - \tau_-)/\bar{\tau} = 0.00055 \pm 0.00071,$$

based on a total of 228 data points. $\chi^2/D = 0.80$ for the weighted average (two degrees of freedom).

*If measurements are $x_i \pm \sigma_i$, the weighted average is $\bar{x} \pm \bar{\sigma}$, where

$$\bar{x} = \frac{\sum_i x_i/\sigma_i^2}{\sum_i 1/\sigma_i^2} \quad \text{and} \quad \bar{\sigma} = \frac{1}{\sum_i 1/\sigma_i^2}.$$

correction, were made both with no uncertainty in the correction and with the actual measurement errors included for the factors in F. The difference between the uncertainties on the lifetime difference obtained by the two methods was attributed to the lateral-slope-correction uncertainty, and was used to compute the number labelled "Lat. Slope Uncert."

The final weighted average gives our best value for the lifetime

ratio:

$$\tau_{\pi^+}/\tau_{\pi^-} = 1.00055 \pm 0.00071.$$

The fact that $\chi^2/D = 0.80$ for the average is an indication of the self-consistency of the three numbers averaged. The result above differs from that published in Ref. 5, which was $\tau_{\pi^+}/\tau_{\pi^-} = 1.00064 \pm 0.00069$. The published ratio is probably less reliable, because it involves a rather crude estimate of the CP lateral-efficiency-variation correction. Furthermore, the published ratio involves a correction to the Run 34B data based on CP efficiency profiles taken before the CP discriminator was lowered. The lifetime ratio used here for Run 34B involves no correction for the effect, since several profiles taken indicated a considerably flatter response after the discrimination threshold was lowered. However, the uncertainty of the Run 34B result has been significantly increased to account for the fact that no high-statistics profile was actually taken at DP4 after the change.

VI. CONCLUSIONS

We have measured the ratio of the mean lifetimes of π^+ and π^- mesons, and found $\tau_{\pi^+}/\tau_{\pi^-} = 1.00055 \pm 0.00071$, where the quoted uncertainty is mostly statistical, but also includes estimates of the error due to major systematic biases. While this result is consistent with the predictions of the CPT theorem, we have not proved CPT invariance, since the equality of lifetimes might be due to some symmetry (e.g. CP) other than CPT. Our result is also consistent with a number of other recent measurements of the same quantity, and it is the most precise determination published to date.

While the quoted lifetime ratio was measured in approximately 400 hours of data taking, a total of 2400 hours of cyclotron time was spent on the experiment. Most of this was used to study possible systematic biases, and resulted in a thorough understanding of the properties of the beam and the two liquid-deuterium Cerenkov counters. One of the most rewarding accomplishments of the experiment was the explanation of the results of the first experiment. The apparent lifetime difference and the anomalously long π^+ absolute lifetime found then were apparently caused by placing the variable cable delay ahead of the pulse-height discriminator of the movable Cerenkov counter. This was one of several potential systematic errors associated with the use of liquid hydrogen as the Cerenkov medium, and eventually led us to use only the data taken with liquid deuterium for the final analysis.

The experiment we finally performed was as symmetric as possible between positive and negative particles. The great majority of the material in the beam was charge-symmetric liquid deuterium, which scattered π^+ and π^- in the same way. Despite the factor of five difference in the

production cross sections of π^+ and π^-, the experiment was performed using equal pion fluxes by reducing the cyclotron's proton-beam intensity when taking data on positive particles. The near equality of accidental coincidences for π^+ and π^- (see Table V) shows that this background was due entirely to beam pions, with completely negligible cyclotron background. Many precautions were taken during set-up to insure identical spatial and momentum distributions of the π^+ and π^- beams, and direct measurements showed that these efforts had been largely successful, although the spatial separation of the positive and negative beams at the end of the decay path was the source of a small systematic bias. One of the largest potential asymmetries was the factor of five difference in the electron contaminations of the positive and negative beams, but this was completely eliminated through the use of the highly efficient electron veto counter A_e, and the monitor Cerenkov counter CM.

Direct checks on systematic errors involved measurements of the lifetime ratio under drastically altered conditions: one data run was taken with CM moved out of the beam, and another with the absorption device, which identified pions by their strong interactions rather than by their velocity. The result of each measurement was equality of lifetimes to about 0.1% accuracy. Another check made on our method was the direct measurement of the absolute lifetime of the π^-, yielding $\tau_{\pi^-} = 25.97 \pm 0.04$ nsec, which is in excellent agreement with the currently accepted value of the π^+ absolute lifetime, measured by an entirely different method. This value of the absolute lifetime can only be checked to 0.15% because of our imprecise knowledge of the beam velocity, as well as the limited precision of the measurements to which it can be compared. However, the statistical uncertainty on the π^- absolute life-

time was 0.05% and the χ^2/D for the fit to a pure exponential was 0.98 for 192 data points at seven different data positions along the decay path. This shows that the decay curves measured were exponential,[45] and is another demonstration that the beam was well confined and the data coincidence due to pions alone.

The ultimate limitation on the accuracy attainable was the stability of the CP central photomultiplier, or alternatively, the interactions in the liquid deuterium, which produced many pulses in the valley of the pion pulse-height distribution and made the efficiency of CP very sensitive to the photomultiplier gain. If either one of these problems had been completely solved, the experiment could probably have produced a measurement of the lifetime difference which was limited only by the knowledge of the equality of the velocities of the π^+ and π^- beams. At the 0.03% level, the measurement is also limited by statistics, and it seems doubtful that the method could determine the lifetime difference to better than this accuracy. In any event, we never succeeded in finding a perfectly satisfactory photomultiplier, and the only way to reduce the number of interactions would be to use a momentum away from the 3/2-3/2 πp resonance, which would require completely redesigned Cerenkov counters. In summary, it seems unlikely that the present method could be improved significantly; the best that could be hoped for would be another factor of two or three in the precision of the measurement.

ACKNOWLEDGEMENTS

I would like to express my appreciation to Professor A. Carl Helmholz and Professor Burton J. Moyer for their constant interest in and guidance of my studies and research at Berkeley.

I wish to thank particularly Dr. Robert W. Kenney, whose friendly support, hard work, and physical insight made this experiment a fruitful and enjoyable experience.

It is a pleasure to acknowledge the help and enthusiastic support of my fellow graduate student, Mr. Arthur J. Greenberg, who assumed complete responsibility for the spark-chamber development and for the time-of-flight studies. He also made major contributions to every phase of the experiment by his hard work and many helpful discussions.

Special thanks also go to my co-workers on the experiment: Dr. David O. Caldwell, Dr. Allan M. Cormack, Dr. Virgil B. Elings, Mr. William P. Hesse, and Dr. Rollin J. Morrison. Without their hard work and many important contributions this experiment could never have succeeded.

I would like to thank Mr. James Vale and the entire cyclotron staff for such trouble-free machine operation. Particular thanks go to Mr. Lloyd B. Houser, Mr. Donald F. Rothfuss, and Mr. Louis A. Sylvia for their help with the design, installation, and smooth operation of the experimental equipment.

The liquid-deuterium Cerenkov counters would never have succeeded without the assistance of Mr. Albert H. Kleid who assembled the flasks with meticulous care, Mr. Edwin F. McLaughlin and Mr. Richard V. Schafer who were responsible for the cryogenic design and proper operation of the counters, and Mr. Rene Bollaert, Mr. Russell F. Ellis, and Mr. Allan R.

Susoeff of the hydrogen-target group, whose hard work kept both counters working and clean despite numerous emergencies. I am also indebted to Dr. James G. Baker for the design of the lens system used in the Cerenkov counters.

I would like to express my gratitude to Dr. Richard J. Kurz for teaching me so much about experimental physics during the first experiment, and for his help in the design of the beam for this experiment.

I owe a special debt of thanks to Miss Miriam L. Machlis, who has cheerfully typed two drafts of this thesis, and who handled efficiently many of the details of my return from Nigeria.

Finally, I would like to thank my wife Kathy for her understanding and encouragement throughout the long hours of running, and during the many crises of the experiment.

This work was done under the auspices of the U. S. Atomic Energy Commission.

REFERENCES

1. M. Bardon, U. Dore, D. Dorfan, M. Krieger, L. Lederman, and E. Schwartz, Phys. Rev. Letters 16, 775 (1966).

2. F. Lobkowicz, A. C. Melissinos, Y. Nagashima, S. Tewksbury, H. von Briesen, Jr., and J. D. Fox, Phys. Rev. Letters 17, 548 (1966). These authors also give the value $\tau_{\pi^+}/\tau_{\pi^-} = 1.0040 \pm 0.0018$, obtained by another method of averaging the data. We have quoted the more conservative result in the text.

3. D. S. Ayres, D. O. Caldwell, A. J. Greenberg, R. W. Kenney, R. J. Kurz, and B. F. Stearns, Phys. Letters 24B, 483 (1967) and Phys. Rev. 157, 1288 (1967). The latter article gives the more complete account of the experiment.

4. V. I. Petrukhin, V. I. Rykalin, D. M. Khazins, and Z. Cisek, Comparison of the Life-Times of the Charged Pions (Preprint), Joint Institute for Nuclear Research, Dubna, USSR, Report No. JINR-P1-3862 (1968), in Russian.

5. D. S. Ayres, A. M. Cormack, A. J. Greenberg, R. W. Kenney, D. O. Caldwell, V. B. Elings, W. P. Hesse, and R. J. Morrison, Phys. Rev. Letters 21, 261 (1968). The result quoted here incorporates an improved correction for the effect of the lateral variation of CP efficiency, and hence differs slightly from the published result. The published lifetime ratio was $\tau_{\pi^+}/\tau_{\pi^-} = 1.00064 \pm 0.00069$, to be compared with the more reliable value quoted here: $\tau_{\pi^+}/\tau_{\pi^-} = 1.00055 \pm 0.00071$.

6. See for example, M. Eckhause, R. J. Harris Jr., W. B. Shuler, R. T. Siegel, and R. E. Welsh, Phys. Letters 19, 348 (1965).

7. R. W. Kenney, D. O. Caldwell, E. F. McLaughlin, W. L. Pope, R. V. Schafer, and B. F. Stearns, Proceedings of the 1966 International Conference on Instrumentation for High Energy Physics (International Union of Pure and Applied Physics and U. S. Atomic Energy Commission, Washington, D. C., 1966), p. 201.

8. C. S. Wu, E. Ambler, R. W. Hayward, D. D. Hoppes, and R. P. Hudson, Phys. Rev. 105, 1413 (1957).

9. R. L. Garwin, L. M. Lederman, and M. Weinrich, Phys. Rev. 105, 1415 (1957).

10. J. H. Christenson, J. W. Cronin, V. L. Fitch, and R. Turlay, Phys. Rev. Letters 13, 138 (1964).

11. T. D. Lee and C. N. Yang, Phys. Rev. 104, 254 (1956), and T. D. Lee, R. Oehme, and C. N. Yang, Phys. Rev. 106, 340 (1957).

12. See for example, J. Schwinger, Phys. Rev. 82, 914 (1951); J. Schwinger, Phys. Rev. 91, 713 (1953).

13. G. Lüders, Kgl. Dansk. Vidensk. Selsk. Mat-Fys. Medd. 28, No. 5 (1954).

14. W. Pauli, Niels Bohr and the Development of Physics (McGraw-Hill, New York and Pergamon, London, 1955).

15. See for example, V. L. Fitch, Comments on Nuclear and Particle Physics, 1, 117 (1967) and 1, 151 (1967).

16. J. J. Sakurai, Invariance Principles and Elementary Particles (Princeton University Press, Princeton, N. J., 1964).

17. G. Lüders, Ann. Phys. (N. Y.) 2, 1 (1957).

18. R. Jost, Helv. Phys. Acta 30, 409 (1957).

19. G. Lüders and B. Zumino, Phys. Rev. 106, 385 (1957).

20. See for example, T. D. Lee and C. N. Yang, Elementary Particles and Weak Interactions, Brookhaven National Laboratory Report BNL-443 (T91), 1957 (unpublished).

21. W. H. Barkas, Ann. Rev. Nucl. Sci. 15, 67 (1967), using the measurement of W. H. Barkas, W. Birnbaum, and F. M. Smith, Phys. Rev. 101, 778 (1956) for the π^+ mass, and the measurement of R. E. Shafer, K. M. Crowe and D. A. Jenkins, Phys. Rev. Letters 14, 923 (1965) for the π^- mass.

22. V. T. Cocconi, T. Fazzini, G. Fidecaro, M. Legros, N. H. Lipman and A. W. Merrison, Phys. Rev. Letters 5, 19 (1960).

23. D. E. Muller, H. C. Hoyt, D. J. Klein, and J. W. M. DuMond, Phys. Rev. 88, 775 (1952). This comparison was the most accurate available at the time of the Third International Conference on Atomic Masses and Related Constants, Winnepeg, Canada (1967).

24. V. L. Fitch, Proceedings of the XIIIth International Conference on High Energy Physics (University of California Press, Berkeley and Los Angeles, 1967), p. 63.

25. S. L. Meyer, E. W. Anderson, E. Bleser, L. M. Lederman, J. L. Rosen, J. Rothberg, and I-T. Wang, Phys. Rev. 132, 2693 (1963).

26. A. Rich and H. R. Crane, Phys. Rev. Letters 17, 271 (1966).

27. R. W. Williams (University of Washington) private communication, October, 1968. The result quoted represents nearly an order of magnitude increase in precision over the previous measurement published at the Berkeley Conference (Ref. 24).

28. See for example, the review article by T. D. Lee and C. S. Wu, Ann. Rev. Nucl. Sci. 16, 471 (1966).

29. Aachen-Bari-Bergen-CERN-Ecole Polytechnique-Nijmegen-Orsay-Padua-Turin collaboration, reported at the Berkeley Conference (Ref. 24).

30. A. T. Alikanov, Tu. V. Galaktionov, Yu. V. Gorodkov, G. P. Eliseyev, Zh. Eksperim. i Teor. Fiz. 38, 1918 (1960), in Russian [English transl.: Soviet Phys. - JETP 11, 1380 (1960)].

31. H. L. Anderson, T. Fujii, R. H. Miller, and L. Tau, Phys. Rev. 119, 2050 (1960).

32. M. L. Goldberger and S. B. Treiman, Phys. Rev. 110, 1178 (1958).

33. 0.012-in. Carlite Transformer Oriented Iron, in 31-in. by 120-in. sheets, obtained from Armco Steel, Lafayette, California.

34. A considerably modified version of the program described by Thomas J. Devlin, OPTIK: An IBM 709 Computer Program for the Optics of High-Energy Particle Beams, Lawrence Radiation Laboratory Report UCRL-9727, Sept. 1961 (unpublished).

35. See for example, Owen Chamberlain, Ann. Rev. Nucl. Sci. 10, 161 (1960).

36. D. A. Hill, D. O. Caldwell, D. H. Frisch, L. S. Osborne, D. M. Ritson, and R. A. Schluter, Rev. Sci. Instr. 32, 111 (1961).

37. See for example, Leonard I. Schiff, Quantum Mechanics (McGraw-Hill Book Co., Inc., New York, 1955), Chap. X.

38. Temperature Sensor Model No. 146AF-1, obtained from Rosemont Engineering Company, Minneapolis, Minn. These sensors had a resistance of about 6 ohms at 20° K, with a sensitivity of about 0.8 ohms/°K.

39. Bell-O-Fram pressure regulator, type 10A, 2 to 25 psi, obtained from Bell-O-Fram Corp., Burlington, Mass. The device maintained a constant pressure within ± 0.01 psi with respect to atmospheric pressure.

40. The ortho-para conversion catalyst used was a nickel-oxide silica gel ($NiO \cdot 2.5\ SiO_2$), obtained from Air Products and Chemicals, Inc., Houdry Industries Div., Allentown, Pennsylvania, under the trade name "Apachi."

41. R. J. Corruccini, Refractive Index and Dispersion of Liquid Hydrogen, National Bureau of Standards Technical Note 323 (1965).

42. The pulse-height analyzer used throughout the experiment was a Series 2200 Nuclear Data Analyzer, with a 1024-channel memory and a 4096-channel Analog-to-digital Converter, obtained from Nuclear Data, Inc., Palatine, Ill.

43. Nearly all of the fast logic used during the experiment was part of the E. G. G. M100 Counting System, obtained from Edgerton, Germeshausen and Grier, Inc. Salem, Massachusetts.

44. Same as Ref. 6. The numbers quoted differ from the published result in accordance with a communication of the authors to A. H. Rosenfeld.

45. Arthur J. Greenberg (Ph. D. Thesis), Lawrence Radiation Laboratory Report UCRL-18485 (unpublished). At the time of writing, this reference, which is devoted entirely to our measurement of the absolute pion lifetime, is still in the early stages of composition. It should be available in final form by January, 1969.

46. See for example, Peter Cziffra and Michael J. Moravcsik, A Practical Guide to the Method of Least Squares, Lawrence Radiation Laboratory Report UCRL-8523 Rev., June, 1959 (unpublished).

This report was prepared as an account of Government sponsored work. Neither the United States, nor the Commission, nor any person acting on behalf of the Commission:

A. Makes any warranty or representation, expressed or implied, with respect to the accuracy, completeness, or usefulness of the information contained in this report, or that the use of any information, apparatus, method, or process disclosed in this report may not infringe privately owned rights; or

B. Assumes any liabilities with respect to the use of, or for damages resulting from the use of any information, apparatus, method, or process disclosed in this report.

As used in the above, "person acting on behalf of the Commission" includes any employee or contractor of the Commission, or employee of such contractor, to the extent that such employee or contractor of the Commission, or employee of such contractor prepares, disseminates, or provides access to, any information pursuant to his employment or contract with the Commission, or his employment with such contractor.